An assessment of the distribution and abundance of dugongs and in-water, large marine turtles along the Queensland coast from Cape York to Hinchinbrook Island

Prepared by Helene Marsh[1], Kym Collins[1], Alana Grech[2], Rachel Miller[1] and Robert Rankin[3]
[1]College of Science and Engineering, James Cook University, Townsville, QLD 4811
[2]ARC Centre of Excellence in Coral Reef Studies, James Cook University, Townsville, QLD 4811
[3]Thomson Reuters, Centre for AI & Cognitive Computing, 120 Bremner Blvd, Toronto, ON Canada.

Acknowledgments:

EXECUTIVE SUMMARY

Project objective

- To assist the Great Barrier Reef Marine Park Authority (GBRMPA) and the Queensland government address the requirements of the Reef 2050 Long-Term Sustainability Plan (the Reef 2050 Plan) by:

  ° Continuing the time series of surveys for dugongs and large marine turtles using the latest advances in distribution and abundance analysis.
  ° Advising GBRMPA about the implications of the findings for the conservation and management of dugongs and large marine turtles in the Great Barrier Reef from just north of Hinchinbrook Island to the southern boundary of the Torres Strait survey region.

Methods

- The intention was to complete the entire survey in November 2018 using two surveys teams and two aircraft. However, in order to obtain weather suitable for aerial surveys, the survey had to be undertaken in three stages: November 2018, June 2019 and November/December 2019.

- The survey design was based on previous aerial surveys conducted by researchers at James Cook University as optimised during the RIMReP process.

Key findings

- The 2018-2019 aerial surveys confirm that the survey region between -18°S and -10°S continues to support globally significant populations of dugongs and marine turtles, both of which have been formally identified as components of the Great Barrier Reef World Heritage Area's outstanding universal values.

- We estimated that the region between north of Hinchinbrook Island and Cape Bedford supported ~550 $\pm$ SE 250 dugongs (Hagihara method) and ~32000 $\pm$ SE 7100 large juvenile and adult in-water turtles (not identified to species, Fuentes method) in November 2018. Because most of this region has not been surveyed for many years using the standard transect technique, we cannot estimate dugong population trends for this region.

- The spatially-explicit models of dugong and turtle distribution and density developed using the results of the November 2018 survey of the region, between the northern end of Hinchinbrook Island and Cape Bedford, indicated that dugongs were sighted at very low densities throughout most of this region. Dugong densities were higher in the area immediately north of Hinchinbrook Island and some of the reefs from the Cape Tribulation region north. In contrast, turtles were sighted at medium densities on the top of many reefs in this region and at high densities on some outer reefs, especially just south of Cape Tribulation and between Cape Tribulation and Cooktown.

- The region north of Cape Flattery supported an estimated ~7000 $\pm$ SE 1600 dugongs (Hagihara method) and ~282000 $\pm$ SE 28000 turtles (Fuentes method) in 2018-2019. The region between ~15°S and ~14°S supported ~85 per cent of the dugongs in the NGBR survey region and the only large herds of dugongs sighted were in this region.

- Bayesian modelling using the N-Mixture estimator suggests that this dugong population has been stable since 2006, assuming that there was no net movement of

animals between the segments surveyed in each of the three stages of the 2018-2019 survey.

- The turtle population estimates were higher in 2018-2019 for all blocks for which comparative data were available from the 2013 survey, with the exception of Lloyd Bay near Lockhart River.

- In addition, relatively few dugongs were sighted in Lloyd Bay in 2019 compared with 2006 or 2013. This region was in the path of a tropical low in December 2018 and severe Tropical Cyclone Trevor in March 2019.
    - The spatially-explicit models developed from data collected during the 2018-2019 surveys of the region from Lookout Point (just north of Cape Flattery) north indicated that:Dugongs were sighted at:
        - very high densities throughout much of the inshore region between Lookout Point and Bathurst Head at the western end of Bathurst Bay, and in local regions of some of the bays on the eastern coast of Cape York between Friendly Point and Shelbourne Bay inclusive; and
        - at medium densities in some bays and associated with many reefs off Cape York.
    - Turtles were sighted at:
        - medium densities throughout most of this region; and
        - at high and very high densities on the top of many reefs and in some inshore waters, especially in the region between Lookout Point and Cape Melville, Princess Charlotte Bay and off Shelburne Bay.

- The percentage of dugong calves is an index of fecundity and neonatal mortality and one of the indices of the health status of dugong population. The percentage of calves was slightly higher than but not significantly different to the results for 2006 and 2013 in the region from Cape Flattery north. This percentage was significantly higher for the surveys of this region conducted prior to 2000 than subsequently, suggesting habitat loss. However, the data on the status of seagrass in the Northern Great Barrier Reef are not adequate to further evaluate this inference.

Recommendations regarding application of the key findings to management arrangements

The key findings of this report suggest that:

- the major priority for dugong management in the Northern Great Barrier Reef continue to be on-going support for the implementation of community-based management by Traditional Owners, by completing Traditional Use Marine Resource Agreements (TUMRA) with Traditional Owners in key hunting communities such as Lockhart River, Hope Vale and the Northern Peninsula Area.

    1) negotiations between Traditional Owners and management agencies consider defining boundaries for the hunting areas of various Traditional Owner Groups (as in the Girrungun TUMRA) in addition to allowable catches or hunting moratoria, especially in view of: the increased challenge of maintaining customary hunting areas as a result of the improvements in road access to remote areas and the increased use of GPS technology;
    2) the challenges of implementing a robust system of catch recording; and
    3) ongoing wider community concerns about Traditional hunting.

- implementation of the Queensland Sustainable Fisheries Strategy 2017-2027 include further reforms to reduce bycatch of Matters of National Environmental Significance such as dugongs and marine turtles in the region, including electronic video surveillance.

- the spatial models of the density of dugongs and marine turtles presented in this report be used to inform the identification of Biologically Important Areas in the Great Barrier Reef World Heritage Area.

- an expert working party be established as soon as possible to enable the next aerial survey of the urban coast of the Great Barrier Reef World Heritage Area scheduled for 2022 to be conducted using an Unmanned Aerial Vehicle (UAV) to reduce the risk to human safety and improve the resolution of the observations. The working party should build on the Dugong technical expert group report submitted as part of the Reef 2050 Integrated Monitoring and Reporting Program design by developing a plan for transitioning the large-scale aerial surveys of dugongs and large in-water turtles to UAVs. The terms of reference of the working party should include:

    1) the logistics of conducting the surveys using a UAV along the urban coast and in remote areas;
    2) whether the boundary of the survey region should be moved to the Whitsundays to reflect dugong stock structure;
    3) how the survey could be funded to include the entire region from Torres Strait to Moreton Bay inclusive; and
    4) the experimental work required to ensure that the results of the UAV surveys can be compared with the historical time series of aerial surveys.

- an expert working party be established as soon as possible to develop a temporal and spatial design for the habitat assessment, health assessment and process monitoring recommended by the Seagrass technical expert group report and to coordinate this monitoring with the aerial monitoring of dugongs and in-water turtles.

Table of Contents

LIST OF FIGURES

Main Text

Appendix Figures

LIST OF TABLES
Main Text

Appendix Tables

ACRONYMS AND ABBREVIATIONS USED IN THIS REPORT

CGBR……… Central Great Barrier Reef
EBK………… Empirical Bayesian Kriging
EPBC Act… Environmental Protection and Biodiversity Conservation Act
GBR............. Great Barrier Reef
GBRMPA...... Great Barrier Reef Marine Park Authority
GBRWHA..... Great Barrier Reef World Heritage Area
JCU..............James Cook University
km............... kilometre
m................. meter
RIMReP........ Reef 2050 Integrated Monitoring and Reporting Program
se................ standard error
NGBR........... Northern Great Barrier Reef
SGBR……… Southern Great Barrier Reef
TUMRA……. Traditional Use of Marine Resources Agreement
UAV............. Unmanned Aerial Vehicle

1. INTRODUCTION

The Great Barrier Reef World Heritage Area (GBRHWA) supports globally significant populations of the dugong (*Dugong dugon*), a coastal marine mammal that feeds mainly on seagrasses (Marsh et al. 2011), and five species of marine turtles, the green (*Chelonia mydas*), loggerhead (*Caretta caretta*), olive ridley (*Lepidochelys olivacea*), flatback (*Natator depressus*) and hawksbill (*Eretmochelys imbricata*) turtles. In addition, leatherback turtles (*Dermochelys coriacea*) are occasionally sighted in the region.

The significance of the Great Barrier Reef World Heritage area for dugongs and green and loggerhead turtles was among the reasons for its World Heritage listing (GBRMPA, 1981). Thus, the status and trends in the distribution and abundance of these species is important information for the management of the World Heritage Area (Commonwealth of Australia 2018).

As the only surviving member of the family Dugongidae (Marsh et al. 2011), the dugong is a species of high biodiversity value. The dugong is listed as 'Vulnerable' to extinction by the International Union for Conservation of Nature (Marsh and Sobtzick 2019), and anecdotal evidence suggests that dugong numbers have decreased throughout most of their range (Marsh et al. 2011). Significant populations persist in Australian waters, which are now believed to support most of the world's dugongs. Dugongs are listed in Appendix 1 of the Convention of Migratory Species. As a signatory to that Convention, and the associated Dugong Memorandum of Understanding, Australia has international obligations to conserve dugongs in its waters and hence the species is listed as a Matter of National Environmental Significance under the Commonwealth *Environment Protection and Biodiversity Conservation Act 1999* (EPBC Act).

All the species of marine turtles occurring in Australasian waters are also Matters of National Environmental Significance by virtue of their listing as threatened, migratory and marine species under the EPBC Act. Leatherback, loggerhead, and olive ridley turtles are listed as 'Endangered'; flatback, green and hawksbill turtles as 'Vulnerable'. As with the dugong, Australia has international obligations to conserve the marine turtles in its waters.

Since the 1980s, aerial surveys have provided information on dugong distribution and abundance for many parts of their distribution in Australia (Marsh et al. 2011), including the GBRWHA. These surveys have been a cost-effective means of assessing the distribution and abundance of dugongs at vast spatial scales (>tens of thousands of km^2). As a key component of this series of surveys, dugongs have been surveyed along the east coast of Queensland using standardised techniques since the mid-1980s. This aerial survey monitoring of dugong distribution and abundance has been coordinated across jurisdictions in this region at the same time of year, over a two-year period, at approximately five-year intervals. JCU teams usually surveyed the entire Queensland coast south from 16.5^{o}S in one year and then the remote Great Barrier Reef region north of -16.5^{o}S plus Torres Strait in a second year, ideally the year after the southern survey. The last survey of the region north of 16.5^{o}S was conducted in 2013 (Sobtzick et al. 2014). The region from the northern end of Hinchinbrook Island south to and including Moreton Bay near Brisbane was last surveyed in 2016 (Sobtzick et al. 2017). The 2016 survey of the southern GBR was unable to include the region between the northern end of Hinchinbrook Island and -16.5^{o}S due to the combined effects of a fixed budget and logistical complications. Hence this region was included in the surveys covered by this report.

The Reef 2050 Plan (Commonwealth of Australia 2018) includes monitoring and reporting actions to inform the evaluation of progress against the key components (underlined) of target (BT4):

- Populations of Australian humpback and snubfin dolphins, <u>dugong, and loggerhead, green, hawksbill and flatback turtles</u> are stable or increasing at Reef-wide and <u>regionally relevant scales.</u>

Thus, the major objective of this study was to help the Great Barrier Reef Marine Park Authority (GBRMPA) and the Queensland government address the requirements of the Reef 2050 Plan (Commonwealth of Australia 2018) by:

- Continuing the time series of surveys for dugongs and large marine turtles using the latest advances in distribution and abundance analysis.
- Advising GBRMPA about the implications of the findings for the conservation and management of dugongs and large marine turtles in the GBR from just north of Hinchinbrook Island to the southern boundary of the Torres Strait survey region.

2. METHODS
2.1 Survey design

The design for the 2018-2019 aerial surveys was based on previous aerial surveys conducted by researchers at James Cook University as optimised during the RIMReP process (Marsh et al. 2019). Figure 1 shows the location of the survey blocks and the orientation and spacing of transects.
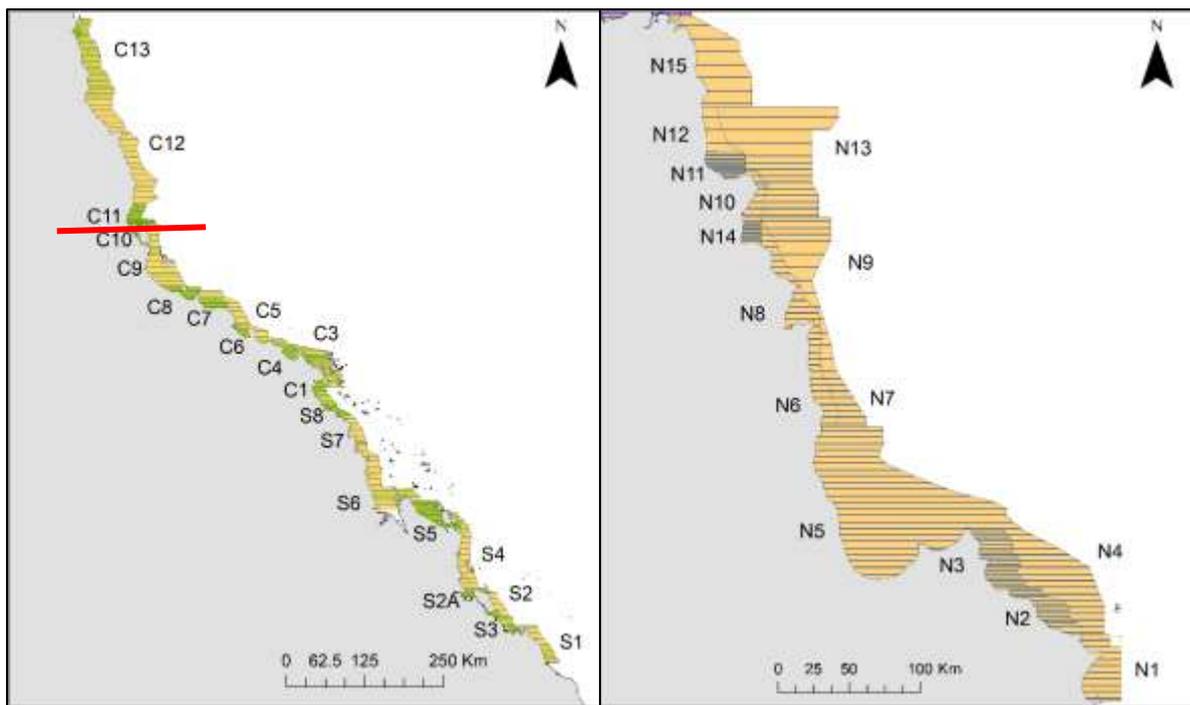
Figure 1. Map of the optimised dugong aerial survey designs for the SGBR (left) and NGBR (right) developed as part of the RIMReP process (Marsh et al. 2019). The blocks north of the red line in the left-hand figure were not surveyed in 2016 as planned and were included in this survey. With the agreement of GBRMPA, Block N1 was not flown in 2018-2019 because in all previous surveys there were too few dugongs sighted in this block to enable a dugong population to be estimated. Thus, Blocks C11-13 and N2-15 were flown in 2018-2019.

We originally planned to complete the entire survey from just north of Hinchinbrook Island (Block C11 southern boundary (-18° 11.294'S) through Block N15 northern boundary

(-10°57.5'S, see Figure 1) in November 2018 using two surveys teams and two aircraft. However after the first few days, the actual and forecast weather conditions experienced were unsuitable for aerial surveys and, after consultation with GBRMPA, we decided to defer the remainder of the survey until 2019. The survey was completed in June and November/December 2019 using a single aircraft. The blocks flown in the various segments of the survey are listed in Table 1 and Appendix Tables 1.1 and 2.1.

Table 1. The data used to calculate the estimates of perception bias for the various survey teams.

Blocks surveyed (see Figure 1)	Date	Data used to correct for Perception Bias	
		Dugong	Turtle
C11, C12, C13	November 2018	Survey Team 1[1]	Survey Team 1
N12, N15	November 2018	Survey Teams 2[2]+4[4]	Survey Teams 2+4
N5	June 2019	Survey Team 3[3]	Survey Team 3
N2, N3, N4, N6, N7, N8, N9, N10, N11, N13, N14	November–December 2019	Survey Team 4	Survey Team 4

[1] Marsh (Leader): Berg Soto, Gonzalez-Paredes, Hanf, Miller
[2] Collins (Leader): Jaeckli, Melvin, Nakamura, Wyatt
[3] Collins (Leader): Carr, Gonzalez-Paredes, Miller, Nakamura
[4] Collins (Leader): Carr, Gonzalez-Paredes, Hanf, Miller

2.2 Survey methodology

All teams consisted of four observers and one survey leader and were (re) trained prior to each survey. We used the same observers as much as possible (see Table 1 and Appendix Table 3.1). Prior to the November 2018 survey, crew members (pilots, survey leaders, observers) received Aircraft Underwater Escape Training.

The aerial survey methodology followed the strip transect aerial survey technique detailed in Marsh and Sinclair (1989a) and used in earlier surveys along the Queensland coast. A 6-seat, high-wing, twin-engine Partenavia 68B (NGBR 2018) or C (all other surveys) was flown along predetermined transects as close as possible to a ground speed of 100 knots. To comply with the requirements of the Civil Aviation Safety Authority, the survey was conducted at a height of 500 feet (152 m) above sea level as opposed to 450 feet (137 m) flown in surveys conducted prior to 2011. The experimental work of Marsh and Sinclair (1989b) indicates that there should be no difference in dugong sightability between survey heights of 152 and 137 m.

Transects 200 m wide on the water surface on each side of the aircraft were demarcated using fiberglass rods attached to artificial wing struts on the aircraft. Distance categories (50, 100, and 150 m) within the strip were marked by colour bands on the artificial wing struts. Two tandem teams of observers on each side of the aircraft (Appendix Table 3.1) scanned their respective transects and recorded their sightings onto separate tracks of an audio recorder. The two members of each tandem team operated independently and could neither see nor hear each other when on transect. The location of the sightings in the distance categories within the survey strip enabled the survey team to decide if simultaneous sightings by tandem team members were of the same group of animals when reviewing the recordings. However, as explained by Pollock et al. (2006), although we found no decline in detection with distance across the strip, there was a large amount of measurement error in the assignment of dugong sightings to distance classes within the transect strip because: (1) dugongs surface cryptically and for only 1–2 seconds (Chilvers et al. 2004); of (2) the inherent limitations of using colour bands on the wing struts (as approved by the Civil Aviation Safety Authority) to define distance categories, and (3) the shape of the aircraft. The

cryptic nature of dugong surfacing and the often high sighting rate also meant that observers could not afford to take their eyes off the water to read an inclinometer. Thus, following Pollock et al. (2006), we decided not to use the distance category as a co-variate in the analyses. The sightings of the tandem observers were also used to calculate survey specific corrections for perception bias (i.e., for animals visible in the survey transect but missed by observers) for each side of the aircraft as outlined below.

The surveys were generally conducted in passing mode with dugongs and large marine turtles as the main focus. For each animal sighting, observers recorded the type of animal (e.g., dugong or turtle), total number of animals seen, position in transect (e.g., low or medium), and a composite index of environmental conditions (see Appendix Tables 4.1 and 4.2). Although dugongs and turtles were the focus of the survey, other megafauna were also recorded (dolphins, large sharks, sea snakes).

The number of calves was recorded for each dugong sighting. Calves were defined as being less than 2/3 of the size of the cow and swimming in close proximity to her. On the relatively rare occasions (see footnotes to Table 7 and Appendix Figures 13.2 and 13.3) when groups of dugongs were sighted that were too large to accurately count in passing mode (generally >9 animals) the aircraft then abandoned the transect and went into circling mode in an effort to obtain an exact census of the group (herd) before resuming the transect. In such cases, the availability bias and detection probabilities were set to 1 (perfect detection and availability).

The survey leader collected data on environmental conditions at the beginning of each flight (cloud cover, cloud height, wind speed and direction, and air visibility) and each transect (cloud cover). Every few minutes during each transect, and whenever conditions changed, the survey leader recorded sea state, visibility, and glare on each side of the aircraft (assessed by the mid-seat observers).

2.3 Population and density estimates
2.3.1 Dugong population estimates

We used the method developed by Hagihara et al. (2014, 2018), henceforth the Hagihara method, to estimate dugong relative abundance and density. The method attempts to correct for availability bias (animals not available to observers because of environmental conditions and animal diving behaviour) and perception bias (animals visible in the survey transect but missed by observers due to imperfect detection). We consider the way this method corrects for availability bias (dugongs that are unavailable to observers because of environmental conditions) to be superior to previous methods (Marsh and Sinclair 1989a and Pollock et al. 2006) for correcting availability bias because it makes fewer assumptions. The additional data required to implement the Hagihara method was also collected for the 2005 and 2016 surveys of the CGBR (survey Blocks N11-N13) and the 2006 and 2013 surveys of the NGBR (Survey Blocks N2-N15), and these results are included here for comparative purposes where available and relevant.

To estimate the perception bias for each aerial survey team, a mark-recapture model was used to calculate the proportion of the 'available' dugongs that were counted during each survey segment (see Marsh and Sinclair 1989a; Pollock et al. 2006). We calculated perception biases separately for each team in November 2018, June 2019, and November/December 2019 (Table 5). We used the data collected by each team with one exception: the number of animals sighted in Blocks N12 and N15 by Team 2 in November 2018 was too low for a precise estimate of perception bias. Consequently, we combined these data with the data collected by Team 4 in an overlapping region at the same time of year in 2019. Following the Hagihara method, the standard error for the population estimate for each block were simulated using the program Python using 5000 iterations. The NGBR

analyses assumed that there was no directional movement of animals between the three 2018-2019 survey periods.

2.3.2 Turtle population estimates

Population estimates for all large juvenile and adult in-water marine turtles (not identified to species) were calculated using the method developed by Fuentes et al. (2015), henceforth the Fuentes method. This methodology uses the same principles as the Pollock et al. (2006) method, but considers green turtle diving behaviour when calculating the availability bias correction factor, which is not depth-corrected.

The population estimates for turtles were unexpectedly large. We explored possible reasons for this result in Appendix 5. Ultimately, modified Fuentes method models were used to generate the population estimates used in the body of this report considering groups of >9 turtles as censused 'herds' (as for dugongs). However, each of the figures generated for sightings of large juvenile and adult marine turtles include all of the sightings (including groups) from each transect (see Appendix Figures 14.1-14.5), and the corrected sightings of groups >9 were also used in the spatial models as per the Fuentes method without modification (see Section 2.4 below).

We calculated perception biases for each team as outlined in Table 8. Standard errors were simulated using the program Python and 5000 iterations. The NGBR analyses assumed that there was no directional movement of animals between the three 2018-2019 survey periods.

2.3.3 Percentage calves - an index of fecundity and neonatal mortality

The overall percentage of calves for the Blocks N2-15 was compared with the historical percentages for the NGBR surveys using Chi-square analyses.

2.3.4 Dugong population trends

These analyses aimed to estimate the annual percent change in dugong population density, as well as a retrospective probability of a decline for the NGBR blocks surveyed in each of 2006, 2013, and 2018-2019 (i.e., Blocks N2-14). The NGBR analyses assumed that there was no directional movement of animals between the three 2018-2019 survey periods.

The data included auxiliary information about transect length, turbidity at sightings, water depth at sightings, and observer identities (i.e., for the different survey teams). Following the Hagihara method, the analyses used estimates of:
- availability biases (denoted $\underline{a_i}$, defined as the probability that a dugong is available for detection by observers, conditional on occupancy); and
- perception biases (denoted p_i, defined as the probability that the observers will sight a dugong, conditional on occupancy and being available for detection).

The availability bias and perception bias (imperfect detection) varied for each dugong sighting, based on local factors such as depth, turbidity, and the identity of the survey team. We used the maximum-likelihood estimates of a_i and p_i, and their standard-errors, to derive probability distributions. We then used Markov Chain Monte Carlo (MCMC) methodology to incorporate these uncertainties into the trend estimates by sampling from the probability distributions of estimates of a and p.

The corrections for availability bias and perception bias led to a distinction between the observed total counts per transect (N^{obs}), versus the 'adjusted total dugong counts' per transect, denoted N^{adj}. The observed number of dugongs per transect was assumed to be much lower than the adjusted counts, i.e., $N^{obs} << N^{adj}$, owning to the corruption by a_i and p_i.

For the purposes of estimating population trends, we focussed on modelling the adjusted counts, N^{adj}, as a log-linear trend over time in a hierarchical model. In order to estimate the adjusted counts from the observed counts, three estimators were developed and explored via simulation: the N-Mixture, the Horvitz-Thompson (HT), and the Hybrid (see Appendices 10 and 12 for more detail). The estimators differed from each other based on how they handled transects with zero-counts. In this report, we focus on estimates produced by the N-Mixture method because this model out-performed the HT and the Hybrid estimators at estimating trends, according to Mean Square Error criteria. The N-Mixture estimator also seemed to be a low-bias/high-variance estimator (see the simulations in Appendix 10 for more details).

Given the imputed values for the adjusted counts, N^{adj}, the trend analyses were a straight-forward application of a log-linear regression model with a Negative Binomial (NB) count distribution:

$$N^{\mathrm{adj}} \sim \mathrm{NB}(\exp\{\mu\}, \theta)$$
$$\mu = \beta_0 + \beta_t \cdot t + \log(\text{transect length})$$

where β_t, β_0, θ are, respectively, the trend parameter, the intercept, and the NB overdispersion parameter. The trend and intercept parameters were estimated per location (NGBR) while the overdispersion parameter was shared among locations along the Queensland coast (NGBR, Southern GBR, Hervey Bay and Moreton Bay based on survey results from those areas[1]).

In accordance with Bayesian inference, the above random variables were given prior distributions:

$$
\begin{aligned}
\pi(\beta_{0,\ell}) &= \mathcal{N}(\mu_{0,\ell}, \sigma_{0,\ell}^2) \\
\pi(\beta_{t,\ell}) &= \mathcal{N}(\mu_{t,\ell}, \sigma_{t,\ell}^2)[a_0, b_0] \\
\pi(\theta) &= \mathcal{U}(c_0, d_0)
\end{aligned}
\tag{1}
$$

where:

$$
\begin{aligned}
\ell &:= \text{location index;} \\
j &:= \text{transect index for } j \in \ell; \\
t &:= \text{time in years;} \\
\beta_{0,\ell} &:= \text{intercept;} \\
\beta_{t,\ell} &:= \text{per-annum trend;} \\
(\mu_{0,\ell}, \sigma_{0,\ell}) &= (0, 10) \text{ for all } \ell \\
(\mu_{t,\ell}, \sigma_{t,\ell}, a_0, b_0) &= (0.03, 0.075, -0.15, 0.07) \text{ for all } \ell \\
(c_0, d_0) &= (0.3, 20)
\end{aligned}
\tag{1}
$$

The prior on the trend parameters was motivated according to the following intuition: the prior placed approximately 55 per cent of its density in the region between -3 per cent and 3 per cent, with an upper cut-off at 7 per cent, and a lower cut-off at -15 per cent. This prior was sufficiently vague around 0, while striving for biologically reasonable upper- and lower-bounds on the intrinsic growth-rate of a large-bodied mammalian population.

The posterior distribution of the intercepts β_0, trend parameters (β_t) and overdispersion parameter

---

[1]   Work done for RimReP (see Marsh et al. 2019)

(l) were sampled via Markov-chain Monte Carlo, specifically, with a Slice Sampler (Neal 2003). The posteriors were as follows:

$$\pi(\beta_{0,l}|\boldsymbol{N}_l^{\mathrm{adj}},\beta_{t,l},\theta,\cdot) = \underbrace{\left(\prod_{j=1}^{J}\mathrm{NB}\big(N_j^{\mathrm{adj}}|\exp\{\beta_{0,\ell}+\beta_{t,\ell}\cdot t\}\cdot A_j,\theta\big)\right)}_{\text{NB likelihood of }N\text{ given }\beta_0\beta_t\theta}\underbrace{\mathcal{N}(\beta|\mu_{0,\ell},\sigma_{0,\ell}^2)}_{\text{Normal prior on }\beta_0}\ \ \text{for each } l$$

$$\pi(\beta_{t,l}|\boldsymbol{N}_l^{\mathrm{adj}},\beta_{0,l},\theta,\cdot) = \left(\prod_{j=1}^{J}\mathrm{NB}\big(N_j^{\mathrm{adj}}|\exp\{\beta_{0,\ell}+\beta_{t,\ell}\cdot t\}\cdot A_j,\theta\big)\right)\mathcal{N}(\beta|\mu_{0,t,\ell},\sigma_{t,\ell}^2)[a_0,b_0]\ \ \text{for each } l \quad (1)$$

$$\pi(\theta|\boldsymbol{N}_l^{\mathrm{adj}},\boldsymbol{\beta}_0,\theta,\cdot) = \left(\prod_{l}^{L}\prod_{j=1}^{J}\mathrm{NB}\big(N_j^{\mathrm{adj}}|\exp\{\eta_j\},\theta\big)\right)\mathcal{U}(\theta|c_0,d_0)$$

As explained above, the availability bias and detection probabilities (perception bias) for 'herds' (groups >9) were set to 1 (perfect detection and availability).

A detailed summary of the methods and simulation experiments are in Appendices 8 and 10, respectively.. Details about calculating availability bias and detection probabilities are in Appendix 9,a description of the simulations for comparing estimators' properties are in Appendix 10, details about vectorizing the N-mixture estimator are in Appendix 11, and additional trend estimates and plots are in Appendix 12.

Parallel analyses were not conducted for turtles because we consider that the historical data and correction factors for turtles are insufficiently robust for such analyses to yield reliable results.

2.4 Spatial modelling

We developed spatially-explicit models of dugong and marine turtle density and distribution using the method of Grech and Marsh (2007) and Grech et al. (2011) with the following improvements as per Sobtzick et al. (2017):

Input data:
   i.   Dugong counts corrected for perception and depth-specific availability probabilities as per the Hagihara method.
   ii.   Marine turtle counts corrected for perception and turtle dive-specific availability probabilities as per the Fuentes method.

The data were modelled using the geostatistical interpolation method *Empirical Bayesian Kriging* (EBK) in ArcGIS 10.7. EBK creates multiple simulations of the semivariogram by sequentially changing input parameters (e.g., model fitted) to find the best-fit parameters for the input data. The semivariogram type was linear and the smoothed search neighbourhood was set to a radius of 5000m. This corresponds with the home range of dugongs at Burrum Heads, Hervey Bay (Sheppard et al. 2006) and the approximate median home range of green turtles in the southern Great Barrier Reef (Shimada et al. 2016).

Relative densities were calculated at a grid size of 1 km^2 for both species. Dugong and turtle densities per grid cell were classified as Low (0 dugongs per km^2); Medium (0-0.5 dugongs per km^2); High (0.5-1 dugongs per km^2), and Very high (>1 dugongs per km^2). Grid cells with 0 dugongs and 0 turtles per km^2 were included: (1) to ensure that the spatial layers of dugong and turtle density extended across the entire survey area; (2) because dugongs and turtles are likely to move across grids where they were not detected during the surveys, and (3) because we have not attempted to estimate abundance for areas where dugongs and

turtles were not sighted (which is theoretically possible but very difficult; see Martin et al. 2014 and this report).

The spatially-explicit models were developed for individual survey years for which the required data were available and as composite of multiple survey years when deemed ecologically relevant (see Table 2).

Table 2. Data used to develop the spatially explicit models of dugong and marine turtle densities and distributions.

Taxon	Input data	Region	Survey year - Model
Dugong	Adjusted number of dugongs as per the Hagihara method	Blocks C11-13, N2-15	2018-2019
		Blocks N1-12	2006, 2013
		Blocks N2-12	2006, 2013, 2018-2019
Large in-water turtles not differentiated to species	Adjusted number of turtles as per the Fuentes method (unmodified)		2018-2019

3. RESULTS

3.1 Survey flight summary

The NGBR (-18º11.294' to -15º17.630') survey region (Figure 1) was surveyed from 5 until 8 November, 2018. Inclement weather caused us to terminate the survey with the agreement of GBRMPA before it could be completed. In June 2019, Block N5 was surveyed from 17 until 24 June, 2019. In November/December 2019, surveys were conducted from 9 November until 2 December, 2019, completing the coverage of the NGBR survey region (-14º 49.676' S to -10º 57.496' S). See Appendices 1 and 2 for details of the daily activities and survey flights for all teams. The sampling intensity of each survey block ranged from 3.8 per cent-24.1 per cent (generally comparable to or better than previous surveys of the same area) (Appendix Table 6.1).

3.2 Conditions

Weather conditions were comparable between November 2018, June 2019, and November 2019. In November 2018, the average wind speed was lower than the average wind speeds in June and November 2019. The average sea state was also lower in November 2018 than during the other survey periods. Overall glare (means of the modes) was highest during the June 2019 survey (Appendix Table 7.1).

3.3 Observations

The data included in this report are based on dugong and marine turtle sightings obtained when the survey team was on transect. Summaries of dugong and turtle sightings are included in Tables 3 and 4; the locations of each dugong, turtle and dolphin sighting is mapped in Appendices 13, 14 and 15 respectively.

3.3.1 Dugong sightings

In the November 2018 surveys of the Great Barrier Reef, 33 dugongs were sighted on transect in the CGBR (Blocks C11 and C13; Table 3, Appendix Figure 13.1). In the November 2018, June 2019 and November 2019 surveys, 428 dugongs were sighted on transect in the NGBR (Table 3, Appendix Figure 13.2-13.5).

Table 3. Number of dugongs and calves encountered, excluding herds, during the surveys conducted in November 2018, June 2019, and November/December 2019.

Region	# dugong sightings	# dugongs	# calves sighted	Group size (excluding groups $\geq$10)[3]		
				Mode	Mean	Range
Central GBR[1]	24	33	1	1	1.38	1–3
Northern GBR[2]	320	428	36	1	1.40	1–7

[1] Surveyed in November 2018
[2] Surveyed in November 2018, June 2019 and in November/December 2019
[3] For details of groups > 10 see footnotes to Table 7

3.3.2 Sightings of large juvenile and adult marine turtles

During the November 2018 surveys, 240 turtles were sighted on transect in the CGBR (Blocks C11 and C13; Table 4, Appendix Figures 14.1). During the June 2019 and November 2019 surveys, 3399 turtles were sighted on transect in the NGBR (Table 4, Appendix Figures 14.2-14.5).

Table 4. Number of turtle sightings, excluding groups of ≥10 turtles, during the surveys conducted in November 2018, June 2019, and November/December 2019. Details of the groups of > 9 turtles are in the footnotes to Table 10.

Region	# turtle sightings	# turtles	Group size (excluding groups $\geq$10)[3]		
			Mode	Mean	Range
Central GBR[1]	213	240	1	1.20	1–8
Northern GBR[2]	2122	3399	1	1.76	1–9

[1] Surveyed in November 2018
[2] Surveyed in November 2018, June 2019 and in November/December 2019
[3] For details of groups > 9 see footnotes to Table 10

3.3.3 Percentage of dugongs sighted classified as calves

One of the 33 dugongs seen in the 2018 survey of the three CGBR blocks was a calf (Table 3). These numbers are too small to draw any inferences. Thirty-six of the 428 dugongs sighted in the 14 NGBR blocks in 2018-2019 (8.17 per cent) were calves, 1-2 percentages higher than but not significantly different (Chi-square $_{2,1}$ = 3.17; p=0.21) from the percentages in 2006 (7.14 per cent) and 2013 (5.56 per cent). However, all these percentages are much lower than those for the five surveys between 1984-2000 inclusive, (Figure 2), which ranged between 11.58 per cent and 12.62 per cent and which were not significantly different from each other (Chi-square $_{4,1}$ = 0.33, p=0.99).
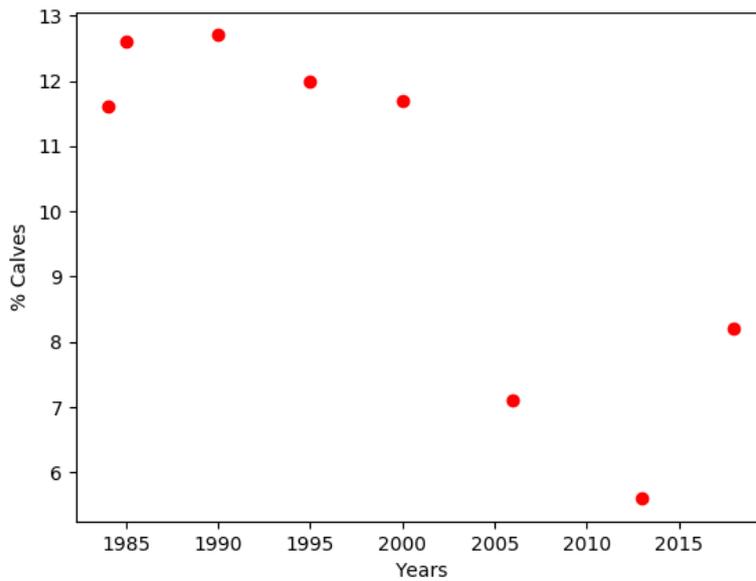
Figure 2. Percentage calves sighted in each of eight aerial surveys of the NGBR conducted from 1984 to 2018-2019.

3.4 Population estimates and trends

3.4.1 Dugong population estimates

The probability of observers sighting dugongs that were available for detection was high for all surveys. The perception probability estimates, based on the generalised Lincoln-Petersen models fitted using program MARK, suggest that the double-observer teams sighted 83–95 per cent of the dugongs that were available during all survey periods (Table 5).

Table 5. Details of models used to calculate the perception bias and the perception probabilities for dugongs for each survey. No model was calculated for the NGBR Team (Team 2) in November 2018 because there were too few dugong sightings to calculate a model for the blocks surveyed.

Month	Model[2]	Probability estimates (± se)[3]	Perception probability for each tandem team
November 2018 Team 1	All observers different	Port primary 0.63 (± 0.11) Port secondary 0.80 (± 0.10) Starboard primary 0.70 (± 0.14) Starboard secondary 0.44 (± 0.12)	Port 0.93 Starboard 0.83
June 2019[1] Team 3	Sides the same as each other	Both port 0.77 (± 0.044) Both starboard 0.65 (± 0.05)	Port 0.95 Starboard 0.88
November/December 2019[1] Team 4	All observers same	All observers 0.75 (± 0.022)	Port 0.94 Starboard 0.94

[1] The observing teams in June and November/December 2019 differed by a single person each time. For the makeup of each team see Table 1 footnotes and Appendix 3.
[2] These models are generalised Lincoln-Petersen models of best fit according to Akaike's Information Criterion (AIC) using the MARK program (White and Burnham 1999), where the perception probability was either the same for all observers, varied according to experience (primary or secondary observers), varied according to side of the aircraft (port or starboard), or was different for every observer
[3] Probability estimate provided by the model

3.4.1.1 Dugongs in the CGBR

The estimated number of dugongs on the CGBR blocks (C11-C13) totalled ~550 $\pm$ SE 250 animals (Table 6). Most (~80 per cent) were in Block C11 just north of Hinchinbrook Island (Appendix Figure 13.1). The number of dugongs sighted in Block C12 (Dunk Island to Port Douglas) was too small to calculate a population estimate. A small population (~100 $\pm$ SE 90) was detected between Port Douglas and Cape Bedford. Thus, there is a large gap between the critical dugong habitats in the Hinchinbrook Island area (-18° S) and the coastal waters north of -15°S. Because most of the C11-13 region was not surveyed in 2005 or 2013 using the standard transect technique, it is inappropriate to make temporal comparisons.

Table 6. Relative abundance of dugongs in November 2018 compared with the corresponding results of the 2005 survey of the same area. All the estimates have been calculated using the optimised survey design developed by Marsh et al. (2019) and the Hagihara method. No herd of dugongs was sighted. The standard errors of each estimate are in brackets.

Block	2005	2018-2019
C11	107 (85)	422 (212)
C12	nc[1]	tfs[2]
C13	ns[3]	114 (91)
Total		**536 (231)**
CV[4]		**0.43**

[1] survey design not comparable
[2] too few seen to estimate population size
[3] not surveyed
[4] Coeffcient of Variation

3.4.1.2 Dugongs in the NGBR

The estimated number of dugongs in the NBGR Blocks N2 through N15 totalled ~7000 $\pm$ SE 1600 animals (Figure 3 and Table 7). As in 2006 and 2015, the highest estimate (~2100 $\pm$ SE 1200) was for Block N5 (Princess Charlotte Bay), the largest block. Blocks N3-4 between Lookout Point (north of Cape Flattery ~15 °S) and Cape Melville (`14.2 °S) supported an estimated ~3800 dugongs, more than half of the animals in the NGBR survey region. Thus, the region between ~15 °S and ~14 °S (Blocks N2-5) supported ~85 per cent of the dugongs in the NGBR survey region, compared with ~77 per cent in 2006 and ~73 per cent in 2013. As in 2006 and 2013, the only large herds of dugongs sighted in 2019 were in this region.
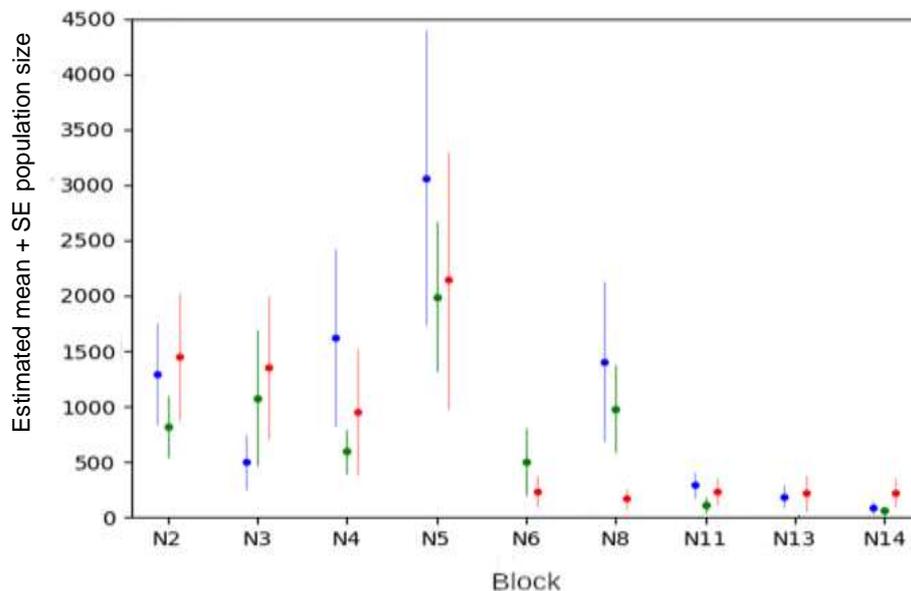
Figure 3. Estimated size of the population of dugongs based on the animals sighted during aerial surveys of the NGBR (Blocks N2-N15 in 2006 (blue), 2013 (green) and 2018-2019 (red). The number of dugongs sighted was too few to estimate population size in Block N6 (2006), Blocks N7, N9 and N10 (all years) and Block N15 in 2018 (the only year in which this block was surveyed using the standard transect technique).

As in the 2006 and 2013 surveys, in 2019 dugongs were sighted in most of the north-facing bays between north of Princess Charlotte Bay and Shelburne Bay inclusive (Blocks N6, N8, N11, N14; Appendix Figures 13.2-13.5). The relative importance of these bays for dugongs varied between surveys (Table 7). Relatively few dugongs were sighted in Lloyd Bay (Block N8) in 2019 compared with 2006 or 2016. Too few dugongs were sighted north of Shelburne Bay (Blocks N12, N15) to calculate a population estimate, indicating another stretch of coast (-11° 45'S to -11° S) that supports low dugong densities between dugong habitats north and south. The only offshore area north of Princess Charlotte Bay where sufficient dugongs were sighted to calculate a population estimate was Block N13, a large block offshore from the Cape Grenville-Shelburne Bay region.

Table 7. Relative abundance (standard errors) of dugongs in the NGBR blocks in November 2018 (Blocks N12 and N15), June 2019 (Block N5) and November/December 2019 (Blocks N2, N3, N4, N6, N7, N8, N9, N10, N11, N13, N14) compared with the corresponding results of the 2006 and 2013 surveys of the same areas. All the estimates have been calculated using the optimised survey design developed by Marsh et al. (2019) and the Hagihara method. The estimates that include herds of dugongs are in bold.

Block	2006	2013	2018-2019
N1	tfs[1]	tfs[1]	ns[2]
N2	**1293 (466)**[5]	**820 (278)**[6]	**1453** (569)[7]
N3	498 (249)	1077 (612)	**1353** (642)[8]
N4	**1619 (802)**[9]	597 (200)	**952** (569)[10]
N5	3061 (1333)	1990 (675)	**2144** (1162)[11]
N6	tfs[1]	504 (306)	231 (148)
N7	tfs[1]	tfs[1]	nds[3]
N8	1407 (725)	979 (394)	167 (88)
N9	tfs[1]	tfs[1]	tfs[1]
N10	tfs[1]	tfs[1]	tfs[1]
N11	293 (116)	108 (71)	235 (121)
N12	tfs[1]	tfs[1]	tfs[1]
N13	189 (105)	nds[3]	216 (165)
N14	89 (57)	58 (40)	219 (134)
N15	nc[4]	nc[4]	tfs[1]
Total	**8449 (1803)**	**6133 (1097)**	**6970 (1581)**
CV	**0.21**	**0.18**	**0.23**

[1] too few sighted to calculate a population estimate
[2] not surveyed
[3] no dugongs sighted
[4] not surveyed using a comparable method
[4] not comparable zig zag transects only and too few dugongs sighted to calculate a population estimate (none in 2013)

[5] Includes herds of 20, 20, 15, 27, 10 dugongs
[6] Includes one herd of 49 dugongs
[7] Includes one herd of 20
[8] Includes one herd of 20
[9] Includes one herd of 10 dugongs
[10] Includes two herds of 12 and 20 dugongs
[11] Includes one herd of 22 dugongs

3.4.2 Turtle population estimates

The probability of observers sighting adult and large juvenile turtles that were available for detection was high during all surveys. The perception probability estimates, based on the generalised Lincoln-Petersen models fitted using program MARK, suggest that the double-

observer teams sighted 78–92 per cent of the adult and large juvenile turtles of all species that were available during all survey periods (Table 8).

Table 8. Details of models used to calculate the perception bias and the resultant perception probabilities for large juvenile and adult turtles for each survey.

Survey period	Model[2, 3]	Probability estimates (± se)[4]	Perception probability for each tandem team
November 2018 Team 1	All observers different	Port primary 0.59 (± 0.04) Port secondary 0.61 (± 0.04) Starboard primary 0.63 (± 0.05) Starboard secondary 0.41 (± 0.04)	Port 0.84 Starboard 0.78
November 2018 Team 2	All observers the same	All observers 0.69 (± 0.01)	Port 0.90 Starboard 0.90
June 2019[1] Team 3	All observers different	Port primary 0.72 (± 0.03) Port secondary 0.70 (± 0.03) Starboard primary 0.45 (± 0.02) Starboard secondary 0.81 (± 0.03)	Port 0.92 Starboard 0.89
November/December 2019[1] Team 4	All observers the same	All observers 0.70 (± 0.01)	Port 0.91 Starboard 0.91

[1] The observing teams in June and November differed by a single person each time. For the makeup of each team see and footnotes of Table 1 and Appendix 3
[2] These models are generalised Lincoln-Petersen models of best fit according to Akaike's Information Criterion using the MARK program (White and Burnham 1999), where the perception probability was either the same for all observers, varied according to experience (primary or secondary observers), varied according to side of the aircraft (port or starboard), or was different for every observer. For these models, all groups of turtles ≥ 10 turtles were removed from the sightings to generate the model
[3] Turtle sightings for the November 2018 NGBR Team were combined with sightings from the November/December 2019 survey team to generate a more robust model
[4] Probability estimates provided by the model

3.4.2.1 Turtles in the CGBR

Large in-water juvenile and adult turtles were sighted in all CGBR survey blocks (C11 through C13) in numbers sufficient to estimate their abundance in the 2018 surveys (Table 9). The estimates for the survey region totalled ~32000 $\pm$ SE 7100 animals, compared with ~9600 $\pm$ SE 4500 for Blocks C11 and C12 only in 2013. The estimates for both Blocks C11 and C12 were higher in 2018 than in 2013.

Table 9. Relative abundance ($\pm$ standard errors) of in-water adult and large juvenile turtles (not identified to species) in the CGBR survey blocks from the November 2018 aerial surveys based on the modified Fuentes method (see Methods).

Block	2006	2018-2019
C11	2361 (1252)	5218 (715)
C12	7227 (4325)	11212 (4812)[1]
C13	nc[2]	15821 (95210)[3]
Total	**9558 (4503)**	**32281 (7128)**
CV	**0.47**	**0.22**

[1] Includes group of 20
[2] not surveyed using a comparable method

[3] Includes groups of: 35, 20, 20, 15, 15, 12, 10

3.4.2.1 Turtles in the NGBR

Large in-water juvenile and adult turtles were sighted in all NGBR survey blocks (N2 through N15) in numbers sufficient to estimate their abundance in 2018-2019 surveys (Figure 4). The combined estimates for the survey region totalled ~282000 $\pm$ SE 28000 animals (Table 10), more than twice the 2013 estimate. The estimates were higher in 2018-2019 for all survey blocks apart from N8 (Lloyd Bay). The greatest difference was for the offshore block closest to Raine Island (Block N13), which supported an estimated 28 per cent of the animals in the NGBR survey region in 2019 compared with 14 per cent in 2013. Possible explanations for the much higher estimates in 2018-2019 than in 2013 are explored in Appendix 5.

Blocks N3-4 between Lookout Point (north of Cape Flattery ~15 °S) and Cape Melville (14.2 °S) supported an estimated ~84000 turtles, about 30 per cent of the animals in the NGBR survey region compared with 19 per cent in 2013. The region between ~15°S and ~14°S (Blocks N2-5) supported ~44 per cent of the large in-water juvenile and adult turtles in the NGBR survey region, compared with 50 per cent in 2013. Block N13, the offshore block closest to the key Grean Island nesting habitats of Raine Island and Moulter Cay supported 28 per cent of the large in-water turtles in 2019 compared with 14 per cent in 2013.
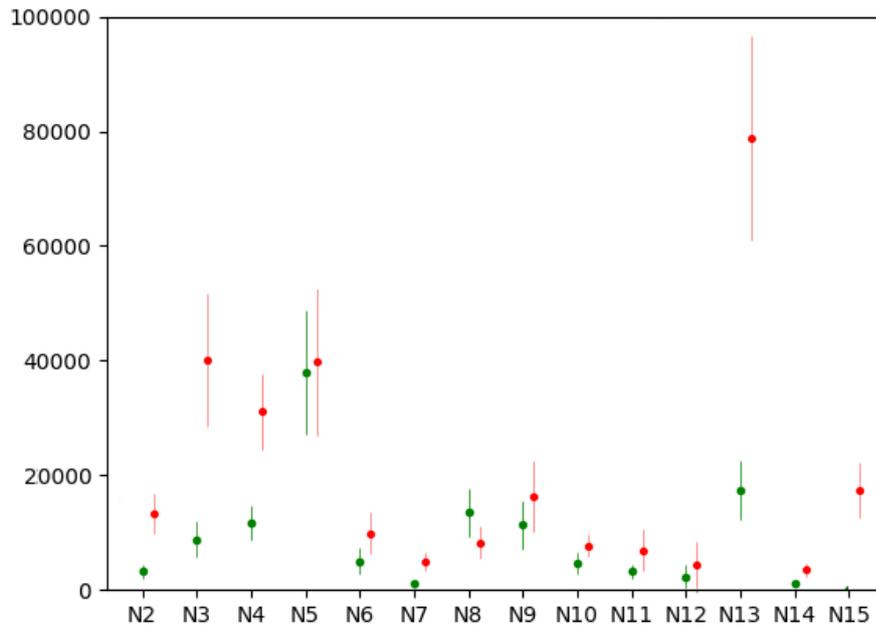
Figure 4. Estimated size of the population of large juvenile and adult turtles (not identified to species) based on the animals sighted during aerial surveys of the NGBR (Blocks N2 to N15 in 2013 (green) and 2018-2019 (red). Block N15 was not surveyed in 2013.

Table 10. Relative abundance (± standard errors) of in-water adult and large juvenile turtles (not identified to species) in the NGBR survey blocks from the June 2019 and November/December 2019 aerial surveys based on the modified Fuentes method.

Block	2013	2018-2019
N1	1709 (1109)	ns
N2	3192 (1237)	13286 (3546)[1]
N3	8804 (3068)	40031 (11667)[2]
N4	11718 (2964)	31101 (6609)[3]
N5	37998 (10820)	39719 (12745)[4]
N6	5056 (2346)	9886 (3600)[5]
N7	1030 (678)	4886 (1594)[6]
N8	13512 (4194)	8281 (2851)
N9	11327 (4148)	16286 (6326)
N10	4617 (1827)	7752 (2009)
N11	3180 (1222)	6897 (3703)
N12	2312 (1989)	4464 (4049)
N13	17344 (5084)	78749 (17931)
N14	1029 (565)	3455 (1135)
N15	nc[7]	17428 (4815)
Total	**122828 (14620)**	**282221 (28259)**
CV	**0.119**	**0.100**

[1] Includes groups of 15, 17, 10
[2] Includes groups of 15, 10, 15, 15, 13, 13, 12, 11, 10
[3] Includes group of 10
[4] Includes group of 10
[5] Includes group of 16
[6] Includes groups of 22,24
[7] not surveyed using a comparable method

3.4.3 Estimates of the trend in the dugong density (2005 to 2018-19)

Figure 5 shows the posterior mean trend-line and per-year densities for the NGBR region (Block N2 through Block N14) using the N-Mixture model. The NGBR trend was upward and positive yielding a 0.5 per cent per year increase (95 per cent CI -3.08 to +4.128). Likewise, the average population-density in 2019 was noticeably higher than 2013 (but still strongly overlapping according to credibility intervals). Overall, it seems that the NGBR is quite stable in terms of both the average trend line and the inter-annual variation (see Figure 5).
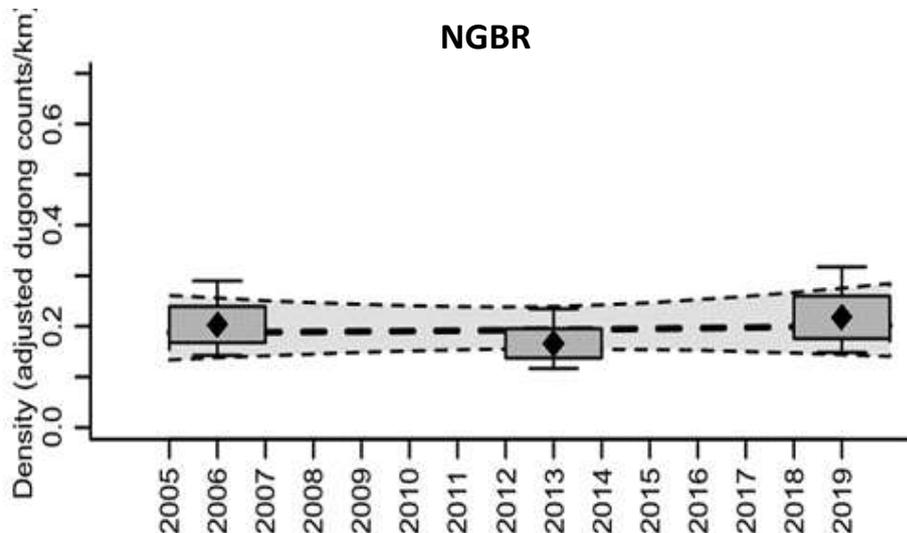
Figure 5. Estimated trend-line (± 95 per cent CI) and per-survey densities (box-plots) for the NGBR (2006 to 2018-2019) according to the N-Mixture estimator.

The Bayesian framework also allowed us to calculate the retrospective probability of decline or *p(decline)*. Some practitioners prefer this statistic to frequentist p-values, which are often confused as evidence in favour of a trend.[2] The *p(decline)* was 0.4 suggesting that there is not a lot of evidence that the population was in a sustained decline over the study period.

3.5 Spatially-explicit models of dugong and marine turtle distribution and density

3.5.1 CGBR 2018-2019: dugongs and turtles

The spatially-explicit models of dugong and turtle distribution and density, developed using the results of the November 2018 survey of the northern end of the SGBR dugong survey region (Figure 6), indicated that dugongs were sighted at very low densities throughout 90 per cent of the region between the northern end of Hinchinbrook Island and Cape Bedford. Dugong densities were higher in the area immediately north of Hinchinbrook Island and some of the reefs from the Cape Tribulation region north. In contrast, turtles were sighted at medium densities over 45 per cent of the region particularly on the top of reefs and at high and very high densities on some outer reefs, especially just south of Cape Tribulation and between Cape Tribulation and Cooktown.

---

[2] A Fisherian p-value is considered evidence of whether a trend parameter is different from zero, and offers support in favour of rejecting the hypothesis that there was no trend. This statistic requires a trend to have a very high magnitude and/or low certainty to meet the 0.05 conventional burden of proof. In contrast, the Bayesian p-value provides direct inference on the trend: what is the probability that it was negative and/or what was the probability that it was positive?
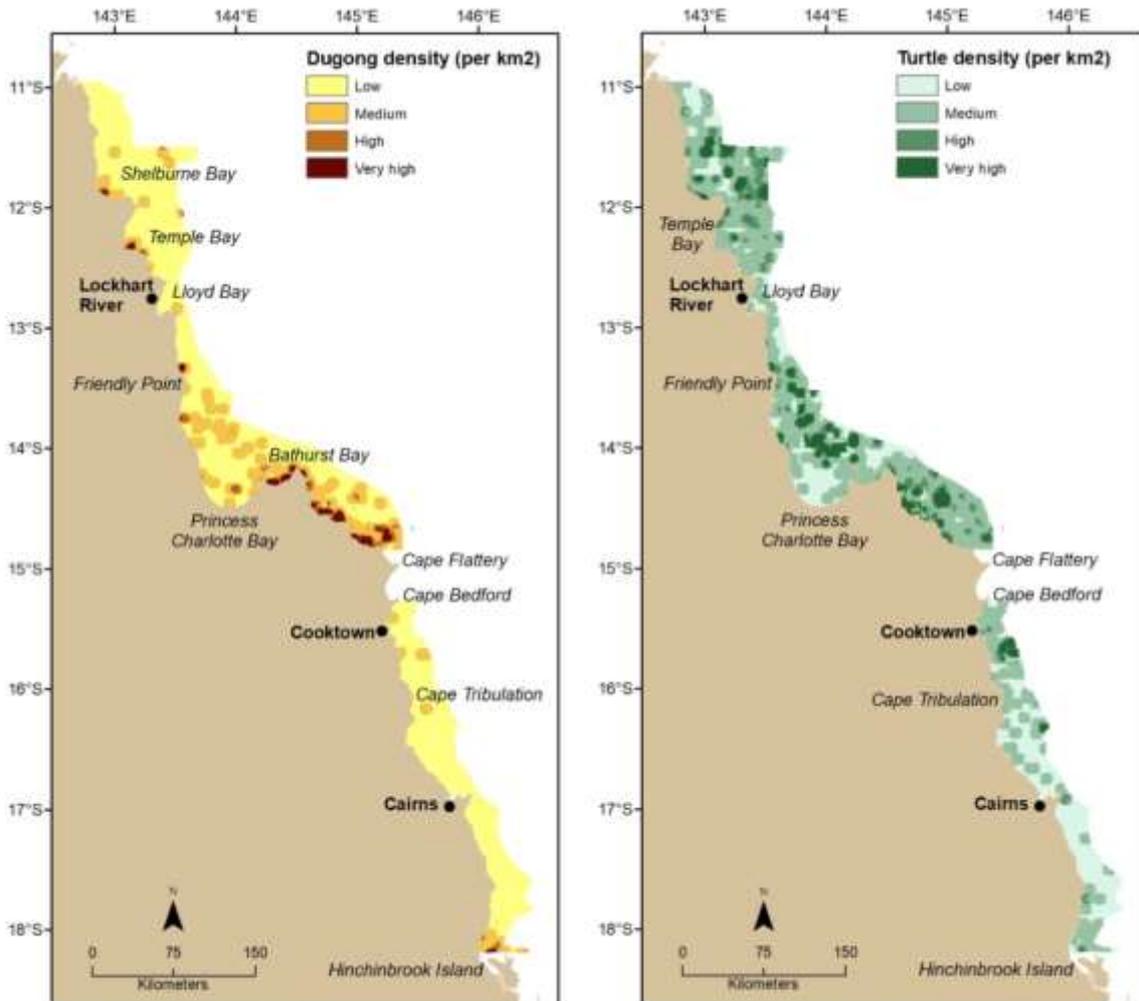
Figure 6. Maps of the relative densities of dugongs and turtles from the spatially-explicit models developed from data collected during the 2018 survey of the region between Hinchinbrook Island and Cape Bedford south and the 2018-2019 surveys between Lookout Point (just north of Cape Flattery) to near the tip of Cape York.

3.5.2 NGBR 2018-2019: dugongs and turtles

The spatially-explicit models developed from data collected during the 2018-2019 surveys indicated that dugongs were sighted at high and very high densities throughout much of the inshore region between Lookout Point (just north of Cape Flattery) and Bathurst Head at the western end of Bathurst Bay (Figure 6), and in local regions of some of the bays between Friendly Point and Shelbourne Bay inclusive. Dugongs were also seen at medium densities in some bays and associated with many reefs in the NGBR survey region. In contrast, turtles were sighted at medium densities throughout ~60 per cent of the region and at high and very high densities over ~25 per cent of the region, particularly on the top of many reefs including the offshore reefs in Princess Charlotte Bay and in some inshore and offshore waters especially in the region between Lookout Point and Cape Melville and Temple and Shelburne Bays.

3.5.3 NGBR 2006 through 2018-2019: dugongs
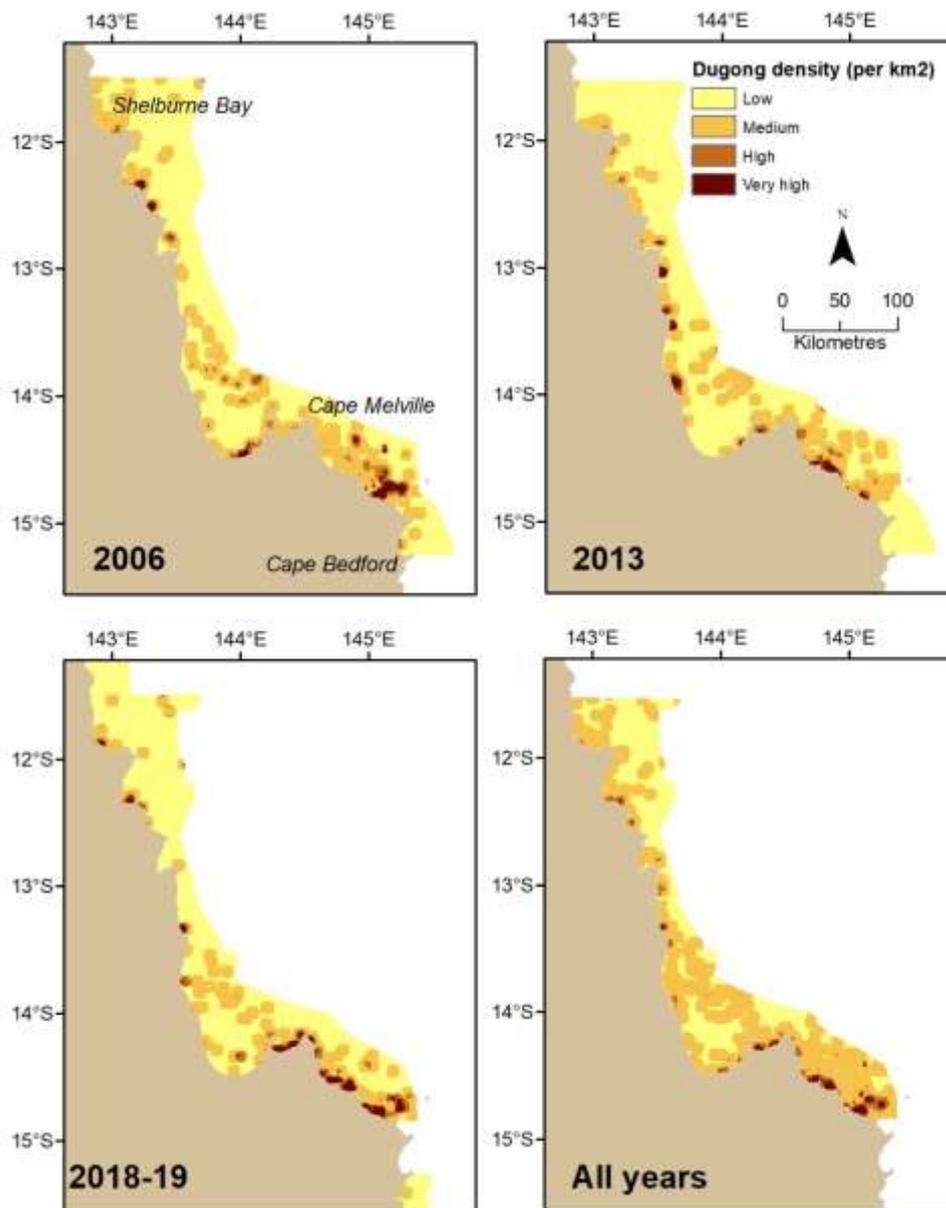
Figure 7. Maps of the relative densities of dugongs from the spatially-explicit models developed from data collected during the 2006, 2013 and 2018-2019 surveys of the region between Cape Bedford (just north of Cooktown) to near the top of Cape York, and for all years combined. The northern and southern boundaries of the survey region differed between years. The composite map (all years) is of the region common to all surveys.

Very High and High densities of dugongs were consistently sighted in the inshore waters between Lookout Point and Cape Melville and in various bays between Cape Melville and Shelburne Bay (Figure 7). Dugongs were also consistently sighted at medium densities in the offshore waters of the GBR lagoon between Lookout Point and Cape Melville and associated with mid-shelf reefs throughout this region (Figure 7).

4. DISCUSSION

4.1 Status of dugongs and large in-water juvenile and adult turtles in the survey areas

Our 2018-2019 aerial surveys confirm that the inshore GBRWHA between -18°S and -10°S continues to support globally significant populations of dugongs and marine turtles, both of which are identified components of the region's World Heritage outstanding universal values.

The standardised relative abundance estimates for dugongs between just north of Hinchinbrook Island and Cape Bedford was ~550 $\pm$ SE 250 dugongs. We cannot estimate population trends for this region because most of it was not surveyed in 2005 or 2016 using the standard technique. The 2018 survey confirmed that a large low-density region occurs between the critical dugong habitats in the Hinchinbrook Island area (-18° S) and the coastal waters of the GBRWHA north to -15°S (Figure 6).

The estimated number of dugongs in the NBGR Blocks N2 through N15 totalled an estimated ~7000 $\pm$ SE 1600 animals. The region between ~15°S and ~14°S supported ~85 per cent of the dugongs in the NGBR survey region and the only large herds sighted in 2019. Relatively few dugongs were sighted in Lloyd Bay (Block N8) in 2109 compared with 2006 or 2013. There were several blocks where too few dugongs were sighted to estimate abundance, including the stretch of coast north of Shelbourne Bay between -11° 45'S to -11° S and all the offshore blocks north of Princess Charlotte Bay other than Block N13.

The N-mixture Bayesian modelling suggests that the NGBR dugong population has been stable since 2006. This analysis assumes that there was no net movement between the regions surveyed in November 2018, June 2019 and November/December 2019. We consider that this assumption is likely to be robust given: (1) the extensive stretch of low-density dugong habitat between the Central GBR area surveyed in November 2018 and the area from Lookout Point to Cape Melville surveyed in November 2019; (2) the low number of dugongs sighted in the blocks at the northern end of the survey regions (Blocks N12 and N15) surveyed in November 2018; and (3) the overall temporal consistency in the pattern of dugongs sighted in Princess Charlotte Bay (surveyed in June 2019) and the areas to the north and south (surveyed in November 2019; see Figure 3), apart from the concerns about Block N8 (see Section 4.3.1 below).

We estimate that the CGBR survey region supported some ~32000 $\pm$ SE 7100 large juvenile and adult in-water turtles; the NGBR survey region ~282000 $\pm$ SE 28000. These NGBR numbers were much larger than in 2013, the only other year for which such data have currently been processed. The reason for this discrepancy is not known. Sufficient turtles were sighted for a population estimate to be calculated for every survey block (Table 9 and 10) indicating that they are widely distributed, especially in inshore waters and on reef tops (Figure 6).

4.2 Neonatal mortality and fecundity of dugongs

As pointed out by Marsh et al. (2019) as part of the RIMReP process, environmental and climatic drivers influence key demographic parameters of the dugong. Extreme weather events (e.g., cyclones and flooding) have been associated with the following impacts on dugongs: mass stranding, increased movements presumably in search of food, loss of weight and fat, delayed reproduction and mortality (see Marsh et al. 2011 and Meager and Limpus 2014 for details). As explained by Fuentes et al. (2016), the proportion of dependant calves sighted during an aerial survey (i.e., calf production) is a reflection of: (1) births (which are expected to reflect the effect on female fecundity of environmental conditions over the previous several years); and (2) neonatal survivorship (which can be affected by the more

immediate effect of an extreme weather event on the mortality of both mothers and calves, as a result of mass stranding associated with a storm surge as well as starvation due to loss of seagrass beds. Marsh et al. (2019) recommended that percentage calves be one of the indices of the health status of the dugong monitored in the GBRWHA. Using a different survey team and data review protocols, Dunshea et al. (2020) have documented observer errors associated with recording calves in manned dugong surveys. We consider that our strict operational procedures overcome most of this problem, the solution of which should be further improved by the use of Unmanned Aerial Vehicles (see below).

Fuentes et al. (2016) investigated how the proportions of dugong calves recorded during the JCU time series of dugong aerial surveys were associated with various sub-regional and ocean-basin climatic covariates at a range of spatially distinct subregions along the east coast of Queensland, including the NGBR. The relationships between the proportion of dependent calves and the climatic drivers varied spatially and temporally, with climatic drivers influencing calf counts at sub-regional scales. In the NGBR, the proportion of calves declined in association with the increase in indices of the El Niño phenomenon: both the Southern Oscillation Index (lagged to four years) and Niño 3.4 (lagged to one year).

In the NGBR, the proportion of dugong calves was significantly higher prior to 2000 than subsequently (Figure 2). The 2018-2019 result was slightly higher than but not significantly different from the results for 2006 and 2013, suggesting habitat loss. However, the data on the status of seagrass in the NGBR are not adequate to further evaluate this inference as explained in Section 4.4.5

4.3 Population sizes and distributions of dugongs and large in-water turtles
4.3.1 Dugongs

As pointed out above, the spatial pattern of dugong relative population size has been relatively stable across the NGBR survey blocks for the last three surveys (2006, 2013, 2018-2019, see Figure 3). From the perspective of the 2018-2019 survey, the low number of dugongs (seen in Lloyd Bay, N8) adjacent to Lockhart River Aboriginal community in November 2019 was the most obvious anomaly. A tropical low (later Cyclone Penny) in late December 2018 was followed by Tropical Cyclone Trevor, which crossed the coast just south of Lockhart River in March 2019 as a severe Category 3 cyclone (Bureau of Meteorology Bureau Home>National Weather Services>Tropical Cyclone Knowledge Centre>Past tropical cyclones>Tropical cyclone reports). Destructive winds from Tropical Cyclone Trevor battered the Lockhart River township for four hours with peak gusts recorded up to 137 km/h. Thus, habitat loss is a plausible explanation for the low numbers of dugongs (and turtles, see Figure 4) seen in Lloyd Bay in November 2019. Nonetheless, the seagrass monitoring at two sites in Lloyd Bay did not record any decrease from 2017 to October 2019 (McKenzie et al. 2020 and unpublished). However, there was no monitoring of intertidal seagrass in Lloyd Bay in 2018. Seagrass monitoring has been conducted at only two sites in other years and is not representative of the entire bay. Thus, the cause of the low numbers of animals sighted in Lloyd Bay in November 2019 is unknown.

4.3.2 Turtles

With the exception of Block N8 (see above, Tables 9 and 10, and Figure 4), the turtle population estimates were higher for all blocks for which comparative data are available in the CGBR in 2018 and the NGBR in 2018 and 2019. We explored possible explanations for these observations in Appendix 5, to see whether the between survey differences could have been due to uncorrected differences in availability bias between surveys, but we did not find a satisfactory explanation for the differences.

We noted that:

- The differences between 2013 and 2018-2019 were less for the segments of the survey conducted in November 2018 and June 2019 than in November/December 2019.

- The Northern GBR green turtle stock nests in the Austral summer and thousands of turtles come to the area to breed at Raine Island and Moulter Cay (Commonwealth of Australia 2017).

- The largest difference was between the estimates for Block N13, the offshore block closest to the major green turtle rookeries at Raine Island and Moulter Cay (Commonwealth of Australia 2017).

- The difference between 2013 and 2019 was not easily explained by inter-annual differences in the size of the green turtle nesting population at Raine Island because both were the highest green turtle nesting seasons in the last 10 years (Andy Dunstan pers. comm. to Marsh 2019).

We conclude that dugong aerial surveys are more appropriate for spatial modeling and risk assessment than for tracking trends in turtle numbers *per se* and have not attempted to do the latter in this report.

4.4 Future monitoring of dugongs and large in-water turtles in the GBRWHA

4.4.1 Boundary between the SGBR and NGBR survey regions

Recent genetic research indicates that the putative stock boundary for dugongs on the east coast of Queensland is in the vicinity of Midge Point (-20.6°S; 148.7°E; McGowan et al. in review). This discovery suggests that the latitude of the division between the northern and southern surveys should be reviewed to better reflect the underlying genetic structure of the dugong populations in the region. The stock structure suggests that the boundary should be around Midge Point.

As our surveys do not identify marine turtles to species, we do not consider that it is as relevant to consider marine turtle stock structure in the design of subsequent surveys.

4.4.2 Transect placement and length

As part of the RIMReP process, Marsh et al. (2019) optimised the design of dugong aerial surveys from Torres Strait through to Moreton Bay in accordance with the principles of adaptive monitoring. All available dugong sighting data were plotted in ArcGIS. Survey intensities in individual blocks were adjusted based on the distribution of the sightings. Survey intensities were reduced in the areas where there were few or no historical dugong sightings and increased in areas with numerous historical dugong sightings. The offshore ends of individual transects were truncated if no dugongs had ever been observed in the offshore area. Aerial survey block sizes were then adjusted to reflect the new survey design. The surveys covered by this report successfully used this survey design demonstrating that it is appropriate for future monitoring of dugongs in these regions.

4.4.3 Survey frequency

Also as part of the RIMReP process, Rankin (2018) in Marsh et al. (2019) conducted prospective power analysis to estimate annual trends using hypothetical datasets under different scenarios, and the Negative Binomial distribution fitted during his accompanying retrospective analyses. Rankin aimed to assess the ability of the large-scale aerial surveys to detect future declines under a variety of simulated sampling regimes, including declines of -1 per cent and-3 per cent per year. The prospective analysis suggested that a -3 per cent decline could be detected with 0.8 probability at intermediate time-horizons (eight years and greater), but that shorter time-scales and more frequent surveys are unlikely to provide the requisite power to detect trends. Marsh et al. (2019) suggested that the five-year survey frequency be strictly maintained for the dugong aerial surveys and that these surveys be taken as one of several lines of evidence used to determine important trends in dugong abundance in the GBRWHA. They provided this advice because of the limited improvement in power achieved by increasing the survey frequency, the statutory five-year reporting period required by the *Great Barrier Reef Marine Park Act 1975* for the Outlook Report, and the requirements of the Reef 2050 Plan (Commonwealth of Australia 2018). We see no reason to change this advice on the basis of the surveys reported here.

4.4.4 Survey platform

Completing this survey was a logistical challenge due to the weather, exacerbated by the few places where AVGAS and accommodation are available north of Cooktown. In addition, the risks associated with surveying from light aircraft were confirmed by the tragic death of our main pilot, Geoff Burry, in an unrelated light aircraft accident some two weeks after the survey ended.

Unmanned Aerial Vehicles (UAVs) offer an attractive 'human-risk free' alternative to using light aircraft to survey dugongs and large juvenile and adult marine turtles. As detailed in Hodgson (2018) in Marsh et al. (2019), the large ScanEagle UAV has sufficient endurance and range to cover the scale of the areas recommended for monitoring dugongs in the NGBR using the optimised design. This approach would significantly reduce the human safety risks associated with manned aircraft.

The optimised survey design could be achieved by using 'hub and spoke' operations whereby repeaters are able to extend the range of the ScanEagle (which we understand would have to be hired from Boeing) by handing off to a nearby communications link. The challenge would be to optimise the placement of the communications links, especially along the remote coasts of Cape York where land access is limited.

One potential logistical limitation in using the ScanEagle is that this system flies at half the ground speed of a manned aircraft, and therefore a survey could take twice as long. However, the ScanEagle has endurance sufficient to fly continually for a whole survey day, as opposed to a manned aircraft with six people-on-board where the maximum flight time is three hours before refuelling. The two-camera imaging system tested in the most recent trial survey of the ScanEagle allows for the same survey design and sampling rate as manned dugong surveys (Amanda Hodgson et al. in prep). Customised dugong detection and mapping software has been developed (with ongoing improvements) so it is realistic to survey large areas and process images in a cost-effective and expedient timeframe, although some manual review of images is currently still necessary. Software to detect large in-water turtles and some seagrass beds is under development.

Preliminary results suggest that sighting rates in UAV images are not affected by sea state and therefore UAV surveys could potentially be flown in a wider range of wind conditions than the manned surveys. This result needs to be examined further as it makes the untested assumption that dugong diving behaviour is unaffected by sea state. The manned aerial surveys overcome this assumption by limiting the sea states in which the surveys are conducted. Both the flight endurance and ability to survey in a wider range of conditions than manned surveys may counteract the effect of slow flight speed of the ScanEagle. However, the logistics of using large UAVs off Cape York need to be investigated and costed in a desktop study preferably well before the next scheduled survey is contemplated, especially as the light aircraft suitable for dugong surveys are becoming less available. The next scheduled survey is the 2022 survey of the SGBR.

Trial surveys suggest that the availability of dugongs is comparable between manned and unmanned aerial platforms, and that it is feasible and appropriate to apply the availability corrections developed for manned surveys to unmanned surveys under the same wind conditions (i.e., Beaufort sea states of ≤ 3). However as pointed out by Hodgson (2018) in Marsh et al. (2019), there are three outstanding matters to resolve before UAV surveys can replace manned dugong surveys in the GBRWHA. These matters are discussed in detail by Hodgson (2018) in Marsh et al., (2019) but are also outlined here:

1. Detection in highly turbid waters and high sea states. The trial surveys conducted to date have been in Shark Bay, Western Australia, where the water is relatively clear – there is very little of the turbid water characteristic of most dugong habitats within the GBRWHA. To ensure that future dugong UAV surveys are directly comparable with historic manned surveys, similar trial surveys need to be conducted in more turbid dugong habitat. Ideally, such surveys would also incorporate further testing of dugong sighting rates in higher sea states. The ScanEagle is capable of flying in higher wind speeds than used in the manned surveys. These trials should be conducted in a relatively turbid habitat that supports predictably large numbers of dugongs such as Hervey Bay, which would be more accessible and much cheaper than doing the work in the NGBR.

2. Capacity to count dugongs in large dispersed groups. Dunshea et al. (2020) report that human observers have difficulty in estimating the size of groups of >5 dugongs in passing mode, and we did not use passing mode for groups of > 9 dugongs (and groups of 5-10 dugongs were rare, see Table 4). The limited trials to date indicate that UAVs are better at counting large dugong groups than human observers in transect mode. This result is currently being investigated and the outcome of these analyses will determine whether further work is needed to resolve this issue.

3. Availability Bias Correction Experiments need to be conducted to ensure that the corrections for availability bias that have been developed for observers in manned aircraft for dugong surveys in the GBRWHA are applicable to unmanned aerial vehicle surveys. These experiments are required maximise the future relevance of the historical time series, which is based on standardised indices of relative abundance as used in this report. The simplest method of conducting this check would be to repeat the dugong model experiments (Hagihara et al. 2016) using a small, multi-rotor UAV with a camera similar to that in the ScanEagle. The UAV could be operated from a boat, similar to methods developed by Dr Chris Cleguer at Murdoch University.

Dunshea et al. (2020) document the observer errors associated with manned surveys. These should also be reduced by using unmanned aerial surveys.

4.4.5 Links to seagrass monitoring

Dugongs are seagrass community specialists (Marsh et al. 2011), a strong argument for linking dugong monitoring to seagrass monitoring in the GBRWHA, as demonstrated by the uncertainty as to why fewer dugongs and large in-water turtles were sighted in Lloyd Bay (Block N8, see above and Figures 3 and 7 and Tables 7 and 10 in 2019 compared with the previous surveys). As part of the RIMReP process, Udy et al. (2019) recommended three levels of monitoring seagrass in the GBR:

1. *Habitat assessment:* to determine the seagrass abundance, species composition and spatial extent of each habitat type within the World Heritage Area across all sites where seagrass has a potential of occurring.

2. *Health assessment:* to provide managers with annual and seasonal trends in seagrass condition and resilience at representative regional sites, for each habitat type.

3. *Process monitoring:* to provide managers with information on cause-and-effect relationships and linkages between different aspects of processes and ecosystems at sites, nested within habitat and health assessment sites.

Seagrass habitat monitoring should be coordinated with the dugong surveys, plus post-event process monitoring of areas impacted by extreme events such as floods, cyclones and marine heatwaves (Arias-Ortize t al. 2018). Unfortunately, Udy et al. (2019) did not develop a temporal and spatial design for their proposed monitoring. We suggest that such a design be developed as a desk-top study as soon as possible using a team of seagrass and marine wildlife experts.

4.5 Management of regulated impacts on the dugong and in-water large juvenile adult marine turtles as Matters of National Environmental Significance (MNES)

4.5.1 Statutory requirements

The dugong is a listed migratory and marine species under the EPBC Act. An action is classified as having a significant impact on a migratory species, such as the dugong, if it meets specified criteria[3] related to an area of important habitat for that species (Commonwealth of Australia 2013). In Australia, areas of important habitat for listed migratory, marine species are typically identified as Biologically Important Areas. Such areas have yet to be formally identified for dugongs on the east coast of Queensland. The spatial models in Figures 6 and 7 should assist with this process.

---

[3]An action is likely to have a significant impact on a migratory species if there is a real chance or possibility that it will: substantially modify (including by fragmenting, altering fire regimes, altering nutrient cycles or altering hydrological cycles), destroy or isolate an area of <u>important habitat</u> for a migratory species; result in an invasive species that is harmful to the migratory species becoming established in an area of <u>important habitat </u>for the migratory species; or seriously disrupt the lifecycle (breeding, feeding, migration or resting behaviour) of an ecologically significant proportion of the population of a migratory species.

The process should also be informed by the recent identification of candidate Important Marine Mammal Areas (cIMMAs)[4] for Australia. The waters of the NGBR from the Northern Boundary of the Great Barrier Reef Marine Park (-10°41'S to -15°S) to the 30m depth contour were identified as a cIMMA with the dugong as the primary species in February 2020. This delineation is currently being peer-reviewed and is expected to be confirmed over the next few months.

The marine turtles that occur in the GBR are all listed as threatened, as well as listed migratory and marine species under the EPBC Act. The significant impact criteria for threatened species are more stringent than for migratory species (Commonwealth of Australia 2013) and depend on whether the species is listed as Critically Endangered/Endangered[5] (leatherback, loggerhead, and olive ridley turtles are listed as Endangered) or Vulnerable (flatback, green and hawksbill turtles), but *inter alia* require information on habitat critical to the survival of the species. Spatial models such as those illustrated in Figures 6 and 7 will assist in the definition of critical in-water habitats for large juvenile and adult marine turtles in the GBRWHA, although more information would be required to identify the animals in the high and very high-density areas to species.

4.5.2 Legal Indigenous hunting

Within the GBRWHA, the practice has been to support Traditional Owners to assert their cultural authority over sea country and voluntarily regulate the dugong and turtle harvest through the Traditional Owners developing formal agreements, the Traditional Resource Use Management Agreements or TUMRAs (Havemann et al. 2005).

Four TUMRAS have been accredited in the Central GBR survey region (Blocks C11-13) considered in this report. Details of these TUMRAS can be found in http://www.gbrmpa.gov.au/our-partners/traditional-owners/traditional-use-of-marine-resources-agreements:

- Girringun TUMRA applies to sea country between Rollingstone and Mission Beach.

---

[4]Important Marine Mammal Areas (IMMAs) are defined as discrete portions of habitat, important to marine mammal species, that have the potential to be delineated and managed for conservation. IMMAs consist of areas that may merit place-based protection and/or monitoring. 'Important' in the context of the IMMA classification refers to any perceivable value, which extends to the marine mammals within the IMMA, to improve the conservation status of those species or populations. IMMAs are being identified at a global scale through a consistent expert process, independent of any political and socio-economic concerns, and will provide valuable input of marine mammals into existing national and international conservation tools with respect to marine protected areas, including Ecologically or Biologically Significant Areas (EBSAs) under the Convention on Biological Diversity (CBD), and Key Biodiversity Areas (KBAs) identified through the IUCN Standard. https://www.marinemammalhabitat.org/immas/

[5]Critically Endangered and Endangered Species Significant Impact Criteria. An action is likely to have a significant impact on a critically endangered or endangered species if there is a real chance or possibility that it will: lead to a long-term decrease in the size of a population; reduce the area of occupancy of the species; fragment an existing population into two or more populations; adversely affect habitat critical to the survival of a species; disrupt the breeding cycle of a population; modify, destroy, remove, isolate or decrease the availability or quality of habitat to the extent that the species is likely to decline; result in invasive species that are harmful to a critically endangered or endangered species becoming established in the endangered or critically endangered species' habitat; introduce disease that may cause the species to decline; or interfere with the recovery of the species. Vulnerable Species Significant Impact criteria. An action is likely to have a significant impact on a vulnerable species if there is a real chance or possibility that it will: lead to a long-term decrease in the size of an important population of a species; reduce the area of occupancy of an important population; fragment an existing important population into two or more populations; adversely affect habitat critical to the survival of a species; disrupt the breeding cycle of an important population; modify, destroy, remove or isolate or decrease the availability or quality of habitat to the extent that the species is likely to decline; result in invasive species that are harmful to a vulnerable species becoming established in the vulnerable species' habitat; introduce disease that may cause the species to decline; or interfere substantially with the recovery of the species.

- Gunggandji traditional land and sea country estate which includes the coastal land and waters immediately to the east of Cairns including: Green Island, Michaelmas Cay, Fitzroy Island, and the surrounding waters. Under this TUMRA no hunting of turtles or dugongs is allowed in these areas.

- Yirrganydji traditional land and sea country estate along the coast from Cairns to Port Douglas. This TUMRA provides the ability to isolate illegal activities that are occurring in the marine park from the care, traditional use and harvest of marine resources by the Yirrganydji people.

- Yuku-Baja-Muliku Regional TUMRA which covers 1088 km^2 south of Cooktown from Monkhouse Point south to Forsberg Point and extending east to just past the Ribbon Reefs. The agreement stipulates that turtles and dugongs cannot be hunted outside of the Traditional Owners' permit management system.

Two TUMRAs have been accredited within the NGBR survey area (Blocks N2 through N15):

- Lama Lama TUMRA covering sea country that extends through Princess Charlotte Bay to the Normanby River.

- Wuthathi TUMRA covering sea country in the Shelburne Bay area of Cape York.

In addition, the implementation of the Kuuku Ya'u People's Indigenous Land Use Agreement (ILUA) is managed in the same way as a TUMRA. This ILUA recognises Traditional Owner native title rights and interests in the management of nearly 2000 km^2 of sea within the GBRMPA, in an area north of Lockhart River. This agreement includes a limit on the annual take of dugongs and turtles from the ILUA area in a calendar year. This number is usually 15 for each species but may vary, subject to determination procedures set out in the ILUA.

Formal agreements have not yet been accredited for the main hunting areas of Traditional Owner Groups from several major hunting communities adjacent to the NGBR, such as Lockhart River, Hope Vale and the Northern Peninsula Area. We understand that some groups of Traditional Owners are in the process of negotiating TUMRAS.

Anecdotal information provided to Marsh by Traditional Owners at Lockhart (in 2014) and Hope Vale (in the 1980s and 1990s) indicates that most hunting occurs close to shore and relatively close to communities. The constraints on hunting are similar to those in Torres Strait (Marsh et al. 2015): the incomes of Traditional Owners are low, fuel is expensive, and outboard engines are often out of commission and unable to be repaired in the community. Thus, at present, we assume that hunting rarely occurs in a very high proportion (probably >90 per cent, Grech and Marsh unpublished) of the high-density dugong habitats off Cape York. Thus, most of the dugong habitat off Cape York currently operates as an unofficial dugong sanctuary with respect to hunting. However, improved road access is opening up much more of the coastal areas of Cape York for legal (and illegal) hunting and potentially other anthropogenic mortality factors. Our survey results indicate widespread distribution of dugongs along much of the Cape York coast (Figures 6 and 7) and improved road access will provide access to many more places to launch boats and stockpile fuel. We suggest that it would be appropriate for the negotiations between the Traditional Owner Groups living in key hunting communities of Cape York and the management agencies to consider the definition and enforcement of the boundaries for the hunting areas of various Indigenous groups (as in the Girrungun TUMRA). This approach could be implemented in addition to allowable catches and/or hunting moratoria, in view of: (1) the improvement in road access; (2) the challenges of implementing a robust system of catch recording; and (3) ongoing wider community concerns about Traditional hunting (e.g. Hansard Australian Senate 2017).

4.5.3 Illegal hunting

As explained above, several of the TUMRAs provide Traditional Owners with the powers to limit illegal take of dugongs, usually by hunters who are not Traditional Owners. The Traditional Owners at Lockhart River advised Marsh in 2014 that they are most concerned about poaching from Indigenous hunters based at Weipa on the western side of Cape York. The Lockhart Traditional Owners try to prevent these poachers hunting in their sea country by blocking their road access with a locked gate. This example reinforces the need to manage road access to the dugong habitats along the Cape York coast that have been documented by the JCU time series of aerial surveys (see Figure 7).

4.5.4 Commercial gillnetting

Gillnetting is considered to be the major source of human-induced mortality of dugongs throughout much of their range (Marsh and Sobtzick 2019), including the GBRWHA. After the 2003 rezoning of the GBRMP, Grech et al. (2008) estimated that commercial netting was banned from approximately 64 per cent of the high-density dugong habitat, 44 per cent of medium-density dugong habitat and 31 per cent of low-density habitat in the GBRWHA based on a spatial risk assessment. The implementation of the Queensland Sustainable Fisheries Strategy 2017-2027 (Queensland Government 2017) provides an opportunity for further changes to reduce bycatch of MNES such as dugongs and marine turtles in the region. In addition, Queensland is required to introduce electronic video surveillance as part of the management plan required as a condition of the Conservation Dependent Listing of the Scalloped Hammerhead shark, *Sphyrna lewini.* This reform *s*hould reduce the mortality of other bycatch species, such as dugongs and turtles, as demonstrated by another Australian fishery where the introduction of electronic surveillance increased the reporting of bycatch of protected species (Emery et al. 2019). WWF-Australia is seeking to establish a 'Net Free North' from just north of Cooktown through to the Torres Strait by purchasing the licence of the last commercial gill netter still operating full-time. WWF has purchased the licence of a gillnet fisher who operated in Princess Charlotte Bay. Taken together, these initiatives have the potential to reduce the bycatch of dugongs and marine turtles in commercial fishing activities, especially gillnetting in the CGBR and NGBR survey areas.

4.5.5 Ports and pollution

In response to concerns about port expansion along the urban Great Barrier Reef coast (e.g., Grech et al. 2013), the Queensland government developed the Queensland Ports Strategy (Queensland Government 2014) as a blueprint for managing and improving the efficiency and environmental management of the state's ports network over the next decade. The Strategy established five Priority Port Development Areas: Abbot Point, Brisbane, Gladstone, Hay Point/Mackay, and Townsville (none of which is in areas covered by the 2018-2019 surveys). The Strategy also prohibits capital dredging outside these Priority Port Development Areas in waters within and adjoining the Great Barrier Reef World Heritage Area until at least 2024, thus prohibiting capital dredging of all ports in our survey area during that period. However, the Strategy *per se* will not prevent the establishment of a proposed port to export coal from the Wongai Project in the Laura Basin, because there is no dredging involved and the proposal pre-dates the Queensland Ports Strategy. The proposed port is in Bathurst Bay, a high-density dugong area (Figure 7), which also supports a population of the Australian snubfin dolphin Parra et al. 2006 and H. Penrose unpublished data 2014; Appendix Figure 15.3), which is listed as Vulnerable by IUCN (Parra et al. 2017 and H. Penrose unpublished data 2014; Appendix Figure 15.3). A port in Bathurst Bay would be of conservation concern because it would increase the risk of mortality from vessel strike to both species of marine mammals, introduce coal dust into the Great Barrier Reef (Burns

2014) and potentially negatively affect seagrass from increased sedimentation from vessel propellers stirring up the seabed in shallow areas. There is also very limited capacity to respond quickly to an oil spill in the remote NGBR region (Tony Preen pers. comm.). There has also been recent concern about the impact of plastic pollution on dugongs see https://www.theguardian.com/environment/2019/aug/17/thailands-sweetheart-dugong-dies-with-plastic-in-stomach, further reason to limit port development in the remote NGBR.

5. Recommendations regarding application of the key findings to management arrangements

The key findings of this report suggest that:

- the major priority for dugong management in the Northern Great Barrier Reef continue to be on-going support for the implementation of community-based management by Traditional Owners, by completing Traditional Use Marine Resource Agreements (TUMRA) with Traditional Owners in key hunting communities such as Lockhart River, Hope Vale and the Northern Peninsula Area.

  1) negotiations between Traditional Owners and management agencies consider defining boundaries for the hunting areas of various Traditional Owner Groups (as in the Girrungun TUMRA) in addition to allowable catches or hunting moratoria, especially in view of: the increased challenge of maintaining customary hunting areas as a result of the improvements in road access to remote areas and the increased use of GPS technology;
  2) the challenges of implementing a robust system of catch recording; and
  3) ongoing wider community concerns about Traditional hunting.

- implementation of the Queensland Sustainable Fisheries Strategy 2017-2027 include further reforms to reduce bycatch of Matters of National Environmental Significance such as dugongs and marine turtles in the region, including electronic video surveillance.

- the spatial models of the density of dugongs and marine turtles presented in this report be used to inform the identification of Biologically Important Areas in the Great Barrier Reef World Heritage Area.

- an expert working party be established as soon as possible to enable the next aerial survey of the urban coast of the Great Barrier Reef World Heritage Area scheduled for 2022 to be conducted using an Unmanned Aerial Vehicle (UAV) to reduce the risk to human safety and improve the resolution of the observations. The working party should build on the Dugong technical expert group report submitted as part of the Reef 2050 Integrated Monitoring and Reporting Program design by developing a plan for transitioning the large-scale aerial surveys of dugongs and large in-water turtles to UAVs. The terms of reference of the working party should include:

  1) the logistics of conducting the surveys using a UAV along the urban coast and in remote areas;
  2) whether the boundary of the survey region should be moved to the Whitsundays to reflect dugong stock structure;
  3) how the survey could be funded to include the entire region from Torres Strait to Moreton Bay inclusive; and
  4) the experimental work required to ensure that the results of the UAV surveys can be compared with the historical time series of aerial surveys.

- an expert working party be established as soon as possible to develop a temporal and spatial design for the habitat assessment, health assessment and process monitoring recommended by the Seagrass technical expert group report and to coordinate this monitoring with the aerial monitoring of dugongs and in-water turtles.

6. REFERENCES

Arias-Ortiz, A., Serrano, O., Masqué, P., Lavery, P.S., Mueller, U., Kendrick, G.S., Rozaimi, M., Esteban, A., Fourqurean, J.W., Marbà, N., Mateo, M.A., Murray, K., Rule, M.J., and Duarte, C.M. 2018. A marine heatwave drives massive losses from the world's largest seagrass carbon stocks. Nature Climate Change 8, 338–344 https://doi.org/10.1038/s41558-018-0096-y.

Burns K. A. 2014. PAHs in the Great Barrier Reef Lagoon reach potentially toxic levels from coal port activities. Estuarine, Coastal and Shelf Science, 144: 39-45.

Chilvers B.L., Delean S., Gales N.J., Holley D.K., Lawler I.R., Marsh H, and Preen A.R. 2004. Diving behaviour of dugongs, *Dugong dugon.* Journal of Experimental Marine Biology and Ecology 304: 203-224.

Commonwealth of Australia 2013. Matters of National Environmental Significance Significant Impact Guidelines 1.1 Environment Protection and Biodiversity Conservation Act 1999.

Commonwealth of Australia 2017. Recovery Plan for Marine Turtles in Australia.

Commonwealth of Australia 2018. The Reef 2050 Long-Term Sustainability Plan July 2018.

Dunshea, G., Groom, R., and Griffiths, A.D. 2020. Observer performance and the effect of ambiguous taxon identification for fixed strip-width dugong aerial surveys. Journal of Experimental Marine Biology and Ecology 526. 10.1016/j.jembe.2020.151338.

Emery, T.J., Noriega, R., Williams, A.J., and Larcombe, J. 2019. Changes in logbook reporting by commercial fishers following the implementation of electronic monitoring in Australian Commonwealth fisheries. Marine Policy 104: 135-145. https://doi.org/10.1016/j.marpol.2019.01.018

Fuentes, M.M.P.B., Bell, I., Hagihara, R., Hamann, M., Hazel, J., Huth, A., Seminoff, J.A., Sobtzick, S., and Marsh, H. 2015. Improving estimates of in-water marine turtle abundance by adjusting aerial survey counts for perception and availability biases. Experimental Marine Biology and Ecology 471:77–83.

Fuentes, M.M.P.B, Beatty, B., Delean, S., Grayson, J., Lavender, S., Logan, M., and Marsh, H. 2016. Spatial and temporal variation in the effects of climatic variables on dugong calf production. PLoS One, 11960 1-14. PONE-D-15-52097R1.

GBRMPA. 1981. Nomination of the Great Barrier Reef by the Commonwealth of Australia for inclusion on the World Heritage List. UNESCO, 37 pp.

Grech, A., and Marsh, H. 2007. Prioritising areas for dugong conservation in a marine protected area using a spatially explicit population model. Applied GIS 3: 1-14.

Grech, A., Marsh, H. and Coles, R. 2008. Using spatial risk assessment to evaluate and address the problem of marine mammal bycatch. Aquatic Conservation 18: 1127-1139.

Grech A., Sheppard J., and Marsh H. 2011. Informing species conservation at multiple scales using data collected for marine mammal stock assessments. PLoS ONE. 6(3): e17993.

Grech, A., Bos, M., Brodie, J., Coles R., Dale, A., Gilbert, R., Hamann, M., Marsh, H., Nei,l K., Pressey, R.L,, Rasheed, M.A., Sheaves, M., and Smith, A. 2013. Guiding principles for the improved governance of port and shipping impacts in the Great Barrier Reef. Marine Pollution Bulletin. 75: 8-20.

Hagihara, R., Jones, R., Grech, A., Lanyon, J., Sheppard, J., and Marsh, H. 2014. Improving population estimates by quantifying diving and surfacing patterns: A dugong example. Marine Mammal Science 30:348–366.

Hagihara, R., Cleguer, C., Preston, S., Sobtzick, S., Hamann, M., Shimada, T., and Marsh, H. 2016. Improving the estimates of abundance of dugongs and large immature and adult-sized green turtles in Western and Central Torres Strait. Report to the National Environmental Science Programme. Reef and Rainforest Research Centre Limited, Cairns, 65 pp.

Hagihara, R., Jones, R.E., Sobtzick, S., Cleguer, C., Garrigue, C., and Marsh, H. 2018. Compensating for geographic variation in detection probability with water depth improves abundance estimates of coastal marine megafauna. PLOSOne 13(1): e0191476.

Hansard Australian Senate. 2017. Senate debates. Wednesday, 13 September 2017. Matters of public importance: management pf protected species. https://www.openaustralia.org.au/senate/?id=2017-09-13.193.2.

Havemann P., Thiriet D., Marsh H., and Jones, C. 2005. Decolonising conservation? Traditional use of marine resources agreements & dugong hunting in the Great Barrier Reef World Heritage Area Environmental & Planning Law Journal 22: 258-280.

Hodgson, A. 2018. Potential use of Unmanned Aerial Vehicles for megafauna monitoring in the GBR: transitioning to the new technology. Appendix 4 in Marsh, H., Hagihara, R., Hodgson, A., Rankin, R., and Sobtzick, S. 2019. Monitoring dugongs within the Reef 2050 Integrated Monitoring and Reporting Program: final report of the Dugong Team in the Megafauna Expert Group, Great Barrier Reef Marine Park Authority, Townsville.

Limpus C.J., and Nicholls N. 1988. The Southern Oscillation regulates the annual numbers of green turtles (*Chelonia mydas*) breeding around Northern Australia. Australian Journal of Wildlife Research. 15:157–61.

Marsh, H., and Sinclair, D.F. 1989a. Correcting for visibility bias in strip transect aerial surveys of aquatic fauna. Journal of Wildlife Management 53:1017–1024.

Marsh, H., and Sinclair, D.F. 1989b. An experimental evaluation of dugong & sea turtle aerial survey techniques. Australian Wildlife Research 16: 639-50.

Marsh, H. and Sobtzick, S. 2019. *Dugong dugon* (amended version of 2015 assessment). *The IUCN Red List of Threatened Species* 2019: e.T6909A160756767. https://dx.doi.org/10.2305/IUCN.UK.2015-4.RLTS.T6909A160756767.en. Downloaded on26 April 2020.

Marsh, H., O'Shea, T.J., and Reynolds, J.E. III. 2011. The ecology and conservation of Sirenia: dugongs and manatees. Cambridge University Press. 521pp.

Marsh, H., Grayson, J., Grech, A., Hagihara, R., and Sobtzick, S. 2015. Re-evaluation of the sustainability of a marine mammal harvest by indigenous people using several lines of evidence. Biological Conservation 192:324-330.

Marsh, H., Hagihara, R., Hodgson, A., Rankin, R., and Sobtzick, S. 2019. Monitoring dugongs within the Reef 2050 Integrated Monitoring and Reporting Program: final report of the Dugong Team in the Megafauna Expert Group, Great Barrier Reef Marine Park Authority, Townsville.

Martin, J., Edwards, H.H., Bled, F., Fonnesbeck, C., Dupuis, J., Gardner, B., Koslovsky, S.M., Aven, A., Ward-Geiger, L., Carmichael, R.H., Fagan, D.E., Ross, M., Reinert, T. 2014. Estimating upper bounds for occupancy and number of manatees in areas potentially affected by oil from the Deepwater Horizon oil spill. PLoS One, 9: e91683.

McGowan, A.M., Lanyon, J.M., Clark, N., Blair, D., Marsh, H., Wolanski, E., Seddon, J.M. In review. Seascape genetics of a mobile marine mammal: evidence of an abrupt break in dugong (*Dugong dugon*, *Müller*) gene flow along Australia's eastern Queensland coast. Conservation Genetics.

McKenzie, L.J., Collier, C.J, Langlois, L.A., Yoshida, R.L., Uusitalo, J., and Waycott, M. 2020. Marine Monitoring Program: Annual Report for Inshore Seagrass Monitoring 2018–19. Report for the Great Barrier Reef Marine Park Authority, Great Barrier Reef Marine Park Authority, Townsville, 202pp.

Meager, J.J., and Limpus C. 2014. Mortality of inshore marine mammals in eastern Australia is predicted by freshwater discharge and air temperature. PLOS One: e94849.

Neal, R. M. 2003. Slice sampling. The Annals of Statistics 31:705–767.

Parra, G.J., Schick, R. and Corkeron, P.K. 2006. Spatial distribution and environmental correlates of Autralian snubfin and Indo-Pacific humpback dolphins. Ecography 29: 396-406.

Parra, G., Cagnazzi, D., and Beasley, I. 2017. *Orcaella heinsohni*. The IUCN Red List of Threatened Species 2017: e.T136315A50385982. http://dx.doi.org/10.2305/IUCN.UK.2017-3.RLTS.T136315A50385982.en.

Pollock, K., Marsh, H., Lawler, I., and Alldredge, M. 2006. Modelling availability and perception processes for strip and line transects: an application to dugong aerial surveys. Journal of Wildlife Management 70:255–262.

Queensland Government 2014. Queensland Ports Strategy 2014. https://www.parliament.qld.gov.au/Documents/TableOffice/TabledPapers/2014/5414T5335.pdf

Queensland Government 2017. Queensland Sustainable Fisheries Strategy 2017-2027.https://www.daf.qld.gov.au/business-priorities/fisheries/sustainable/sustainable-fisheries-strategy/what-it-means-for-commercial-fishers

Rankin, R. 2018 Appendix 1 Trend analysis and probabilities of declining dugong populations. In Marsh, H., Hagihara, R., Hodgson, A., Rankin, R., and Sobtzick, S. 2019. Monitoring dugongs within the Reef 2050 Integrated Monitoring and Reporting Program: final report of the Dugong Team in the Megafauna Expert Group, Great Barrier Reef Marine Park Authority, Townsville.

Royle, J. A. 2004. N-mixture models for estimating population size from spatially replicated counts. Biometrics 60:108–115.

Sheppard, J., Preen, A.R., Marsh, H., Lawler, I.R., Whiting, S., and Jones, R.E. 2006. Movement heterogeneity of dugongs, *Dugong dugon* Müller over large spatial scales Journal of Experimental Marine Biology & Ecology 334: 64–83.

Shimada, T., Jones, R., Limpus, C., Groom, R., and Hamann, M. 2016. Long-term and seasonal patterns of sea turtle home ranges in warm coastal foraging habitats: implications for conservation. Marine Ecology Progress Series, 562:163-179.

Sobtzick, S., Hagihara, R., Penrose, H., Grech, A., Cleguer, C., and Marsh, H. 2014. An assessment of the distribution and abundance of dugongs in the Northern Great Barrier Reef and Torres Strait. A Report for the Department of the Environment, National Environmental Research Program (NERP). August 2014.

Sobtzick, S., Cleguer, C., Hagihara, R., and Marsh, H. 2017. Distribution and abundance of dugong and large marine turtles in Moreton Bay, Hervey Bay and the southern Great Barrier Reef. A report to the Great Barrier Reef Marine Park Authority. Centre for

Tropical Water & Aquatic Ecosystem Research (TropWATER) Publication 17/21, James Cook University, Townsville.

Udy, J., Waycott, M., Carter, A., Collier, C., Kilminster, K., Rasheed, M., McKenzie, L., McMahon, K., Maxwell, P., Lawrence, E., and Honchin, C. 2019, Monitoring seagrass within the Reef 2050 Integrated Monitoring and Reporting Program: Final Report of the Seagrass Expert Group, Great Barrier Reef Marine Park Authority, Townsville.

White G., and Burnham K. P. 1999. Program MARK: survival estimation from populations of marked animals. Bird Study 46: 120-139.

7. APPENDICES

Appendix 1: Daily activities for each team during the surveys in 2018–2019

Appendix Table 1.1. Daily activities for each team during their respective surveys in 2018–2019.

Abbreviations used: No Survey (NS), Survey (S), Transit (T), Training Course (TC), Training Flight (TF). Refer to Figure 1 to locate the blocks mentioned in this table.

| Date | Team 1 - November 2018 | | Team 2 - November 2018 | |
	Activity	Block (s) surveyed	Activity	Block(s) surveyed
30-Oct-18	TC	N/A	TC	N/A
31-Oct-18	TF, TC	N/A	TF, TC	N/A
1-Nov-18	TC	N/A	TC	N/A
2-Nov-18	TF, TC	N/A	TF, TC	N/A
3-Nov-18	TF, T	N/A	TF, T	N/A
4-Nov-18	T	N/A	T	N/A
5-Nov-18	S	C11, C12	NS	N/A
6-Nov-18	S	C12, C13	NS	N/A
7-Nov-18	S	C13	S	N8, N9
8-Nov-18	S	N2	S	N12, N13, N15
9-Nov-18	T	N/A	S	N8, N9
10-Nov-18	NS	N/A	NS	N/A
11-Nov-18	NS	N/A	NS	N/A
12-Nov-18	NS	N/A	NS	N/A
13-Nov-18	NS	N/A	NS	N/A
14-Nov-18	NS	N/A	NS	N/A
15-Nov-18	NS	N/A	NS	N/A
16-Nov-18	T	N/A	T	N/A
17-Nov-18			T	N/A

Date	Team 3 - June 2019	
	Activity	Block surveyed
1-Jun-19	TC	N/A
9-Jun-19	TF	N/A
10-Jun-19	TF	N/A
15-Jun-19	T	N/A
16-Jun-19	T	N/A
17-Jun-19	S	N5
18-Jun-19	S	N5
19-Jun-19	S	N5
20-Jun-19	NS	N/A
21-Jun-19	S	N5
22-Jun-19	NS	N/A
23-Jun-19	S	N5
24-Jun-19	S	N5
25-Jun-19	T	N/A
26-Jun-19	NS	N/A
27-Jun-19	NS	N/A
28-Jun-19	T	N/A
29-Jun-19	T	N/A

| Date | Team 4 – November/December 2019 | |
	Activity	Block(s) surveyed
1-Nov-19	TC	N/A
8-Nov-19	T	N/A
9-Nov-19	S	N2/ N4
10-Nov-19	S	N3
11-Nov-19	NS	N/A
12-Nov-19	NS	N/A
13-Nov-19	S	N4
14-Nov-19	S	N3
15-Nov-19	NS	N/A
16-Nov-19	NS	N/A
17-Nov-19	NS	N/A
18-Nov-19	NS	N/A
19-Nov-19	NS	N/A
20-Nov-19	NS	N/A
21-Nov-19	T	N/A
22-Nov-19	T	N/A
23-Nov-19	S	N6, N7, N8, N9
24-Nov-19	NS	N/A
25-Nov-19	S	N8, N9
26-Nov-19	S	N10, N13, N14
27-Nov-19	S	N11
28-Nov-19	NS	N/A
29-Nov-19	NS	N/A
30-Nov-19	NS	N/A
1-Dec-19	NS	N/A
2-Dec-19	S	N13
3-Dec-19	NS	N/A
4-Dec-19	T	N/A
5-Dec-19	T	N/A

Appendix 2: Completion schedule for the survey work

Appendix Table 2.1. Completion schedule for the survey work. See Figure 1 for the position of the survey blocks.

Block number	Transects	Date completed
C11	3311-3323	5-Nov-18
C12	3324-3368	6-Nov-18
C13	3369-3396	7-Nov-18
N1		Not Attempted by agreement with GBRMPA
N2	4021-4034	19-Nov-19
N3	4035-4053	14-Nov-19
N4	4064-4080	13-Nov-19
N5	4081-4104	23-Jun-19
N6	4213-4221	23-Nov-19
N7	4105-4113	23-Nov-19
N8	4114-4136	25-Nov-19
N9	4138-4158	25-Nov-19
N10	4160-4166	26-Nov-19
N11	4167-4178	27-Nov-19
N12	4180-4184	8-Nov-18
N13	4186-4201	2-Dec 19
N14	4203-4212	26-Nov-19
N15	4301-4307	8-Nov-18

Appendix 3: Members of each aerial survey team during the 2018–2019 aerial surveys

Appendix Table 3.1. The membership of each aerial survey team during the 2018-2019 aerial surveys. The order of the names reflects the position each observer was sitting in the aircraft (e.g., the first observer sitting on the port side was the primary port observer for that survey).

Team 1: Central Great Barrier Reef Team (November 2018)	
Port	Starboard
Daniella Hanf	Alvaro Soto Berg
Daniel Gonzalez-Paredes	Rachel Miller
Team 2: NGBR Team (November 2018)	
Erin Wyatt	Jane Melvin
Anya Jaeckli	Nao Nakamura
Team 3: NGBR Team (June 2019)	
Daniel Gonzalez-Paredes	Rachel Miller
Leah Carr	Nao Nakamura
Team 4: NGBR Team (November/December 2019)	
Daniel Gonzalez-Paredes	Daniella Hanf
Leah Carr	Rachel Miller

Appendix 4: Scales used to describe the environmental conditions encountered during the aerial surveys

Appendix Table 4.1. Water visibility scale.

Visibility	Water quality	Depth range	Visibility of sea floor
1	Clear	Shallow	Clearly visible
2	Variable	Variable	Visible but unclear
3	Clear	Deep	Not visible
4	Turbid	Variable	Not visible

Appendix Table 4.2. Glare scale.

Glare	Proportion of view affected
0	No glare
1	<25 per cent of view affected
2	25-50 per cent of view affected
3	>50 per cent of view affected

Appendix 5: Exploration of differences between surveys in marine turtle numbers

We were puzzled by the very large 2018/2019 population estimates of large juvenile and adult in-water marine turtles compared with the estimates from the most recent survey in 2013 using the optimum design (see Tables 9 and 10 and 11 and Figure 4).

We noted that:

- Any differences in survey conditions should have been accommodated by the use of sighting specific corrections for availability bias and the Fuentes methodlogy.

- Most of the turtles seen from the aircraft were likely to have been green turtles.

- The differences between 2013 and 2018-2019 were less for the segments of the survey conducted in November 2018 and June 2019 than in November/December 2019. The NGBR green turtle stock nests in the Austral summer and thousands of turtles come to the area to breed (Commonwealth of Australia 2017).

- The largest difference was between the estimates for Block N13, the offshore block closest to the major green turtle rookeries at Raine Island and Moulter Cay (Commonwealth of Australia 2017).

In an effort to explain this situation, we first considered whether the differences in the November population estimates between 2013 and 2018-2019 could be due to the inter-annual differences in the size of the green turtle nesting population and the consequent migration into the region (Limpus and Nicholls 1988). We were advised that the situation in 2013 and 2019 should have been very similar; both were the highest green turtle nesting seasons in the last 10 years (Andy Dunstan pers. comm. to Helene Marsh 2019).

We then undertook three approaches in an attempt to determine whether the between survey differences could have been due to differences in availability bias between surveys. We had a turtle specialist in our team and he was very good at spotting small turtles in clear water. The approaches were as follows:

1) the standard Fuentes et al. (2015) method used to analyse the data for the 2013 survey for RIMReP (Marsh et al. 2019);
2) the standard Fuentes et al. (2015) method with sightings in Visibility 1 conditions (clear water bottom visible) uncorrected for bias and added on at the end; and
3) population estimates with groups > 9 turtles uncorrected for bias and added on at the end. This approach parallels the Hagihara method for dugongs and assumes these turtles have been censused and is the approach used in the body of this report (see Tables 9 and 10).

Appendix Table 5.1 shows that none of these approaches explained the high 2018-2019 estimates. We conclude that the turtles must have been more available in 2018-2019 for some unknown reason.

Appendix Table 5.1. Comparisons of mean population estimates per survey block of large juvenile and adult in-water marine turtles using three approaches. The previous surveys of the N Blocks occurred in 2013. Those of the C Blocks in 2006. All results were based on the optimal survey design.

Block	Most recent survey prior to 2018	Standard method 2018-2019	Standard method with turtles sighted in Visibility 1 conditions uncorrected for bias 2018-2019	Standard method with groups >10 uncorrected for bias 2018-2019
C11	2361	5300	5300	5218
C12	7227	11306	10576	11212
C13	ns	17428	14642	15851
N2	3192	16412	15820	13286
N3	8804	44053	42946	40031
N4	11718	30935	29080	31101
N5	37998	58716	45689	39719
N6	5056	9802	9519	9886
N7	1030	5286	4237	4886
N8	13512	8034	78560	8281
N9	11327	15880	15634	16286
N10	4617	7615	7493	7752
N11	3180	7616	7498	6897
N12	2312	7978	7976	4464
N13	17344	76890	75886	78749
N14	1029	3398	3379	3455
N15	nc	32703	17123	17428
Total	**130707**	**359352**	**391358**	**314502**

Appendix 6: Sampling intensities for individual blocks during the surveys

Appendix Table 6.1. Sampling intensities for individual blocks during the November 2018, June 2019 and November/December 2019 surveys.

| Block | Most recent survey prior to 2018 | | 2018–2019 | |
	Block Size (km^2)	Sampling Intensity (per cent)	Block Size (km^2)	Sampling Intensity (per cent)
C11	351[1]	18.1	675	17.9
C12	5511[2]	9.5	5483	4.9
C13	ns[3]	ns[3]	2955	9.5
N2	674[4]	19.4	677	17.2
N3	1052[4]	19.8	1055	17.3
N4	2383[4]	10.1	2392	8.6
N5	7276[4]	10.1	7276	8.9
N6	464[4]	10.0	464	9.1
N7	601[4]	10.1	600	9.3
N8	981[4]	9.8	979	8.5
N9	1837[4]	6.8	1833	6.0
N10	278[4]	10.4	278	9.2
N11	430[4]	28.6	429	24.1
N12	415[4]	4.2	413	3.8
N13	4012[4]	7.0	4003	6.1
N14	226[4]	22.9	225	22.8
N15	ns[3]	ns	1960	4.9

[1] Last surveyed in 2005
[2] Last surveyed in 2011
[3] Not surveyed
[4] Last surveyed in 2013

Appendix 7. Weather conditions encountered during the 2018-2019 aerial surveys of the Great Barrier Reef.

Appendix Table 7.1. Weather conditions encountered during the 2018-2019 aerial surveys of the Great Barrier Reef.

Weather Conditions	November 2018	June 2019	November/December 2019
Max. Wind Speed (kn)	<10	<15	<15
Cloud Cover (oktas)	1.23	2.69	3.68
Min. Cloud Height (ft)	2000	3333	1300
Beaufort Sea State (range)	1.67 (0–3)	2.59 (1–4)	2.34 (1-3)
Glare (range)	1.83 (0–3)	3 (0–3)	2 (0–3)
Air Visibility (km)	10+	10+	10+

Appendix 8: Various Estimators for Adjusted Counts (N^{adj})

The following appendix describes three estimators that were used to model adjusted-counts, N_j^{adj} based on observed counts, and the availability bias and detection probabilities (y,a,b). The estimators were:

1. Horvitz-Thompson-like (HT) estimator;
2. N-Mixture estimator; and
3. Hybrid HT/N-Mixture.

Before running the analyses in the main report, we ran simulations to compare the properties of the different estimators, especially how they each negotiated the "bias-variance" trade-off. See Appendix 11 for a detailed description of the simulation experiments.

8.1 Horvitz-Thompson-like Estimator (HT)

The first method used the popular Horvitz-Thompson correction for estimating population abundance under individual heterogeneous covariates (McDonald and Amstrup 2001):

$$N_j \approx \sum_{i=1}^{n_j} \frac{y_i}{a_i \cdot p_i}$$

where:

$$n_j = \text{total counts of dugongs at transect } j$$

$$y_i = 1 \text{ for observed dugong } i \text{ at transect } j$$

$$p_i = \text{detection probability assigned to the } i^{th} \text{ dugong}$$

$$a_i = \text{availability bias assigned to the } i^{th} \text{ dugong}$$

The method is easily integrated into a MCMC sampler for estimating the regression parameters (β, θ), as follows: for each MCMC iteration, new values of a and p were drawn from their distributions; a new N_j was calculated for each non-zero transect j; and then, conditional on $\{N_j\}_{j=1}^J$ the β and θ variables were updated according to their posterior distributions (as detailed in the main report).

The method assumes that the availability bias and detection probability (perception bias) were similar between: i) points where dugongs were positively observed, and ii) points where dugongs were present but missed. The method is undefined for transects where no dugongs were observed (because there are no values of a and p to record if there are no dugongs present). As discussed in Appendix 11, the method has a slight positive bias but has lower variance compared to other methods discussed. The method is inappropriate at low values of detection probability (less than 0.1) because as the denominator approaches 0, the estimator explodes to infinity.

8.2 N-Mixture Model

The second estimator used a Binomial mixture on N and a Negative Binomial prior on N (aka, the N-mixture distribution, inspired by Royle (2004)), in order to sample N from its posterior distribution.

The distribution is summarised as:

$$\pi\left(N|n_j,\eta_j,\boldsymbol{a},\boldsymbol{p}\right) = \frac{1}{\mathcal{Z}}\pi(n_j|N,a\cdot p)\pi(N|\exp\{\eta_j\},\theta)$$

$$= \frac{1}{\mathcal{Z}}\;\underbrace{\mathrm{Bin}(n_j|N,a\cdot p)}_{\substack{\text{Binomial likelihood}\\\text{of }n\text{ given }N,p,a}}\;\underbrace{\mathrm{NB}(N|\exp\{\eta_j\},\theta)}_{\substack{\text{NB prior on}\\N\text{ given }\eta,\theta}}$$

where:

$$n_j = \text{sum of observed counts of dugongs at transect } j$$

$$(\eta_j,\theta) = \text{log-linear mean and overdispersion at transect } j$$

$$\mathcal{Z} := \text{normalising function to ensure that } \sum_{N=n_j}^{\infty} \pi\left(N|n_j,\eta_j,\boldsymbol{a},\boldsymbol{p}\right) = 1$$

The method can be integrated into an Markov Chain Monte Carlo sampler for estimating the regression parameters (β,θ) in the following way: for each MCMC iteration, a and p are drawn from their distributions, a new $\tilde{N}_j$ is drawn for transect j from its distribution conditional on β and θ, and then β and θ are updated conditional on the (imputed) values of all adjusted counts $\tilde{N}$.

Additional computational details are presented in Appendix 10. Nonetheless, the description above reveals some key points about the N-mixture estimator:

- The distribution can handle transects with zero dugong observations (unlike the HT estimator).
- The method does not suffer from an explosion of N towards infinity as a and p get close to zero (unlike the HT); this is because N has a Negative Binomial prior which reigns in the density of N towards lower values near the expectation of $\mathrm{NB}(N|\exp(\eta),\theta)$.
- The posterior distributions of β and θ should have larger dispersions compared to the HT estimator, given that N is now a random variable with its own uncertainty; this uncertainty should propagate to the other random variables. In other words, the N-mixture is a high-variance estimator, but it is less biased than the HT estimator (as demonstrated in the Appendix 10 simulations).
- The distribution of N includes a summation over infinity, reflecting the fact that, theoretically, there could be a very large number of unseen dugongs, especially when the availability bias and detection probability are very low.

The final point requires a slight modification of the MCMC sampler, due to the dilemma of how to account for values of (a,p) for animals that were present but were not detected (one cannot measure the values of (a,p) at $y=0$, because such animals were not observed). In order to use the N-mixture distribution, we required estimates of a and p for every $N \subset [n_j,\infty]$. In other words, we require a means to account for the values of a,p for a large number of dugongs who theoretically may have been present but were not detected.

Our solution to this dilemma was to make the assumption that such unseen values could be approximated according to the background distribution of a, p, which we sampled regularly along the transect, regardless of the presence of dugongs. We denote these background values $(a^\varnothing,p^\varnothing)$. These served as approximate values of (a,p) for unseen dugongs. Computationally, within each MCMC iteration, we sampled-with-replacement from the empirical distribution of $(a_j^\varnothing,p_j^\varnothing)$ within each transect, in order to approximate the values of (a,p) when $y_i = 0$.

To integrate these background values into the N-Mixture, we exploited a useful factorization of the Binomial distribution into a series of Bernoullis, and in particular, into a product of two series: one series for the subset of cases where all y=1 (observed dugongs), and a second series for cases where all y=0 (unobserved dugongs). Consider the general case of a Binomial distribution where the observations have been factored into N independent Bernoullis:

$$\text{Bin}(n|N,p) = \binom{N}{n} \prod_{i=1}^{N} \text{Bern}(y_i;p)$$

$$= \binom{N}{n} \underbrace{\left(\prod_{y_i \in \boldsymbol{y}^+}^{n} \text{Bern}(y_i;p_i) \right)}_{\substack{\text{product of Bernoullis} \\ \text{for } y=1}} \underbrace{\left(\prod_{y_i \in \boldsymbol{y}^{\varnothing}}^{N-n} \text{Bern}(y_i;p_i) \right)}_{\substack{\text{product of Bernoullis} \\ \text{for } y=0}}$$

$$= \binom{N}{n} \left(\prod_{y_i \in \boldsymbol{y}^+}^{n} p_i^{y_i}(1-p_i)^{(1-y_i)} \right)^1 \left(\prod_{y_i \in \boldsymbol{y}^{\varnothing}}^{N-n} p_i^{y_i}{}^1(1-p_i)^{(1-y_i)} \right) \quad (1)$$

$$= \binom{N}{n} \left(\prod_{y_i \in \boldsymbol{y}^+}^{n} p_i \right) \left(\prod_{y_i \in \boldsymbol{y}^{\varnothing}}^{N-n} (1-p_i) \right)$$

where :

$$n = \sum_{i=1}^{N} y_i$$

$$N = |\boldsymbol{y}|$$

$$\boldsymbol{y}^+ = \text{set of elements in } \boldsymbol{y} \text{ where all } y_i = 1$$

$$\boldsymbol{y}^{\varnothing} = \text{set of elements in } \boldsymbol{y} \text{ where all } y_i = 0$$

The last line shows the Binomial factored into two series of Bernoulli distributions, one for positive counts (all $y_i=1$) and the other for unseen dugongs (all $y_i=0$), which is useful for the N-mixture model, because we can represent the positive counts of dugongs (and their observed values of a,p) as the Bernoulli-series dedicated to $\boldsymbol{y}^+$, and we can represent the undetected dugongs as the Bernoulli-series dedicated to $\boldsymbol{y}^{\varnothing}$. The vector $\boldsymbol{y}^+$ has fixed-length equal to n_j, which is the total number of dugongs observed on transect j; whereas $\boldsymbol{y}^{\varnothing}$ represents the excess 0's and has a dynamic length $N^{\text{adj}} - n_j$ (and can theoretically be infinite length).

It is important to note the relationship between the series $\boldsymbol{y}^+$ and the empirical values of a and p, as well as the relationship between the dynamic series $\boldsymbol{y}^{\varnothing}$ and the distribution of $(a^{\varnothing}, p^{\varnothing})$. The observed dugongs ($\boldsymbol{y}^+$) have values of a and p recorded at their sighting, whereas the imputed/unobserved dugongs that make-up the series $\boldsymbol{y}^{\varnothing}$ have no values of a and p, and so these values were imputed, randomly, by sampling-with-replacement from the background distribution $(a^{\varnothing}, p^{\varnothing})$.

We denote this special series-expansion, which combines observed and background values of (*a,p*) as $\mathrm{Bin}^*(n_j|N, \boldsymbol{a}_j, \boldsymbol{p}_j, \boldsymbol{a}^\varnothing, \boldsymbol{p}^\varnothing)$. We also use Monte-Carlo (MC) imputation to integrate over the background distribution of $(a^\varnothing, p^\varnothing)$. We define our distribution as:

$$\mathbb{E}[\mathrm{Bin}^*(n_j|N, \boldsymbol{a}_j, \boldsymbol{p}_j, \boldsymbol{a}^\varnothing, \boldsymbol{p}^\varnothing)] \approx \sum_{m=1}^{M_{\mathrm{mcmc}}} \mathrm{Bin}^{(m)}(n_j|N, \boldsymbol{a}_j, \boldsymbol{p}_j, \boldsymbol{a}_m^\varnothing, \boldsymbol{p}_m^\varnothing)$$

where :

$$\mathrm{Bin}^{(m)}(n_j; N, \boldsymbol{a}_j, \boldsymbol{p}_j, \boldsymbol{a}_m^\varnothing, \boldsymbol{p}_m^\varnothing)$$

$$= \binom{N}{n_j} \underbrace{\left(\prod_{y_i \in \boldsymbol{y}_j^+}^{n_j} (a_i \cdot p_i)^{y_i}(1 - a_i \cdot p_i)^{(1-y_i)} \right)}_{\substack{\text{product of Bernoullis} \\ \text{for observed } \boldsymbol{y}_j}} \underbrace{\left(\prod_{y_i \in \boldsymbol{y}_j^\varnothing}^{N-n_j} (a_i^\varnothing \cdot p_i^\varnothing)^0(1 - a_i^\varnothing \cdot p_i^\varnothing)^{(1-0)} \right)}_{\substack{\text{product of Bernoullis} \\ \text{for excess zeros for } (n_j+1) \to N}}$$

(1)

$$= \binom{N}{n_j} \left(\prod_{y_i \in \boldsymbol{y}_j^+}^{n_j} (a_i \cdot p_i) \right) \left(\prod_{y_i \in \boldsymbol{y}_j^\varnothing}^{N-n_j} (1 - a_i^\varnothing \cdot p_i^\varnothing) \right)$$

where :

n_j = sum of observed counts of dugongs at transect j

$\boldsymbol{y}_j$ = vector of 1s for observed dugongs at j

$\boldsymbol{a}_j$ = vector of a for observed dugongs at j

$\boldsymbol{p}_j$ = vector of p for observed dugongs at j

$\boldsymbol{a}_m^\varnothing$ = sample from background a at MCMC iteration m

$\boldsymbol{p}_m^\varnothing$ = sample from background p at MCMC iteration m

The first line says that the distribution can be approximated by Monte Carlo integration over the background empirical values of $(a_i^\varnothing \cdot p_i^\varnothing)$. In the second and third lines, the background samples are used within the second term $(a_i^\varnothing \cdot p_i^\varnothing)^0(1 - a_i^\varnothing \cdot p_i^\varnothing)^{(1-0)}$ to represent the excess 0's (unseen dugongs) who must be accounted for in cases where $N_j > n_j$, that is, where the adjusted counts are greater than the observed counts.

In practice, the above equation has a simple vectorized calculation (Appendix 11), and the inner MC integration is performed simultaneously as the global MCMC sampling algorithm (i.e., we need only sample background values of $(a^\varnothing, p^\varnothing)$ once per MCMC iteration).

Altogether, our N-mixture model has the following MCMC pseudo-algorithm:

for $m \in [0, M_{\mathrm{mcmc}}]$, do :

draw $a_i \sim \hat{\pi}(\hat{\mu}_a, \hat{\sigma}_a)$ for all i observations in j transects, and all j in location l

draw $p_i \sim \hat{\pi}(\hat{\mu}_p, \hat{\sigma}_p)$ for all $i \in j$ and all j in location l

sample with replacement $\boldsymbol{a}_{(m)}$ and $\boldsymbol{p}_{(m)}$ from their background distributions, for all $j \in l$

calculate $\eta_j = \beta_{0,l} + \beta_{t,l} \cdot t$ for all j, t, l

sample $N_j \sim \mathrm{Bin}^{(m)}(n_j|N, \boldsymbol{a}_j, \boldsymbol{p}_j, \boldsymbol{a}_{(m)}^\varnothing, \boldsymbol{p}_{(m)}^\varnothing) \cdot \mathrm{NB}(N|\exp\{\eta_j\}, \theta)$ on support $N \in [n_j, \infty)$

$$\text{sample } \beta_{0,l} \sim \underbrace{\left(\prod_{j=1}^{J} \mathrm{NB}(N_j|\exp\{\eta_j\}, \theta) \right)}_{\text{NB likelihood } N|\beta_0\beta_t\theta} \underbrace{\mathcal{N}(\beta|\mu_{0,\ell}, \sigma_{0,\ell}^2)}_{\text{Normal prior on } \beta_0} \text{ for each locations } l \qquad (1)$$

$$\text{sample } \beta_{t,l} \sim \left(\prod_{j=1}^{J} \mathrm{NB}(N_j|\exp\{\eta_j\}, \theta) \right) \mathcal{N}(\beta|\mu_{0,t,\ell}, \sigma_{t,\ell}^2)[a_0, b_0] \text{ for each locations } l$$

$$\text{sample } \theta \sim \left(\prod_{l}^{L} \prod_{j=1}^{J} \mathrm{NB}(N_j|\exp\{\eta_j\}, \theta) \right) \mathcal{U}(\theta|c_0, d_0)$$

8.3 Hybrid Estimator

Our third estimator was a hybrid: it involved the N-mixture distribution, just like the previous estimator, but used a truncated data-set equivalent to the truncation that occurs when using the HT-estimator, i.e., it was defined only for those transects where the sum-of-dugongs was non-zero.

The benefit of the Hybrid estimator is that it is asymptotically equivalent to the HT-estimator, under the assumption that the background values of (*a,p*) share the same distribution as values where dugongs are observed. However, in practice, the two distributions seem to be different.

Other properties of the HT-estimator are explored in Appendix 10, such that the Hybrid estimator seems to be less-biased than the HT estimator and seems to have lower variance than the N-Mixture estimator.

Appendix 9: Details on Calculating Availability Bias and Detection Probabilities

9.1 Availability Probabilities

The availability probability (*a*) is a bias correction factor to account for the subsurface diving behaviour of dugongs, whereby animals are infrequently at the surface, and therefore not available for detection (Pollock et al. 2006). Water conditions and depth affect this bias.

The availability biases *a* and their standard errors *se(a)* were estimated in previous studies using models of turbidity and depth, per year and per location, as detailed in Hagihara et al. (2014, 2018). Depth and turbidity measurements were discretised into 13-15 different category bins per year and location. Each observation of a dugong was assigned a depth/turbidity category. For each category, the maximum likelihood estimates of the biases $(\hat{\mu}_a, \hat{\sigma}_a)$ were transformed into approximating Beta distributions, to facilitate sampling of a^* for each MCMC iteration.

$$\hat{\pi}(a; \hat{\mu}_a, \hat{\sigma}_a) \approx \text{Beta}(a; s_1 + 1, s_2 + 1)$$

where :

$$s_1 = \frac{(1 - \hat{\mu}_a)\hat{\mu}_a^2}{\hat{\sigma}_a^2} - \hat{\mu}_a \qquad (1)$$

$$s_2 = s_1 (\frac{1}{\hat{\mu}_a} - 1)$$

We call these *pseudo* posterior distributions, because they were approximated from frequentist estimators, and not subject to Bayesian updating during the MCMC routine.

9.2 Detection Probabilities[6]

Elsewhere in the report, we simplified our description about sampling the detection probabilities according to the short-hand:

$$\text{draw } p_i \sim \hat{\pi}(\hat{\mu}_p, \hat{\sigma}_p) \text{ for all } i \in j \text{ and all } j \text{ in location } l$$

This description omitted several nuances about the detection probabilities and their mark-recapture models (Pollock et al. 2006). Because the method is well-documented in previous articles, we have refrained from excessive exposition here, and just focus on the key points.

Consider that each dugong observation (y_i) comes with an estimate of its availability probability (*a*) and a detection probability (p_s), where the latter was conditional on the *side* of the aircraft that the observation took place (hence the subscript *s* for *port* and *starboard*).

Recall that each survey team included four observers seated in four quadrants of the aircraft: one in the mid-section on the port side, one in the mid-section on the starboard side, one in the back on the port side, and one in the back on the starboard side. We assume that dugongs on the port side were only observable by the observers on the port side, and likewise for dugongs on the starboard side.

---

[6] Referred to as Perception Bias by Pollock et al. (2006) and in many places in this report

Therefore, the effective detection probability on the port-side and starboard-side were:

$$\hat{p}_{\text{port}} = 1 - (1 - \hat{\rho}_{\text{PortFront}})(1 - \hat{\rho}_{\text{PortBack}})$$

$$\hat{p}_{\text{starboard}} = 1 - (1 - \hat{\rho}_{\text{StarboardfFront}})(1 - \hat{\rho}_{\text{StarboardBack}})$$

These decompositions reveal that, in order to assign each dugong a single unified detection probability, we require estimates of four detection probabilities $\{\hat{p}_{\text{PortFront}}, \hat{p}_{\text{PortBack}}, \hat{p}_{\text{StarboardfFront}}, \hat{p}_{\text{StarboardBack}}\}$.

The above four detection probabilities were estimated in previous capture-recapture studies. Pollock et al. (2006) motivated four models to reduce the complexity of the capture-recapture models, by assuming homogeneity in detection probabilities among different groupings of observers:

- *M_All*: all observers have the same detection probability, $\hat{\rho}_{\text{all}}$;
- *M_Independent*: all observers have different detection probabilities, $\{\hat{\rho}_{\text{PortFront}}, \hat{\rho}_{\text{PortBack}}, , \hat{\rho}_{\text{StarboardfFront}}, \hat{\rho}_{\text{StarboardBack}}\}$;
- *M_FrontBack*: the front two observers share the same detection probability, as do the back two observers $\{\hat{\rho}_{\text{Front}}, \hat{\rho}_{\text{Back}}\}$; and
- *M_PortStarboard*: the two port-side observers share the same detection probability, as do the two starboard-side observers $\{\hat{\rho}_{\text{Port}}, \hat{\rho}_{\text{Starboard}}\}$

Each model was also assigned a model probability $\hat{p}(M)$ where $M \in \{M_{\text{all}}, M_{\text{independent}}, M_{\text{FrontBack}}, M_{\text{PortStarboard}}\}$. The model probabilities were derived from AIC weights.

Given the model probabilities and the model-specific detection probabilities (estimated by maximum likelihood), and their standard errors, we used the following sampling routine within our MCMC algorithm.

For each MCMC iteration, do:
1. for each team, sample
   $M^* \sim [\hat{p}(M_{\text{all}}), \hat{p}(M_{\text{independent}}), \hat{p}(M_{\text{FrontBack}}), \hat{p}(M_{\text{PortStarboard}})]$ using AIC-weight-derived model probabilities
2. conditional on *M**, sample the quadrant-specific detection probabilities:

$i.$ if $M^* = M_{\text{all}}$,
$$\rho^*_{\text{all}} \sim N(\hat{\rho}_{\text{all}}, \hat{se}(\rho_{\text{all}})|M)$$
$$\hat{p}_{\text{port}} = 1 - (1 - \hat{\rho}_{\text{all}})(1 - \hat{\rho}_{\text{all}})$$
$$\hat{p}_{\text{starboard}} = 1 - (1 - \hat{\rho}_{\text{all}})(1 - \hat{\rho}_{\text{all}})$$

$ii.$ if $M^* = M_{\text{FrontBack}}$,
$$\rho^*_{\text{Front}} \sim N(\hat{\rho}_{\text{Front}}, \hat{se}(\rho_{\text{Front}})|M)$$
$$\rho^*_{\text{Back}} \sim N(\hat{\rho}_{\text{Back}}, \hat{se}(\rho_{\text{Back}})|M)$$
$$\hat{p}_{\text{port}} = 1 - (1 - \hat{\rho}_{\text{Front}})(1 - \hat{\rho}_{\text{Back}})$$
$$\hat{p}_{\text{starboard}} = 1 - (1 - \hat{\rho}_{\text{Front}})(1 - \hat{\rho}_{\text{Back}})$$

$iii.$ if $M^* = M_{\text{PortStarboard}}$,
$$\rho^*_{\text{Port}} \sim N(\hat{\rho}_{\text{Port}}, \hat{se}(\rho_{\text{Port}})|M)$$
$$\rho^*_{\text{Starboard}} \sim N(\hat{\rho}_{\text{Starboard}}, \hat{se}(\rho_{\text{Starboard}})|M)$$
$$\hat{p}_{\text{port}} = 1 - (1 - \hat{\rho}_{\text{Port}})(1 - \hat{\rho}_{\text{Starboard}})$$
$$\hat{p}_{\text{starboard}} = 1 - (1 - \hat{\rho}_{\text{Port}})(1 - \hat{\rho}_{\text{Starboard}})$$

$iv.$ if $M^* = M_{\text{Independent}}$,
$$\rho^*_{\text{FrontPort}} \sim N(\hat{\rho}_{\text{FrontPort}}, \hat{se}(\rho_{\text{FrontPort}})|M)$$
$$\rho^*_{\text{FrontStarboard}} \sim N(\hat{\rho}_{\text{FrontStarboard}}, \hat{se}(\rho_{\text{FrontStarboard}})|M)$$
$$\rho^*_{\text{BackPort}} \sim N(\hat{\rho}_{\text{BackPort}}, \hat{se}(\rho_{\text{BackPort}})|M)$$
$$\rho^*_{\text{BackStarboard}} \sim N(\hat{\rho}_{\text{BackStarboard}}, \hat{se}(\rho_{\text{BackStarboard}})|M)$$
$$\hat{p}_{\text{port}} = 1 - (1 - \hat{\rho}_{\text{FrontPort}})(1 - \hat{\rho}_{\text{BackPort}})$$
$$\hat{p}_{\text{starboard}} = 1 - (1 - \hat{\rho}_{\text{FrontStarboard}})(1 - \hat{\rho}_{\text{BackStarboard}})$$

After calculating values for $\hat{p}_{\text{starboard}}$ and $\hat{p}_{\text{port}}$ for each team, these values were assigned to each dugong observation based on what side of the aircraft the dugong was observed.

These values were also imputed for the background values of $(p^{\varnothing}, a^{\varnothing})$, assuming that 50 per cent of the (undetected) animals were on the port-side, and 50 per cent are on the starboard-side.

Appendix 10: Simulations for Comparing Estimators

The purpose of the simulations was to study the frequency properties of three estimators. The estimators were used in the analyses' MCMC routine to map counts of observed dugongs to inflated "adjusted counts" that included hypothetically unseen dugongs. The three estimators were: the Horvitz-Thompson-like estimator (HT), the N-Mixture estimator (Nmix) and the Hybrid estimator. These estimators resulted in different population estimates and concomitant trends. It was the goal of these simulations to determine whether they could accurately estimate a population trend (τ) of -3 per cent/year over 10 years, under various scenarios.

The different scenarios included different combinations of the following simulation parameters: i) total number of transects over all years: 400, 800, and 1600; and ii) the background density of dugongs (counts per km): 0.1, 0.2, 0.4, and 0.8. Each scenario was repeated 100 times, for a total of 1600 simulations.

These scenarios allowed us to observe how the estimators behaved under different magnitudes of "sample size". By sample size, we have two different but related meanings: the amount of research effort as measured by the number of survey-transects (fewer transects = smaller sample size; more transects = larger sample size), and the true population density of dugongs. In the latter case, consider that low dugong densities result in many zeros in the simulated response variable (counts of dugongs). Such zero-inflated counts are difficult to analyse by Poisson or Negative Binomial count distributions.

To assess the performance of the estimators under the various scenarios, we focused on the estimated posterior means of the trend variable $(\bar{\beta}_t)$ versus the true trend (τ), and looked at several statistics between the two, including:
- Bias: $\mathbb{E}[\bar{\beta}_t - \tau]$
- Root-Variance: $\mathbb{V}[\bar{\beta}_t]^{\frac{1}{2}}$
- Mean Square Error: $\mathbb{E}[(\bar{\beta}_t - \tau)^2]$
- Nominal Coverage vs Realised Coverage of the 95 per cent credibility interval:
  $$1 - \mathbb{P}[\tau < q_{0.025}(\pi_{\beta_t})] - \mathbb{P}[\tau > q_{0.975}(\pi_{\beta_t})]$$
- Average Expected Cost (iMSE): $\dfrac{1}{100} \displaystyle\sum_{s=1}^{100} \int_{\pi_{\beta_t}} (\beta_t - \tau)^2 d\beta_t$

… where the expectations were over 100 simulations.

The first three statistics are popular frequentist criteria to study the bias-variance trade-off. For estimation tasks, frequentists generally prefer the MSE statistic as an overall performance measure (a.k.a., the generalization error), because it incorporates both bias and variance. The final statistic, the Average Expected Cost, is a posterior error statistic favoured by Bayesians, which integrates the square-error over the entire posterior distribution of $\bar{\beta}_t$, where the outer average is over all 100 simulations.

Additional notes about the simulations:

- The simulated counts were generated by a Negative Binomial distribution; true counts were corrupted by availability bias and imperfect detection probabilities.
- The values of the availability bias and detection probabilities were generated by sampling-with-replacement from the empirical values collected from field studies, as used in the main report.

- The total length of kilometres-surveyed were simulated by sampling-with-replacement from the empirical distribution of transect lengths in the main article.
- The simulation over-dispersion parameter was set to be a multiple of the average expected value of the Negative Binomial distribution, per simulation. The multiple was 2.5, resulting in more dispersion for higher true densities.
- After simulating data, the Bayesian estimation procedure involved posterior approximation via MCMC, as in the main report. We ran 50,000 MCMC iterations, and used the same vague priors that were used in the main report for real data. The frequency statistics used the posterior means of these MCMC-sampled distributions.

10.1 Simulation Results

Appendix Figure 10.1 shows the performance of the estimators according to different scenarios (number of transects and population density) and the accompanying table.

10.1.1 General Results

The results are consistent with the interpretation that the estimators occupy different points along a bias-variance trade-off, such that the N-Mixture was less-biased but had higher-variance, and the HT/Hybrid estimators had lower variance, but suffered a high bias, especially at low sample-sizes and low population density.

10.1.2 Results in Detail

The N-Mixture estimator was the least biased, although all three estimators had a positive bias. The N-Mixture was also the best according to the MSE statistic. Its realised coverage was also closest to the nominal coverage (i.e., it gave a more honest estimate of uncertainty). However, the N-Mixture was a higher-variance estimator, whereby its root-variance was highest among estimators; it also had a higher iMSE statistic, meaning that for any given point within its posterior distribution, such a point was, on average, further away from the "truth" as compared to the other estimators. The HT and Hybrid estimators we more similar to one another, although the Hybrid generally beat the HT for most statistics, except coverage. The Hybrid estimator was the best according to the iMSE statistic.

These general results broadly match the results at the per-scenario level, whereby the N-Mixture estimator generally dominated the other two estimators according to bias and MSE, but had higher root-variance and iMSE.

The granular results show that all estimators were sensitive to the number-of-transects, such that performance varied a lot within the range of 400 to 600 transects, after which there was a plateau in performance. In contrast, there was a gradual monotonic reduction in error as the true population density increased. In other words, having more transects results in diminishing returns, while a larger population density always results in less error.

Given these results, there is no definitive "winning" estimator. Choosing an estimator will depends on our measure of error: according to the Bayesian Average Expected Error/iMSE, the Hybrid was the best overall estimator; whereas according to the frequentist MSE statistic, the N-Mixture was the best overall estimator.
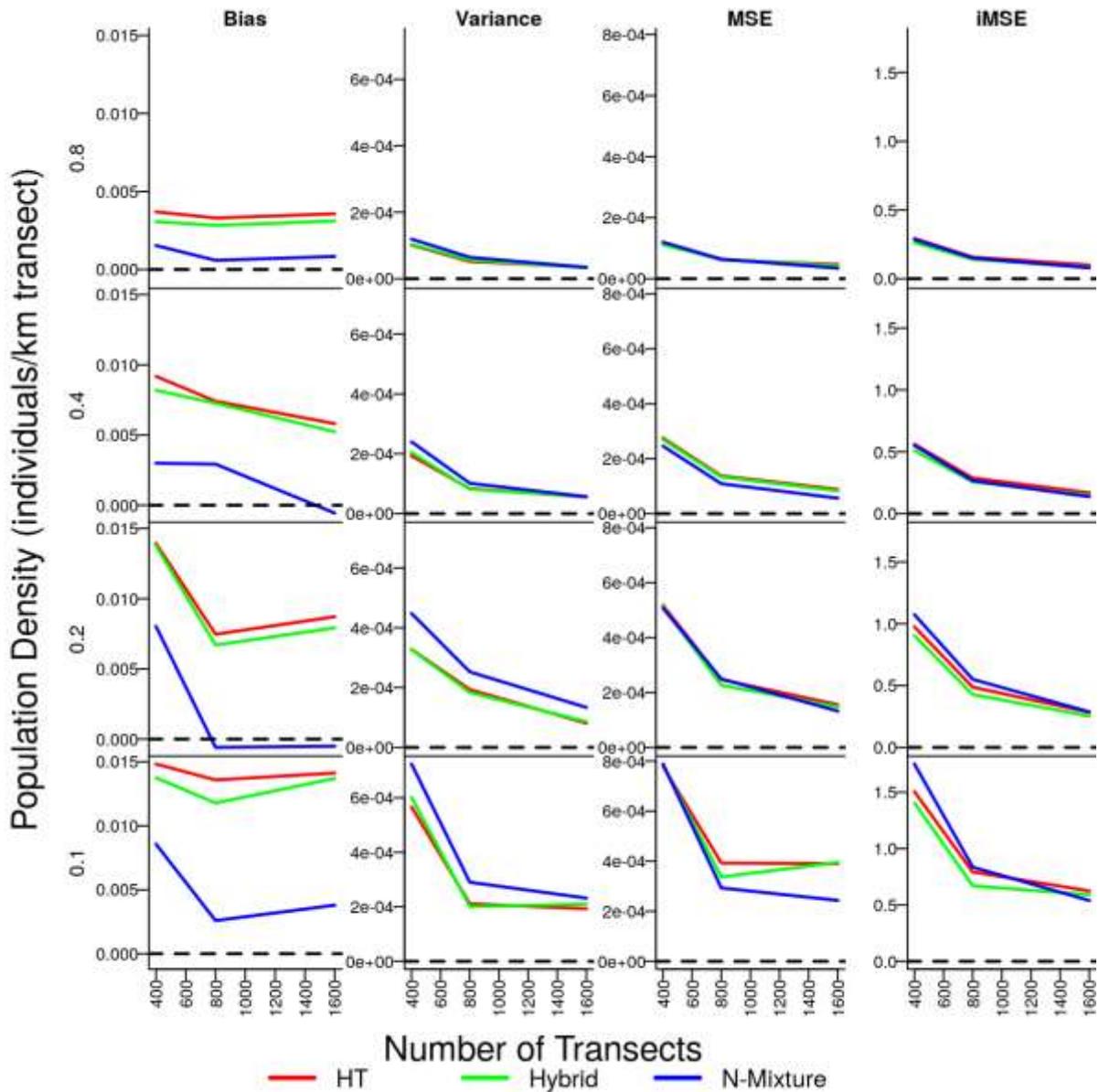
Appendix Figure 10.1. Simulation results for estimating a -3 per cent/year trend, comparing three estimators (coloured lines): Horvitz-Thompson-like (HT), N-Mixture, and a Hybrid between the former two. There were 100 simulations per scenarios, whereby scenarios varied by the true background density of dugongs (major y-axis) and the total number of sampled transects (minor x-axis). Columns represent different statistics to compare the estimators.

10.2 Discussion

Given how the estimators occupy different regions of the bias-variance trade-off, the answer as to which estimator is "best" is partially dependent on one's values. Is it more important to be less-biased and trust the accuracy of the 95 per centCI (i.e., close correspondence between the nominal vs realised coverage)? If the answer to these is yes, then the N-mixture is best. Alternatively, is it better to sacrifice some bias and be closer to the "truth" (lower variance and lower iMSE)? By such criteria, the Hybrid performed best.

An interesting point is that, no matter one's values, the HT under-performed the other two estimators, and the choice is really between the Hybrid vs. N-Mixture.

69

In terms of the relationship between sample size (density and effort), and statistic performance, the results suggest that running more transects has diminishing returns, whereas a higher population density is always better. Unfortunately, the latter is uncontrollable from a survey-design perspective.

Appendix Table 10.1. Estimator simulation results over all scenarios

Estimator	Horvitz-Thompson	Hybrid	N-Mixture
Bias	8.55	7.88	2.45
Variance	0.014	0.014	0.015
MSE	0.00027	0.00026	0.00024
iMSE	0.52	0.47	0.54
Coverage	0.92	0.90	0.96

Appendix 11: N-Mixture Calculation

This appendix provides a detailed algorithm to calculate the N-Mixture probability distribution. The distribution is not conceptually difficult to understand nor mathematically difficult to calculate, but given the large amount of N-Mixture calculations in the MCMC routine, we found it was necessary to develop an efficient version in order to get quick MCMC results.

Recall that if there was perfect detection and no availability bias, then the true number of

$$N_j = \left(\sum_{y_i \in \boldsymbol{y}_j} y_i \right) = n_j$$

dugongs on a transect would equal the total observed counts, , where n_j is the total observed counts on transect j. However, due to availability bias and imperfect detection probabilities, we must calculate adjusted counts, N_j, which are bounded below by $N_j \geq n_j$ and could very large if $(a \times p) \ll 1$.

The posterior distribution of the adjusted counts is an N-mixture distribution, which is an integer-valued distribution that goes up-to infinity (theoretically). We call this series the $\mathrm{pmf}(N_j|n_j) = [n_j, n_j + 1, n_j + 2, \ldots, \infty)$, i.e., the adjusted count is some integer plus the observed counts n_j at transect j. The observed counts provide a lower bound, but there is no upper-bound.

The challenge of the MCMC sampler is to be able to sample from this discrete *pmf* series, meaning that we require the probabilities for each element of the series, and that the series must sum to one.

$$\sum_{N \geq n_j}^{\infty} \pi \left(N|\boldsymbol{y}_j, \boldsymbol{\beta}, \theta, \boldsymbol{a}, \boldsymbol{p} \right) = 1$$

Having a sum over an infinite series is difficult: to make the calculation tractable, we place an upper-bound on the *pmf* : $[n_j, \ldots, N_{\max}]$, whereby the final term of the series $p(N_{max}|y)$ is below some threshold 10^{-6}. A good way to guess a reasonable N_{max} is provided below.

11.1 Calculating the N-Mixture Series

The goal of this section is to motivate a vectorised calculation of the N-Mixture probability mass function to facilitate efficient sampling of N_j for all transects, as used within one MCMC sampling loop.

Recall that the definition of the N-Mixture is a product of a Binomial likelihood term on the observed counts y given N, and a prior distribution on the adjusted counts N (such as a Poisson or Negative Binomial):

$$p(N = x|\boldsymbol{y}\mu, \theta, p) \propto \underbrace{\binom{x}{n_j} \prod_{i=1}^{x} p_i^{y_i} (1 - p_i)^{(1-y_i)}}_{\text{Binomial term } y \text{ given } N = x} \underbrace{\frac{(\theta + x - 1)!}{(\theta - 1)!x!} \left(\frac{\theta}{\theta + \mu} \right)^{\theta} \left(\frac{\mu}{\theta + \mu} \right)^{x}}_{\text{NB probability of } N = x}$$

where $n_j = \sum_i y_i$; p_i is a product of availability bias and detection probability, *NB* is the Negative Binomial distribution parameterised by its mean and overdispersion (μ, θ). Notice that the Binomial term is expressed as a product-series of Bernoullis (this will be important later on).

The above formula has a recursive form, under the assumption that, at least for the recursive portion of the series, all $y_i = 0$. This is helpful for our particular situation because 100 per

cent of the hypothetical y_i for $N > n_j$ are, by definition, dugongs who were present but were not detected (hence $y_i = 0$ for all i beyond n_j). Later, we will exploit this fact and use it to factor the Binomial likelihood into two series of Bernoullis.

With some expansion and collection of terms, we can reveal the recursive nature of the formula:

$$p(N=x|\boldsymbol{y}, \cdot) =$$

$$\binom{x}{n_j}\frac{\binom{x-1}{n_j}}{\binom{x-1}{n_j}}(1-p_x)\prod_{i=1}^{x-1}p_i^{y_i}(1-p_i)^{(1-y_i)}\frac{\theta+x-1}{x}\frac{(x+\theta-2)!}{(\theta-1)!(x-1)!}\left(\frac{\theta}{\theta+\mu}\right)^\theta\frac{\mu}{\theta+\mu}\left(\frac{\mu}{\theta+\mu}\right)^{x-1}$$

$$= \frac{\binom{x}{n_j}}{\binom{x-1}{n_j}}(1-p_x)\left(\frac{\theta+x-1}{x}\right)\left(\frac{\mu}{\theta+\mu}\right)\underbrace{\binom{x-1}{n_j}\prod_{i=1}^{x-1}p_i^{y_i}(1-p_i)^{(1-y_i)}}_{\text{Binomial term } y \text{ given } N=x-1}\underbrace{\frac{(\theta+x-2)!}{(\theta-1)!(x-1)!}\left(\frac{\theta}{\theta+\mu}\right)^\theta\left(\frac{\mu}{\theta+\mu}\right)^{x-1}}_{\text{NB probability of } N=x-1}$$

$$= \underbrace{\left(\frac{\binom{x}{n_j}(1-p_x)(\theta+x-1)\mu}{\binom{x-1}{n_j}(\theta+\mu)x}\right)}_{\text{recursive increment } \chi_x}p(N=x-1|\boldsymbol{y}_{-x}, \cdot)$$

$$= \exp\{\chi_x\}\cdot p(N=x-1|\boldsymbol{y}_{-x}, \cdot)$$

This shows that we can calculate the probability that *N=x* given that we already know the probability that $N = x-1$, multiplied by a simple function called the *recursive increment*. On the log scale, the recursive increment is:

$$\chi_x = \log\binom{x}{n_j} + \log(1-p_x) + \log(\theta+x-1) + \log(\mu) - \log\binom{x-1}{n_j} - \log(\theta+\mu) - \log(x)$$

Although seemingly unwieldy, the term is actually very easy to calculate and facilitates vectorisation. The recursive increment "starts" at the lower bound with an initial log-probability of $\log p(N=n_j|\boldsymbol{y}_{n_j}, \cdot)$: this is the probability that *N* equals its lower-bound (the total number of observed dugongs at transect *j*). In other words, we can seed the recursive series by first calculating the lower-bound of $N_j=n_j$, and then calculate all higher log-probabilities $\log p(N=x|x>n_j, \cdot)$ by accumulating the recursive increments.

Vectorisation is possible by creating a vector whose first element is the lower-bound $\log p(N=n_j|\boldsymbol{y}_{n_j}, \cdot)$ and all subsequent elements are the recursive-increments χ for each *x* up to *x=Nmax*. The cumulative summation of this vector is another vector which represents the log-probability mass function of the N-mixture (un-normalised, truncated to N_{max}):

$$\log p(N=x|\boldsymbol{y}, \cdot) := \text{cumsum}\left(\left[\log p(N=n_j|\boldsymbol{y}_{n_j}, \cdot), \chi_{n_j+1}, \chi_{n_j+2}, \dots, \chi_{N_{max}-1}, \chi_{N_{max}}\right]^\top\right)$$

In other words, the *cumsum* operator is recursively adding $\chi_x + \log p(N=x-1|\boldsymbol{y}_{n_j}, \cdot)$, and creating a new vector that is the un-normalised log probability mass function.

Finally, the un-normalised log probability mass function is normalised according to the well-known "log-sum-exp" trick. After normalisation, the *pmf* sums to one and can be sampled. For the sake of MCMC sampling of N_j, we can take the normalised *cumsum series*, exponentiate it, and use the resulting probabilities as the input for a categorical-distribution sampler with categories $[n_j, n_j+1, \dots, N_{max}]^\top$. This is repeated for every MCMC iteration and every transect.

11.2 Heuristic to estimate an N_{max}

The above formulation benefits from vectorisation, thereby avoiding expensive if/then statements and while-loops. The crux of this benefit is having a reasonable upper-bound on the *cumsum* series N_{max}; this is essential for stopping the recursive calculation at a reasonable point for normalising the series into a probability distribution that sums to 1.

To reduce approximation error, we require that the N-mixture probability mass function has near-zero probability beyond N_{max}. Generally, it is not possible to set a very large number and hope that it applies to all N-Mixture distributions. This is because a "reasonable" upper-bound N_{max} is different for every transect, and conditional on regression parameters $(\beta_0, \beta_t, \theta)$ which change per MCMC iteration. Therefore, we need to recompute a "local" upper-bound per transect and per MCMC iteration.

One way to set this upper-bound is to increment N_{max} until $p(N_{max} | y, .)$ is sufficiently small, such as $<10^{-6}$. However, we found that constantly calculating $p(N_{max} | y, .)$ and checking whether it was sufficiently small was prohibitively expensive (i.e., $p(N | y, .)$ is expensive to compute). Another obvious way is to set a very large global upper-bound, regardless of the transect or current MCMC parameters, but this makes every single draw from the N-Mixture *pmf* needlessly over-burdensome.

Therefore, we developed a fast and principled heuristic to guess the upper-bound per MCMC iteration and transect:

$$N_{\max} = \text{mean} \left(q\text{NB} \left(0.99; \exp\{\beta_0 + \beta_t \cdot t\} \cdot A_j, \theta\right), \nu \left(\sum_{i=1}^{n_j} \frac{y_i}{a_i \cdot p} + 1 \right) \right)$$

where :

$$q\text{NB}(q; e^\eta, \theta) := \text{Negative Binomial quantile function}$$
$$A_j := \text{total area of transect } j$$
$$\nu := \text{safety factor, } 1 < \nu < 3$$

(1)

Notice that this N_{max} heuristic has two terms, each of which provides a principled and independent guess at an upper-bound to the distribution of N. The first term is the expected 0.99-quantile of the Negative Binomial distribution, parameterised by the current MCMC-sampled values of $(\beta_0, \beta_t, \theta)$. The second term is a modified Thompson-Horvitz-like estimator that depends on the availability bias and the detection probabilities for transect j (multiplied by a safety factor $\nu > 1$). Intuitively, the qNB term is acting like a prior, guessing N_{max} based on the upper-tail low-probability region of the NB distribution. The HT-term is a purely data-driven quantity approximating the expectation of a Binomial term (

$$\sum y_i \approx a \cdot p \cdot N_j \text{)}.$$ Notice that the latter term is inflated by a safety factor ν.

We found that it was most computationally efficient to do a trial MCMC run where we tried several safety factors ν and monitored the number of incidences where the density at the upper-bound $p(N_{max} | y, .)$ exceeded a threshold (10^{-6}). We then adjusted the safety-factor ν so that there was only a tiny (but non-zero) number of incidences where the density at N_{max} exceeded the threshold 10^{-6}. Too many incidences meant that our approximating distribution was too inaccurate, and no incidences meant that we were wasting computing-resources on trivially-small regions of the N-Mixture distribution. This pre-tuning was faster than coding multiple if/then statements to adjust N_{max} on the fly, or setting a global large upper-bound.

Appendix 12: Results from Other Methods for Estimating Dugong Population Density

This appendix presents the estimates of dugong trend-lines (2006 to 2018-2019) and dugong population densities for the NGBR, per year, according to three estimators. The N-Mixture was the focus of this technical report, while the Horvitz-Thompson estimator (Middle in Appendix Figure 12.1) and Hybrid (Bottom) are presented for comparison.
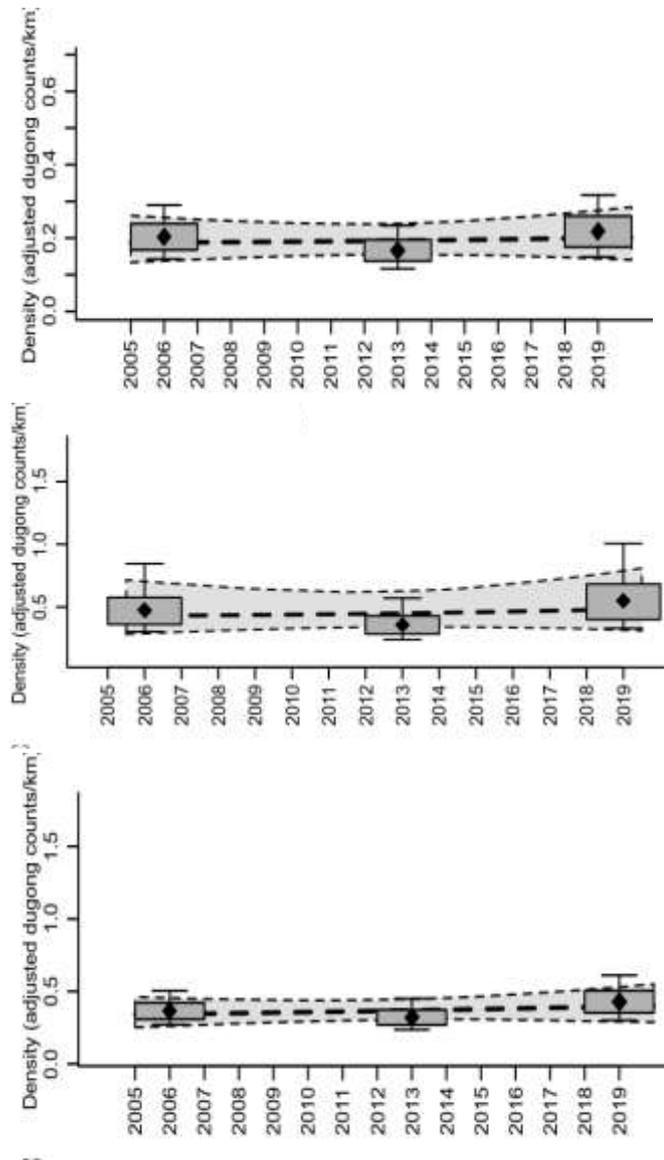

Appendix Figure 12.1. Per-year estimates of dugongs (box-and-whiskers) and trend-line ($\pm$ 95 per cent CI) for NGBR according to three estimators. Top: N-Mixture; Middle: Horvitz-Thompson; Bottom: Hybrid

Appendix Table 12.1. Comparison of trend estimates for NGBR dugongs 2006-2018-2019 for the N-Mixture, Hybrid and Horvitz-Thompson (HT) estimators.

N-Mixture				Hybrid				Horvitz-Thompson HT			
Mean	SE	95 per centCI	p(decline)	Mean	SE	95 per centCI	p(decline)	Mean	SE	95 per centCI	p(decline)
0.5	1.83	(-3.084; 4.128)	0.4	1.12	1.75	(-2.287; 4.525)	0.26	0.92	2.66	(-4.601; 6.167)	0.36

The three estimators all suggest that the dugong population has been stable been across the period from 2006 to 2018-2019.
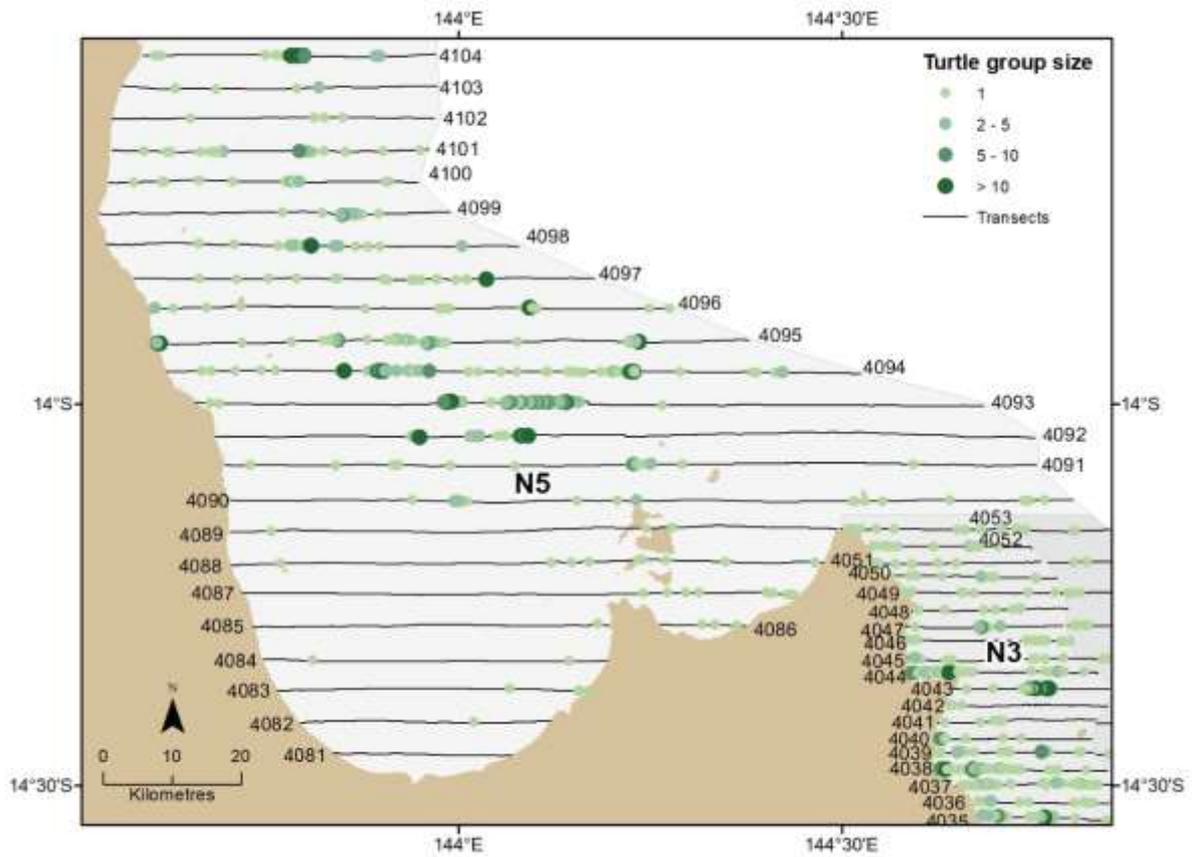
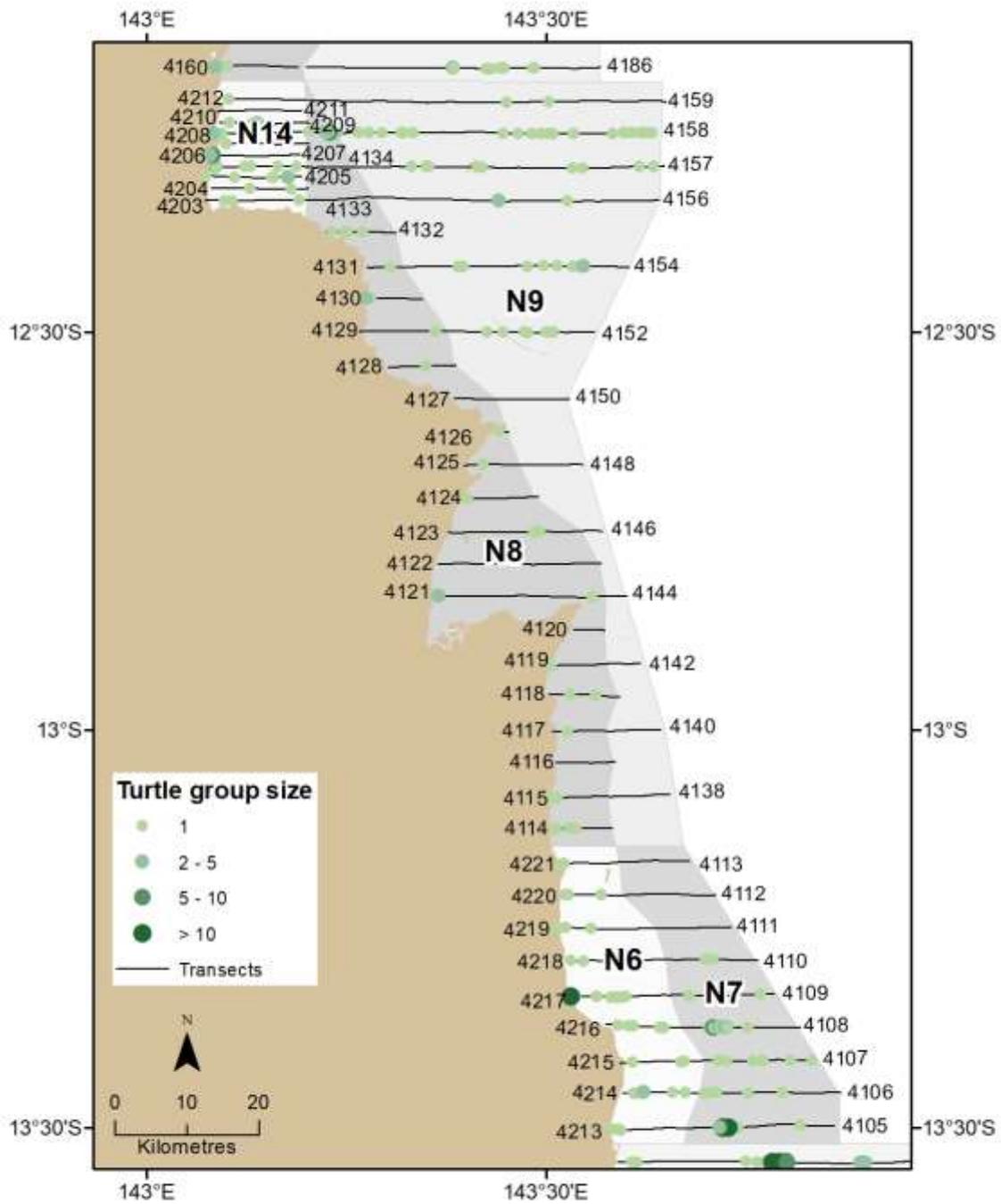# Appendix 13: Dugong sightings in the CGBR and NGBR during the 2018–2019 surveys
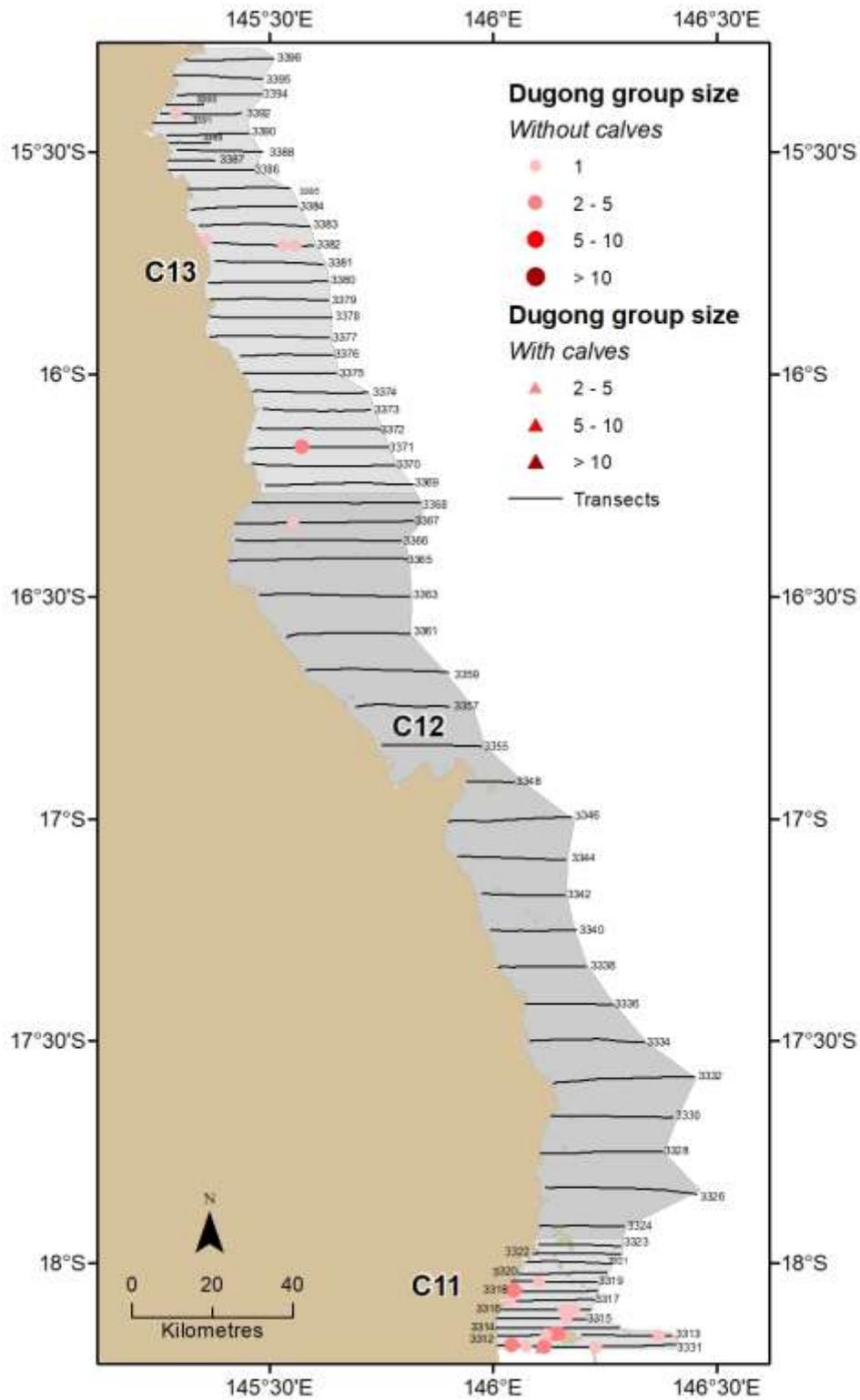
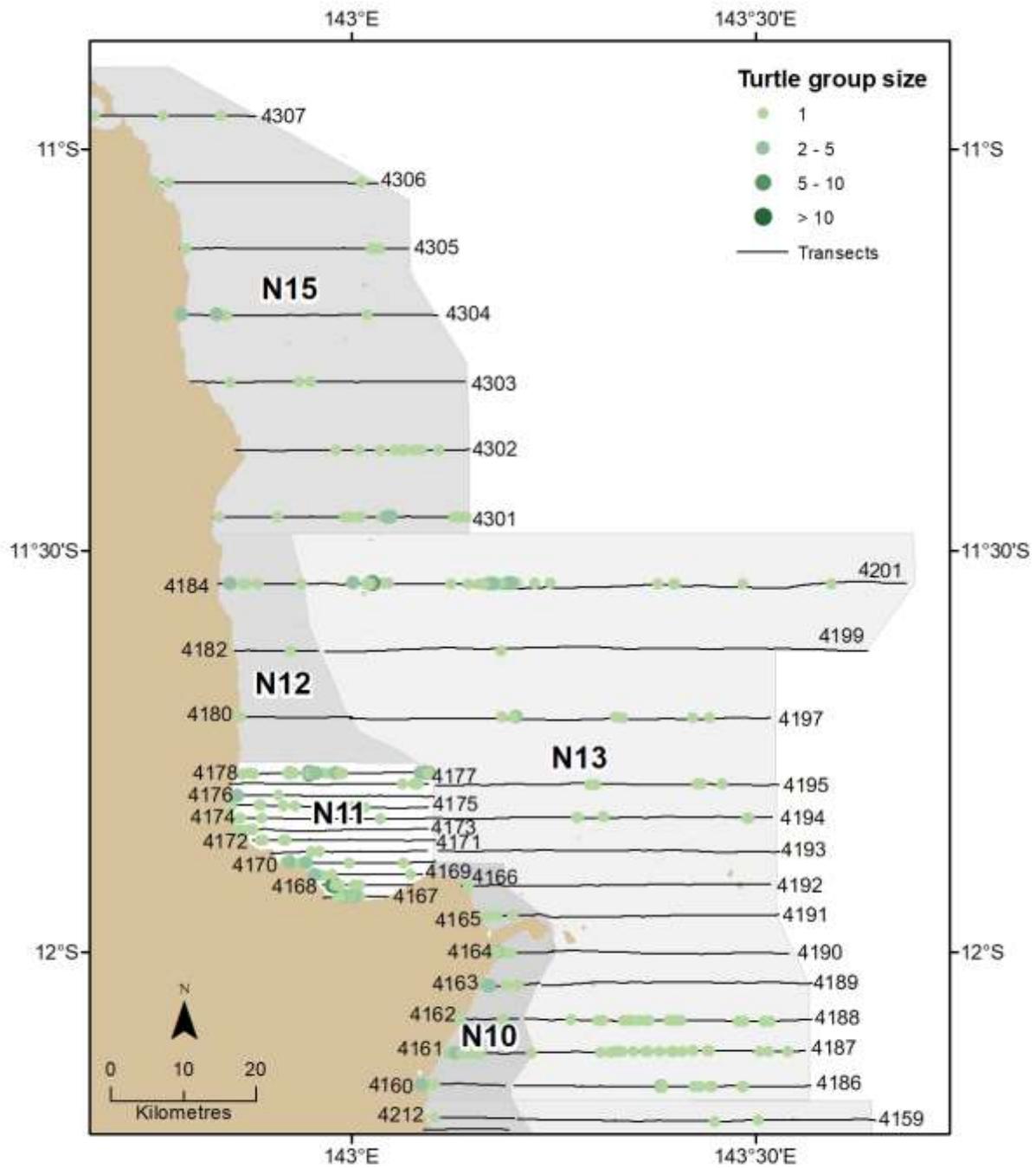**Appendix Figure 13.1**. Distribution of dugongs in the CGBR surveyed in November 2018.
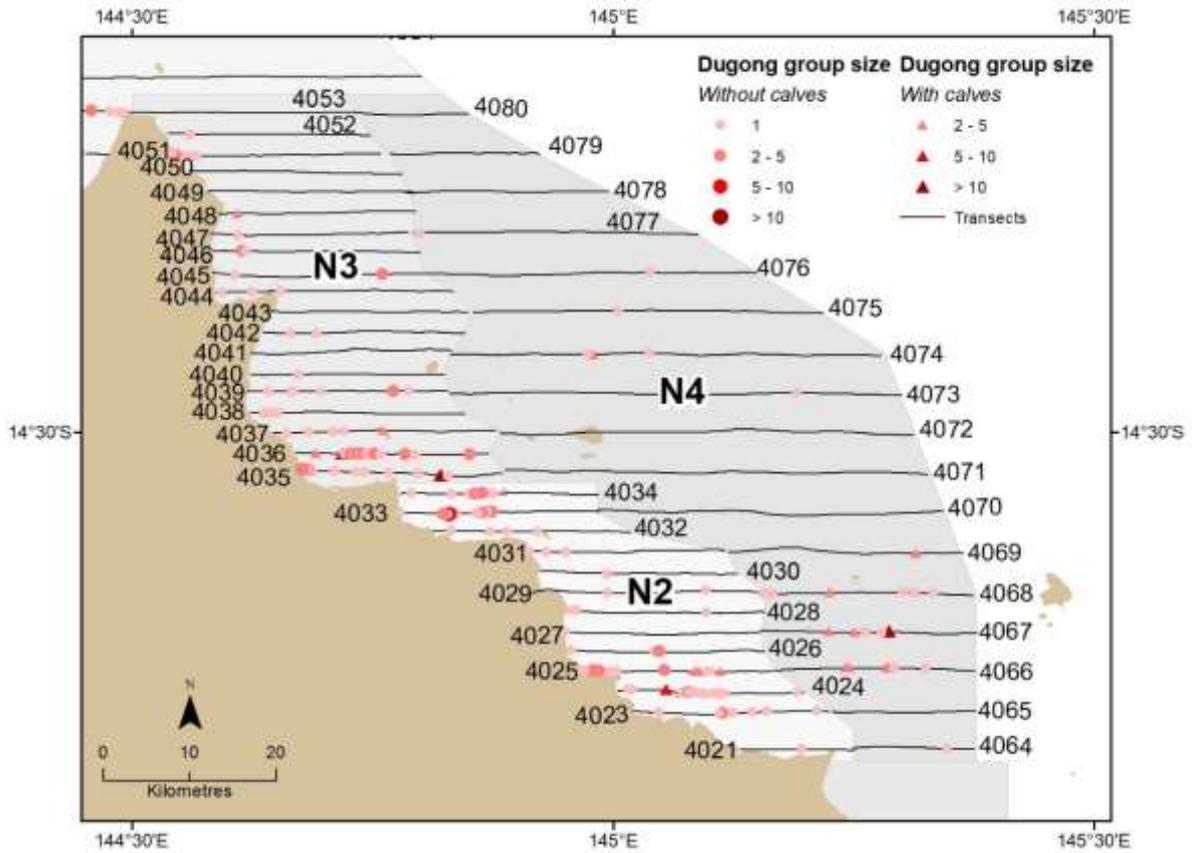
Appendix Figure 13.2. Distribution of dugongs in Blocks N2, N3, and N4 of the NGBR surveyed in November 2019.
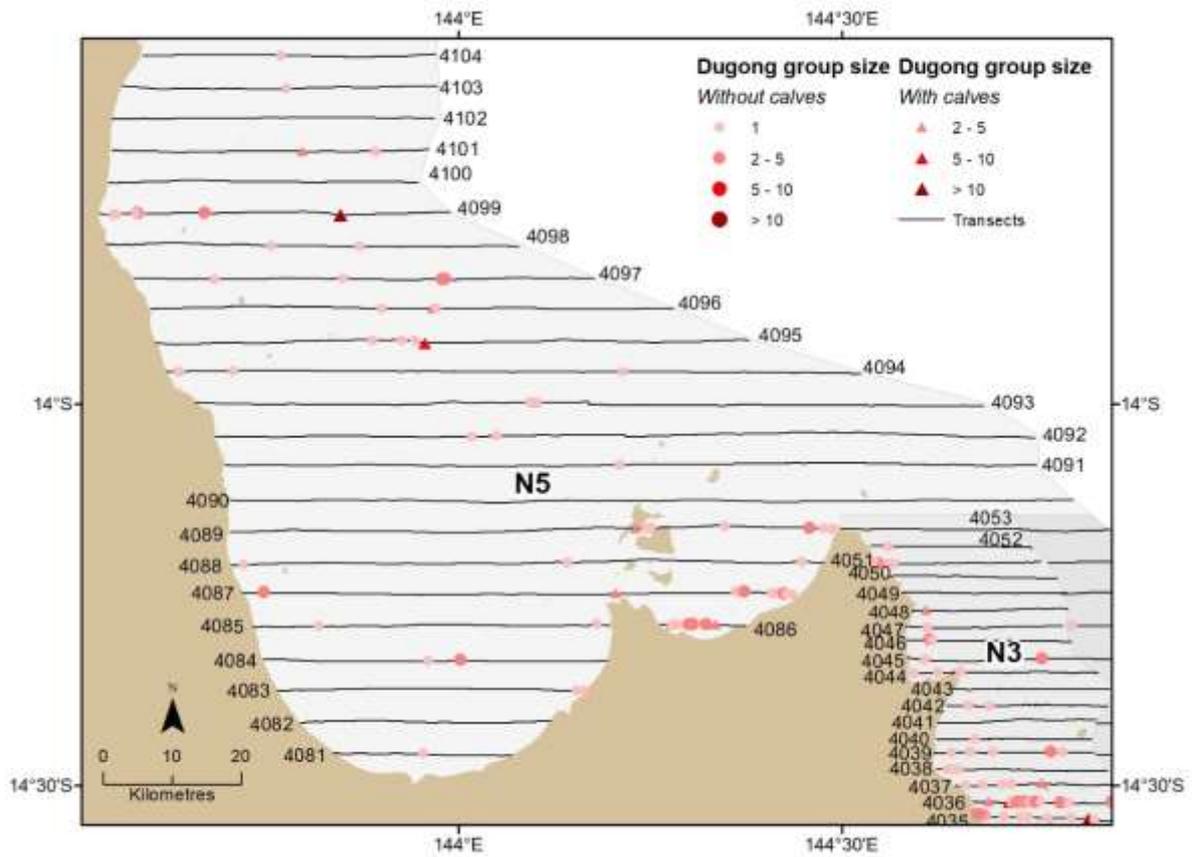
Appendix Figure 13.3. Distribution of dugongs in Blocks N3 and N5 of the NGBR surveyed in November 2019 and June 2019 respectively.
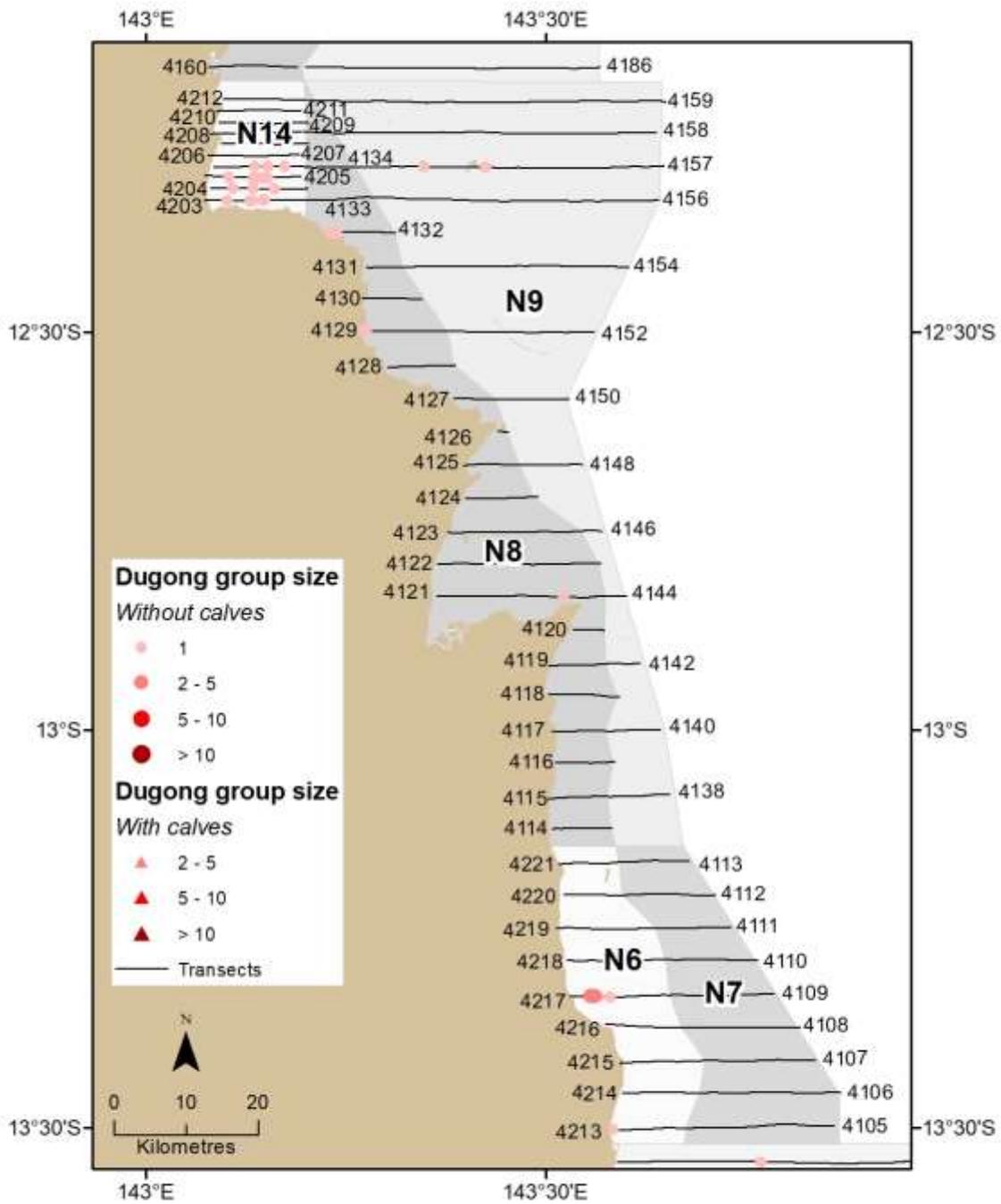
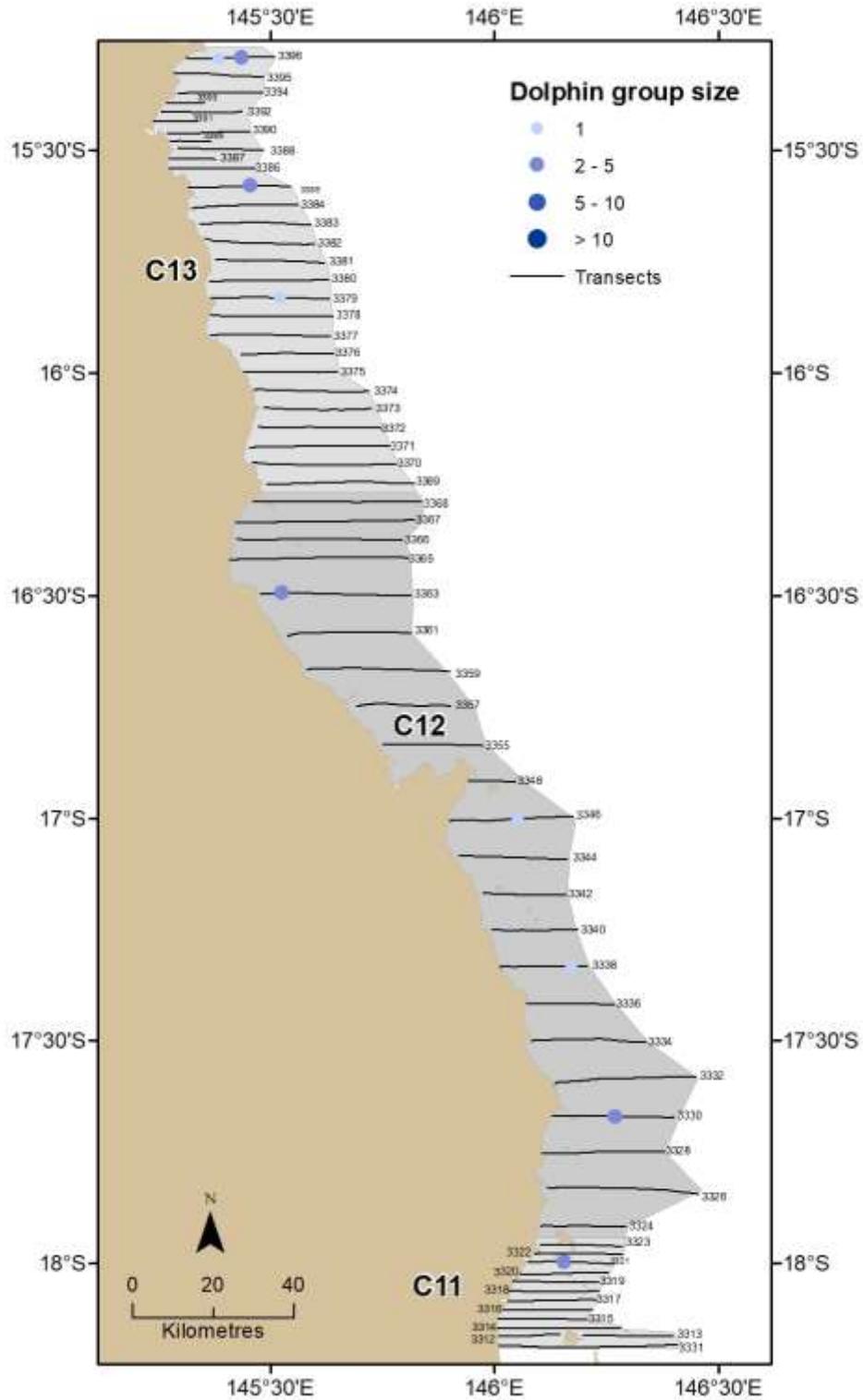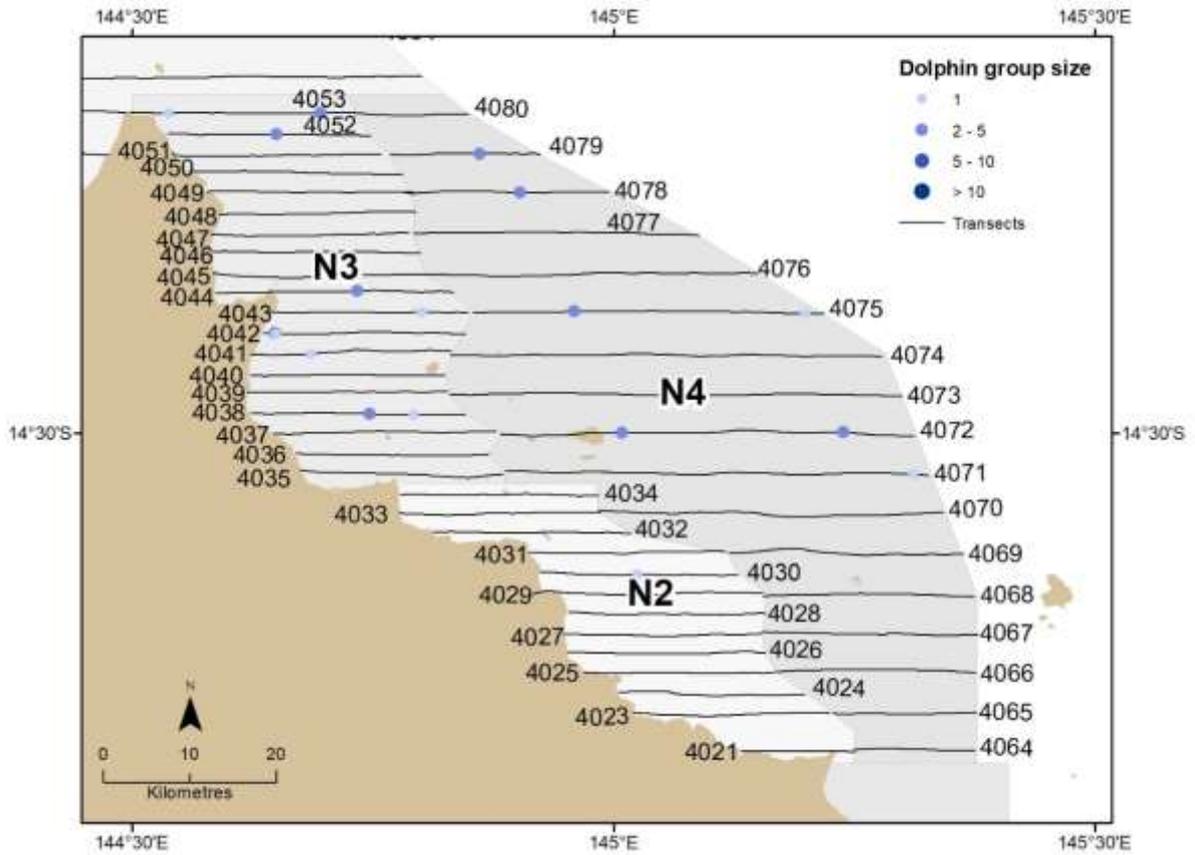**Appendix Figure 13.4**. Distribution of dugongs in Blocks N6, N7, N8, N9, and N14 of the NGBR surveyed in November 2019.
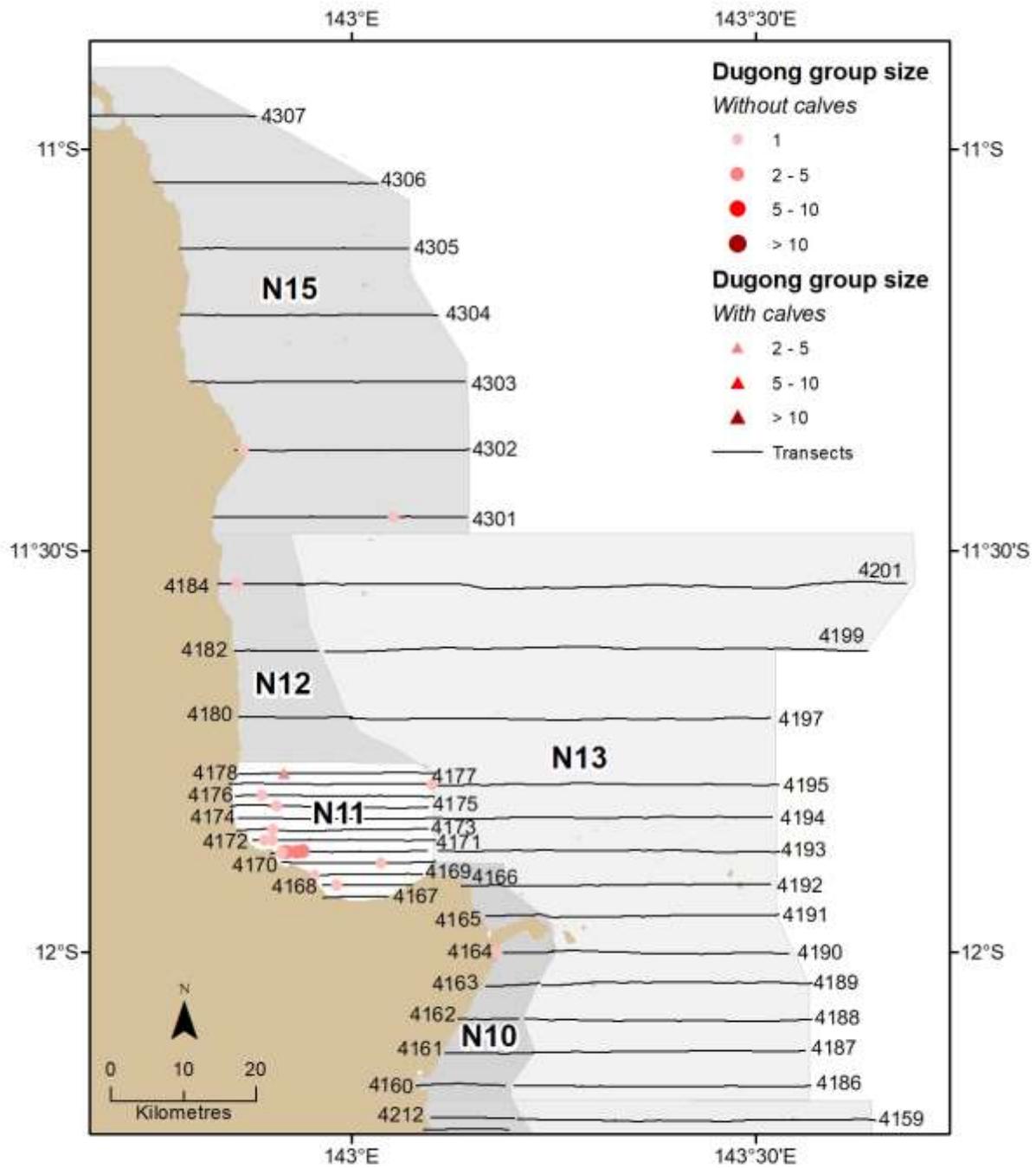
Appendix Figure 13.5. Distribution of dugongs in Blocks N10, N11, N12, N13, and N15 of the Northern Great Barrier Reef. Blocks N12 and N15 were surveyed in November 2018, Blocks N10 and N11 in November 2019 and Block N13 in November/December 2019.

Appendix Figure 14.1. Distribution of turtle sightings in the CGBR surveyed in November 2018.
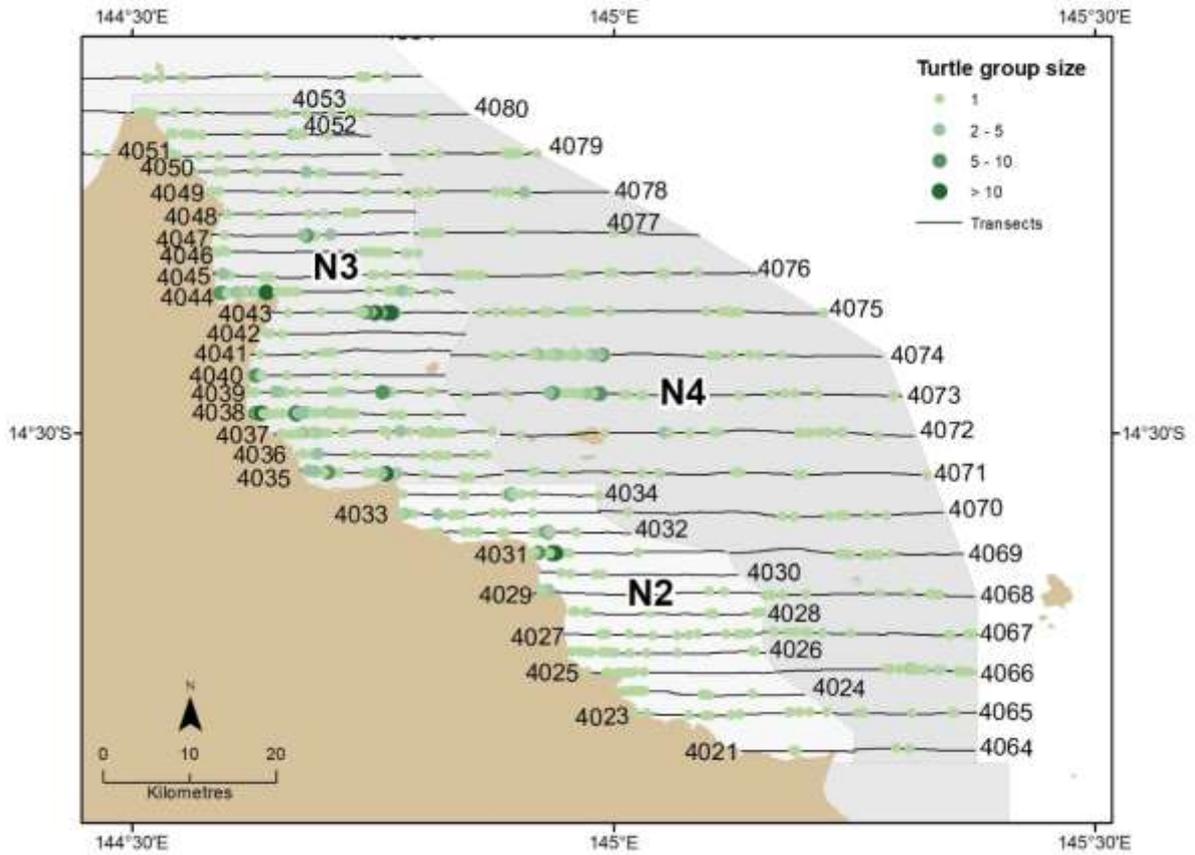
Appendix Figure 14.2. Distribution of turtle sightings in Blocks N2, N3, and N4 of the NGBR surveyed in November 2019.

Appendix Figure 14.3. Distribution of turtle sightings in Blocks N3 and N5 of the NGBR surveyed in November 2019 and June 2019 respectively.

Appendix Figure 14.4. Distribution of turtle sightings in Blocks N6, N7, N8, N9, and N14 of the NGBR surveyed in November 2019.

Appendix Figure 14.5. Distribution of turtle sightings in Blocks N10, N11, N12, N13, and N15 of the Northern Great Barrier Reef. Blocks N12 and N15 were surveyed in November 2018, Blocks N10 and N11 in November 2019 and Block N13 in November/December 2019.
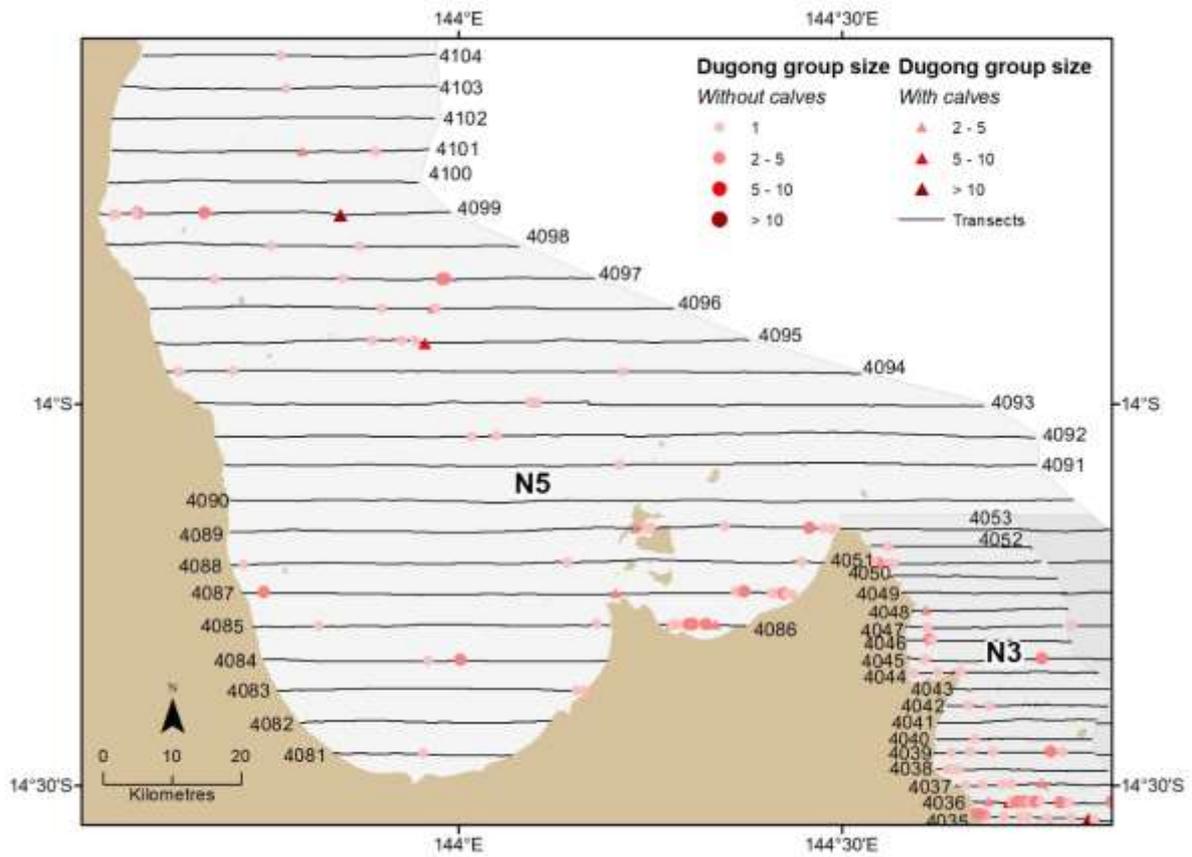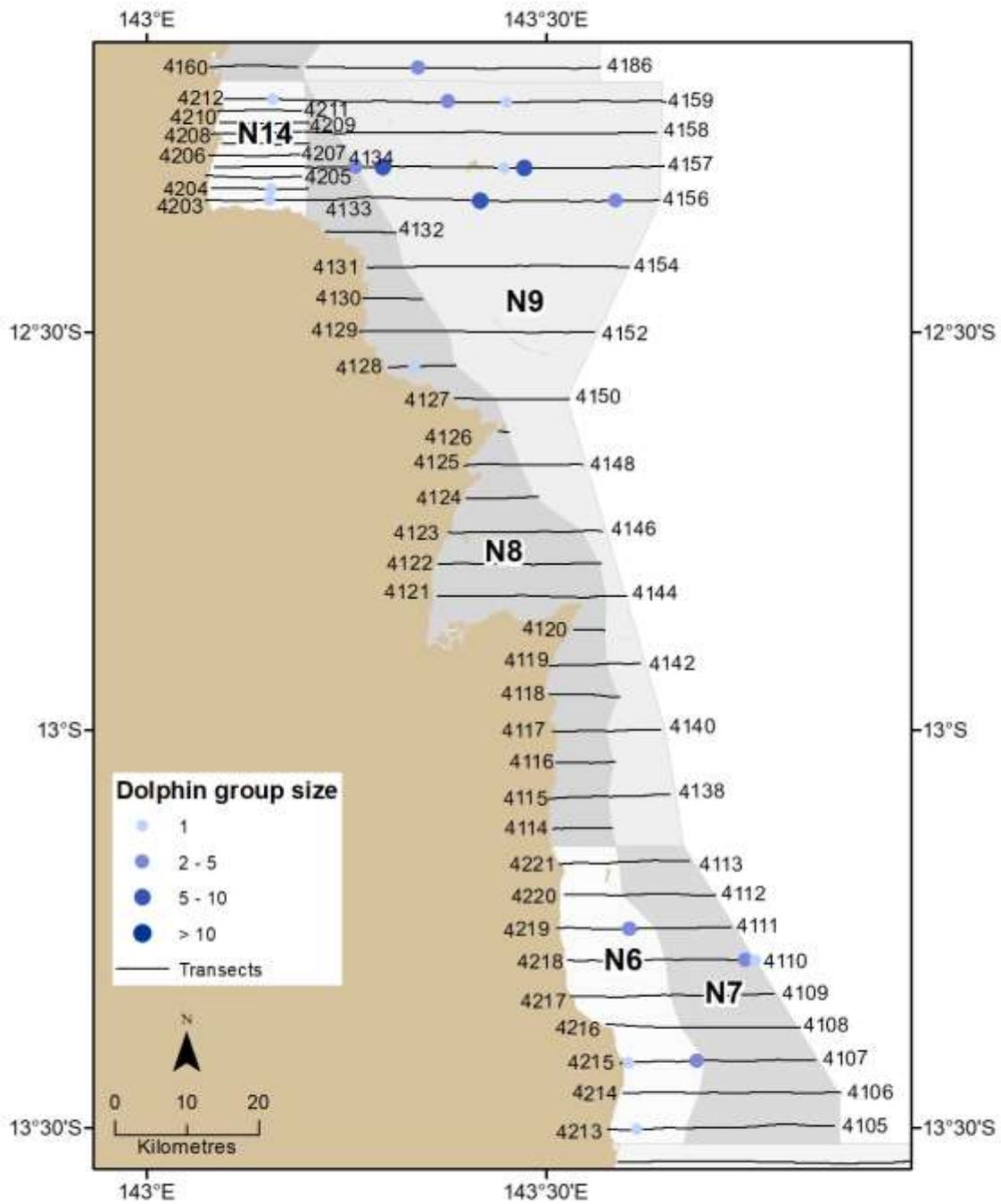
Appendix Figure 15.1. Distribution of dolphins sighted in the CGBR in November 2018.
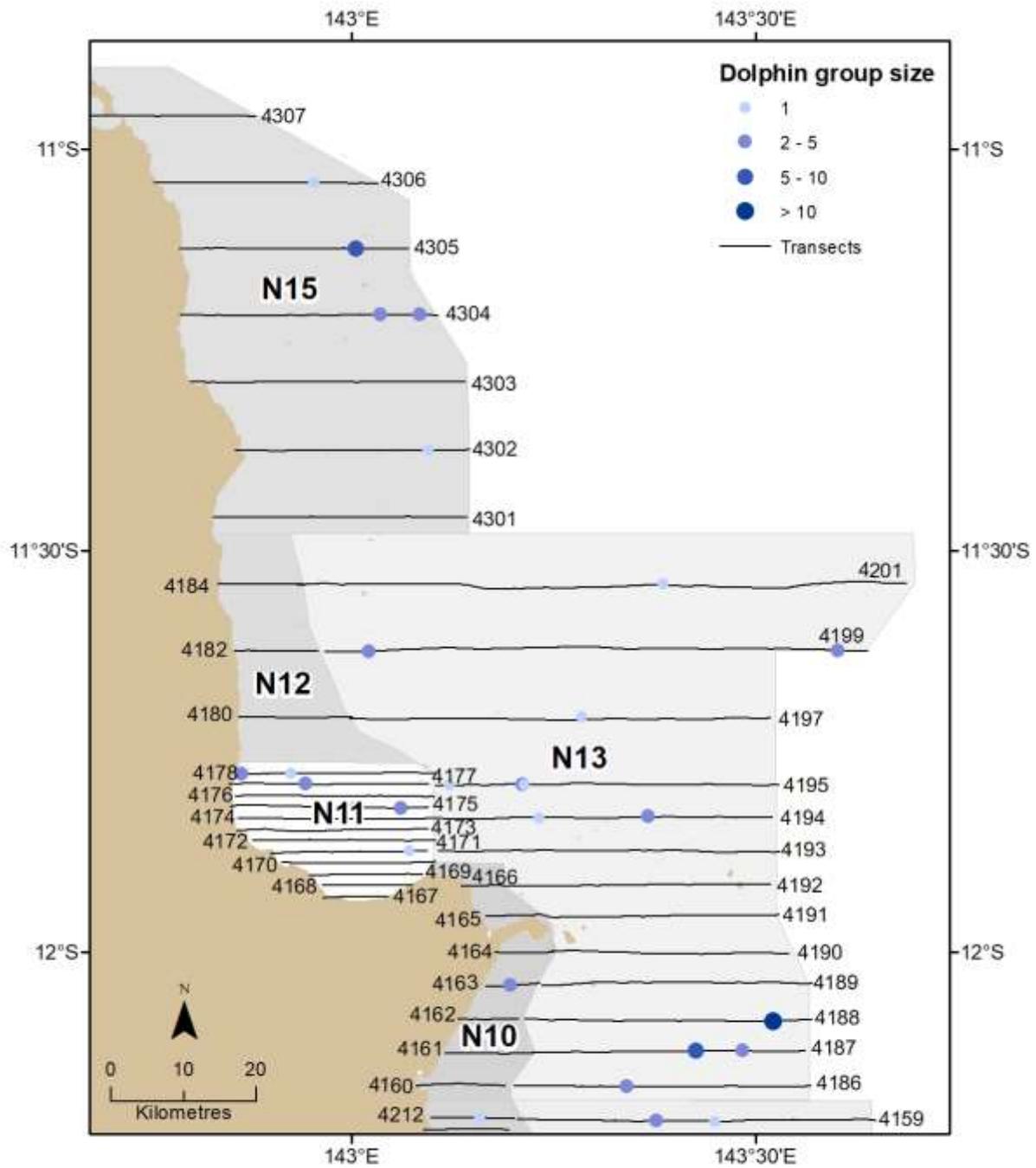
Appendix Figure 15.2. Distribution of dolphins in Blocks N2, N3, and N4 of the NGBR surveyed in November 2019.

Appendix Figure 15.3. Distribution of dolphins in Blocks N3 and N5 of the NGBR surveyed in November 2019 and June 2109 respectively.

Appendix Figure 15.4. Distribution of dolphins in Blocks N6, N7, N8, N9, and N14 of the NGBR surveyed in November 2019.

Appendix Figure 15.5. Distribution of dolphins in Blocks N10, N11, N12, N13, and N15 of the Northern Great Barrier Reef. Blocks N12 and N15 were surveyed in November 2018, Blocks N10 and N11 in November 2019 and Block N13 in November/December 2019.